TECHNISCHE UNIVERSITÄT MÜNCHEN

Wissenschaftszentrum Weihenstephan für Ernährung, Landnutzung und Umwelt
Lehrstuhl für atmosphärische Umweltforschung

Ecosystem-Atmosphere Exchange over a wind-throw-disturbed upland spruce forest in the Bavarian Forest National Park

Matthias Lindauer

Vollständiger Abdruck der von der Fakultät Wissenschaftszentrum Weihenstephan für Ernährung, Landnutzung und Umwelt der Technischen Universität München zur Erlangung des akademischen Grades eines

Doktors der Naturwissenschaften (Dr. rer. nat.)

genehmigten Dissertation.

Vorsitzender:		Univ.-Prof. Dr. Jörg Völkel
Prüfer der Dissertation	1.	Univ.-Prof. Dr. Hans Peter Schmid
	2.	Univ.-Prof. Dr. Harald Kunstmann Universität Augsburg

Die Dissertation wurde am 17.12.2015 bei der Technischen Universität München eingereicht und durch das Wissenschaftszentrum Weihenstephan für Ernährung, Landnutzung und Umwelt am 04.05.2016 angenommen.

Abstract

Net ecosystem exchange of CO_2 (NEE) as well as fluxes of water vapor and energy were measured in a wind-throw-disturbed upland spruce forest in the Bavarian Forest National Park (Germany) continuously over five years, from 2009 to 2013, by the eddy covariance method. Estimated annual NEE (positive values stand for a net carbon source) of the non-cleared wind-throw resulted in 347 ±104, 255 ±77, 221 ±66, 240 ±52, and 167 ±50 g C m^{-2} for the successive years, respectively. However, two to six years after the storm event (windstorm Kyrill, January 2007) gross ecosystem production (GEP) was already strong, increasing from 393 (2009) to 649 g C m^{-2} yr^{-1} (2013). Ecosystem respiration showed a high inter-annual variability during the measurement period, ranging from 656 to 816 g C $m^{-2}yr^{-1}$. Carbon dioxide (CO_2) fluxes during snow-covered periods averaged about 0.8 µmol m^{-2} s^{-1} with only little variation. The present study is worldwide the first to track the post-disturbance C-exchange continuously over more than a year in an intact wind-throw area.

The contributions of spruces and grasses to the overall carbon exchange, and the differentiation into autotrophic and heterotrophic respiration were estimated by the biogeochemical model LandscapeDNDC. Results have shown that this model can reasonably represent the measured carbon dioxide fluxes, apart from a slight but systematic underestimation of ecosystem respiration at very high fluxes and during winter. Thus, model deviations tend to increase with time. A long-term simulation of the carbon balance development predicts that the ecosystem most likely will switch from a net carbon source to a net carbon sink within the next 10 years. Simulations also show that the “biome-time-scale” – the time scale over which all post-disturbance emitted carbon will have been fixed again by the ecosystem – is about 20 years.

Overall, the results show that 1) low productive mountainous forest sites may switch from a carbon source to a carbon sink within relatively few years after disturbance, and 2) main uncertainties in process understanding originate from poorly resolved dynamics in soil respiration, decomposition of large debris, and succession of ground cover species development. Evidence from the present study suggests that the carbon release of non-cleared wind-throws does not follow a simple pattern which is mainly a function of biomass, but that changing structural and micro-climate conditions have to be taken into account.

An additional outcome of the present work was a simple model for incoming short-wave radiation, requiring only screen-level relative humidity data (and site specific astronomical information). The model was developed and parameterized using high quality global radiation data, covering a broad range of climate conditions. Despite its simplicity, the new model clearly outperforms conventional approaches, and it comes close to more labor- and data-intensive alternative models.

Zusammenfassung

Von 2009 bis 2013 wurden der Netto Ökosystemaustauch von CO_2 (net ecosystem exchange - NEE) sowie Energie und Wasserdampfflüsse über einem naturbelassen Windwurfgebiet im Bayerischen Wald mittels der Eddy Kovarianz Methode bestimmt. Die jeweiligen Nettosummen für den CO_2-Austauch dieser Jahre (positive Werte bedeuten CO_2-Emission) ergaben 347 ±104, 255 ±77, 221 ±66, 240 ±52 und 167 ±50 g C m^{-2}. Zwei bis sechs Jahre nach dem Sturm (Wintersturm Kyrill, Januar 2007) war jedoch die jährliche brutto CO_2-Aufnahme (gross ecosystem production - GEP) bereits sehr hoch und stieg von 393 (2009) auf 649 g C m^{-2} (2013) an. Die Respiration des Ökosystems (R_{eco}) zeigte eine hohe Variabilität über den Messzeitraum mit Werten zwischen 656 und 816 g C m^{-2} a^{-1}. Die CO_2-Austauschraten während Zeiträumen mit geschlossener Schneedecke betrugen im Mittel etwa 0.8 µmol m^{-2} s^{-2}. Die vorliegende Arbeit ist weltweit die erste, die den störungsbedingten Kohlenstoff Haushalt kontinuierlich über mehr als ein Jahr in einem intakten Windwurf Gebiet verfolgt.

Die Beiträge von Fichten und Gräsern zum gesamten Kohlenstoffumsatz und die Unterscheidung zwischen autotropher und heterotropher Respiration wurde mit Hilfe des biogeochemischen Models LandscapeDNDC bestimmt. Die Ergebnisse haben gezeigt, dass dieses Modell die gemessenen CO_2-Flüsse korrekt wiedergibt, abgesehen von einer geringen aber systematischen Unterschätzung der Respiration bei hohen Emissionsraten und im Winter. Die kumulativen Modellabweichungen steigen dabei mit der Zeit an. Eine Langzeitsimulation des Kohlenstoffumsatzes prognostiziert dass sich das Ökosystem innerhalb der nächsten 10 Jahre von einer netto CO_2-Qelle zu einer netto CO-Senke entwickeln wird. Die Simulationen zeigen auch, dass die „Biom-Zeitskala“ – die Zeitskala in der der gesamte Kohlenstoff, der nach der Störung emittiert wurde, wieder fixiert worden ist – ungefähr 20 Jahre ist.

Im Allgemeinen zeigen die Ergebnisse, dass 1) sich Standorte an langsam wachsenden Bergwäldern innerhalb weniger Jahre nach einer Störung von einer Kohlenstoffquelle wieder in eine Senke umwandeln dürften und 2) die hauptsächlichen Unsicherheiten beim Prozessverständnis in der Bodenrespiration, in der Zersetzung von Totholz und in der Entwicklung der Bodenvegetation begründet sind. Die Resultate dieser Studie weisen darauf hin, dass die Kohlenstofffreisetzung naturbelassener Windwurfgebiete nicht einem einfachen Schema abhängig von der Biomasse folgt, sondern dass sich ständig verändernde strukturelle und mikroklimatische Bedingungen ebenfalls berücksichtigt werden müssen.

Ein zusätzliches Produkt dieser Arbeit war ein einfaches Model zur Bestimmung der eingehenden kurzwelligen Solarstrahlung (Globalstrahlung) welches nur die relative Feuchte (und astronomische Informationen) als Eingangsparameter benötigt. Das Model wurde mit qualitätsgeprüften Globalstrahlungsdaten, die ein breites Spektrum von Klimaverhältnissen umfassen, entwickelt und pa-

rametrisiert. Trotz seiner Einfachheit, übertrifft das Modell herkömmliche Ansätze und reicht nah an mehr Arbeits- und Datenintensivere Modell heran.

Table of Contents

Motivation

On January 18th/19th in 2007 the severe winter storm Kyrill, with gusts up to 60 m s^{-1}, swept over large parts of Europe (Figure 1) and left a trail of devastation. The overall economic damage was estimated at ten million US$ (≈7.4 million €) (Munich Re, 2007) and 49 people lost their lives. Public transport systems were disrupted for some days in many places. For the first time in its history the German railway company DB had to stop all intercity rail-traffic in the evening of January 18th due to Kyrill. Thousands of houses were without electricity for many hours during these two days. In addition, the silvicultural damage was disastrous. An amount of almost 60 million m³ of timber all over western Europe was uprooted – 37 million m³ of these in Germany. Although Kyrill had the biggest impacts in the mid-western parts of Germany (e.g., Thuringia and North-Rhine-Westphalia), there were also large areas affected within the southern part of Germany, especially in the Bavarian Forest National Park. A large area about 600 m in diameter (30 ha) of a Norway spruce forest (*Picea abies* (L.) H. Karst) on the Lackenberg hill was almost completely uprooted by Kyrill.

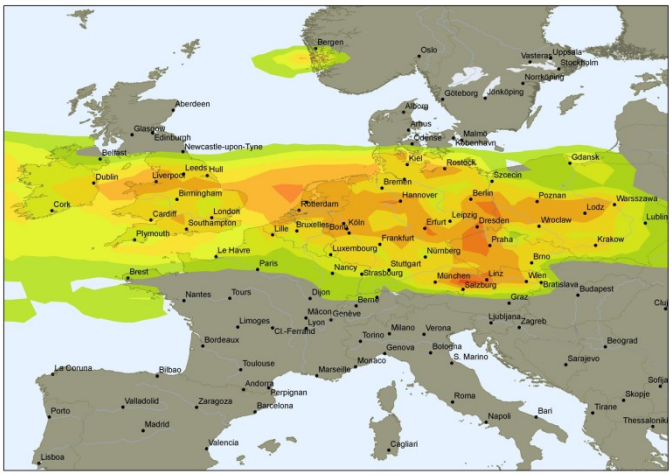

Figure 1: Storm track of Kyrill. The color indicates the maximum wind speed from green (22-25 ms^{-1}) to red (> 40 ms^{-1}). From: Munich Re (2007)

After such a severe wind-storm all fallen trees are usually removed, to salvage the wood, and to protect the remaining forest from insect infestation. Thus, the whole wind-throw is commonly cleared and eventually new seedlings of the predominant trees are planted afterwards. Not so in the Bavarian Forest National Park. Due to a policy of conservative forest management, succinctly put in the slogan "Natur Natur sein lassen", engl.: "let nature be nature", the administration of the National Park decided not to clear this area. All dead-wood remained on site at the Lackenberg wind-throw, thereby creating an almost unique opportunity to investigate and observe an ecosystem that was recently affected by severe disturbance during ecological succession without anthropogenic intervention. Within the project "bark-beetle-attack on wind-throw areas: process analysis for course of action" (Schopf et al., 2008; funded by Bavarian State Ministry of the Environment and Public Health), the first part was to study the development of bark-beetles (*Ips typographus* (L.)) on wind-throw disturbed Norway spruce forests. In the second part of the project the climatic parameters, energy budget, and exchange of water vapor, VOCs (Wolpert, 2012) as well as of CO_2 were estimated.

Particularly concerning the exchange of carbon and energy between such disturbed ecosystems and the atmosphere there is only sparse knowledge up to now. Therefore, investigating carbon and energy exchange in this wind-throw was promising to deliver new scientific findings about the basic processes of carbon and energy transport (short time-scales) but also about the long-term dynamics of carbon cycling in this particular ecosystem over longer time periods. Thus, in this work the carbon and energy exchange of the wind-throw disturbed forest at the Lackenberg is examined. With regard to anthropogenic global warming, understanding the processes and dynamics that are driving carbon exchange within all kinds of ecosystems is of high importance, not only for scientists, but also for policy makers. Sound knowledge of these processes and dynamics will help to specify the expected consequences of global warming more reliably and is necessary for the evaluation of future climate mitigation actions (Pan et al., 2011).

1 Introduction

1.1 Global carbon cycle and climate change

Anthropogenic global warming as a major driver of climate change with all the associated risks, such as rising temperatures, rising sea-levels, increasing extreme weather situations, extinction of many species, and many more is well documented and widely accepted (e.g., IPCC, 2013). However, there is still uncertainty about the magnitudes of climate change impacts on Earth. That is, how much will the temperature increase be, how fast will sea-levels rise, and so on. Constraining these uncertainties is an important contribution to improve scientifically based climate change impact assessment and decision support.

In this context it is essential to quantify regional and global greenhouse gas (GHG) budgets. CO_2 and CH_4 are the two main contributors of human-induced climate forcing - "CO_2 alone accounts for 80% of the current growth in climate forcing…" (Canadell et al., 2010). Thus, CO_2 has been the focus of much research for many years (IPCC, 2013).

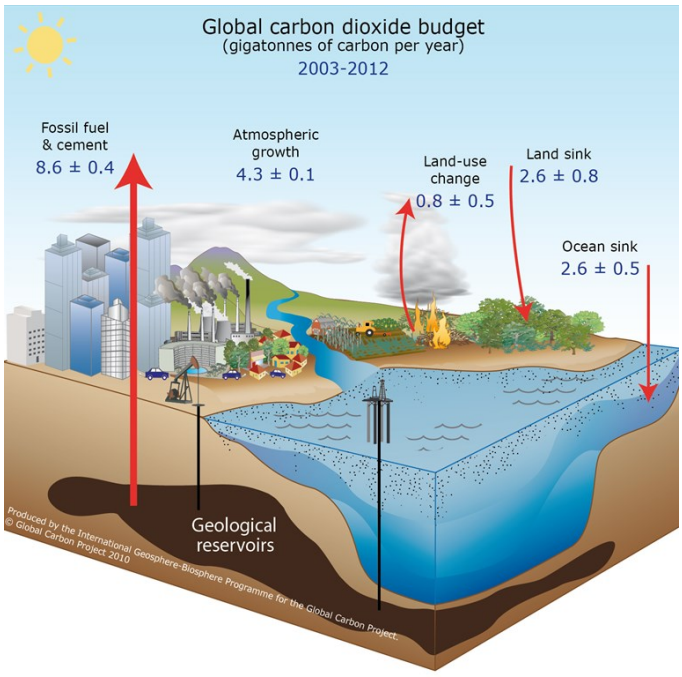

Figure 2: Global carbon dioxide budget from 2003 - 2012 Source: globalcarbonproject.org

The global carbon budget is roughly divided into a terrestrial part (net Land sink), an oceanic part (net Ocean sink), atmospheric growth, emissions from fossil fuel combustion and cement production, and emissions from land-use change. Dynamics and global magnitudes of the several fluxes are shown in Figure 2 and Table 1. Estimates of these exchange rates are based on energy use statistics, statistics of land use change (fossil fuel emissions and emissions from land-use change respectively), atmospheric measurements (atmospheric growth), and models (ocean sink). The terrestrial (land) sink is usually calculated as the residual of the sum of all sources minus atmosphere + ocean sinks. However, as Le Quéré (2010) notes, "this equation transfers all uncertainties to the land CO_2 sink, and does not test our understanding of the underlying processes". Thus, in recent years there have been efforts to calculate the terrestrial sink also from models (Canadell et al., 2007b; Heimann and Reichstein, 2008; Le Quéré et al., 2009; Le Quéré, 2010).

Table 1: Global carbon budget of recent years. Values are in gigatonnes of carbon per year. Data from: Le Quéré et al. (2012)

Year	Fossil fuel + cement	Land-use change	Atmospheric growth	Ocean sink	Land sink
2004	7.81	0.85	3.41	2.36	2.88
2005	8.09	0.83	5.15	2.45	1.32
2006	8.37	1.06	3.69	2.51	3.23
2007	8.57	0.66	4.45	2.55	2.22
2008	8.78	0.68	3.77	2.39	3.30
2009	8.74	0.77	3.50	2.61	3.40
2010	9.17	0.68	5.17	2.60	2.07
2011	9.46	0.63	3.63	2.71	3.75
2012	9.67	0.85	5.15	2.90	2.46

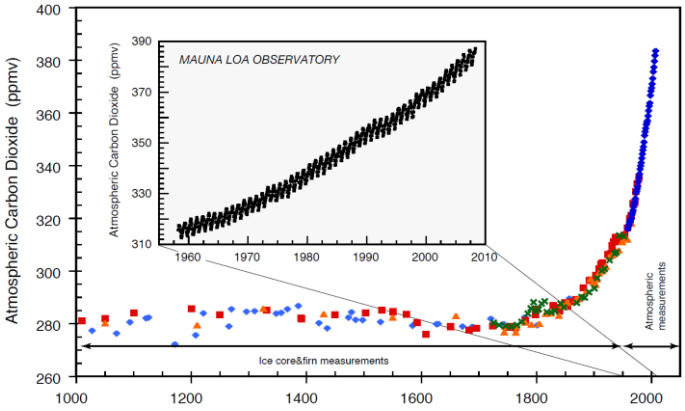

Figure 3: Atmospheric carbon dioxide. Data until 1958 is estimated from Antarctic ice cores. Data from 1958 onward is from the Mauna Loa Observatory in Hawaii. Inner graph shows monthly Mauna Loa measurements; main graph shows annual means. From: Sarmiento et al. (2010)

Due to the rising level of CO_2 concentration in the atmosphere (Figure 3), the potential of individual ecosystems to emit or store carbon, that is whether they act as a carbon source or sink, is of growing interest. As can be seen in Figure 2, there is still a high uncertainty of the estimated carbon exchange, especially in the terrestrial part (Goodale et al., 2002; Houghton, 2003).

Figure 4 shows that, for the terrestrial part of the global carbon balance, there is also a large inter-annual variability (Le Quéré et al., 2009; Schimel et al., 2001). The high uncertainty, together with this large inter-annual variability, indicate that there is still lack of knowledge, which has led to intense efforts quantifying the net exchange of CO_2 in different terrestrial ecosystems. Thus, natural carbon sources and sinks were studied with increasing intensity (Baldocchi et al., 2001; Canadell et al., 2007a; Falkowski et al., 2000; Le Quéré et al., 2013; Raupach, 2011). Forests, as large and highly dynamic carbon pools, attract special attention in this respect (Bonan, 2008b; Janssens et al., 2005; Luyssaert et al., 2008; Pan et al., 2011; Schulze et al., 1999). Generally, forest ecosystems are reported to serve as strong carbon sinks (Dragoni et al., 2011; Gruenwald and Bernhofer, 2007; Knohl et al., 2003; Valentini et al., 2003). Analyzing carbon accumulation of European forests, Ciais et al. (2008) emphasized that European forests are important carbon sinks and could maintain this property for several decades. Nabuurs et al. (1997) report a carbon sink strength of European forests on the order

of 0.10 $GtCyr^{-1}$. From 2001 to 2007 the European terrestrial biosphere took up about 0.17 $GtCyr^{-1}$ as estimated by Peters et al. (2010).

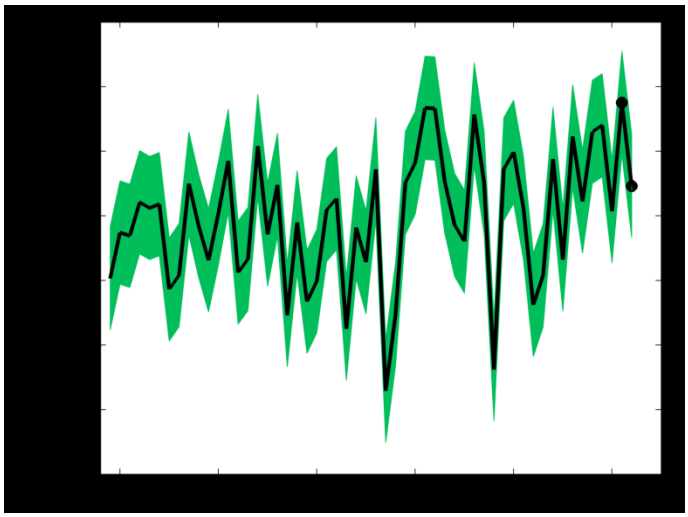

Figure 4: Land sink: average from calculations of five different models (Le Quéré et al., 2013).

In comparison to oceans, the land surface is very heterogeneous with a large variety of ecosystems. The amount of carbon that is exchanged between the atmosphere and the terrestrial biosphere varies not only in time but also in space. Thus, the up-scaling from regional to continental or even global scale of the global carbon balance is very difficult over the land surface, due to its high degree of heterogeneity. For this reason there is a high demand for CO_2 flux-data over every kind of ecosystem and a need for a global network of CO_2-flux measurements, in addition to inventory data, remote sensing, terrestrial biosphere models, or a global air sampling network.

The eddy covariance (EC) method is a well approved tool to quantify the carbon exchange between biosphere and atmosphere at the ecosystem scale (Baldocchi, 2003; Canadell et al., 2000). By capturing the net exchange of matter of a relatively large area (up to ≈ 1km²) from measurements at a single point, the eddy covariance technique is the most direct flux measurement at this scale. To be able to obtain more and better flux datasets, regional networks of flux observation stations, each estimating exchange of carbon, water vapor, and energy at the ecosystem scale, were established – globally coordinated in the FLUXNET project. The scope of this “network of networks” is to collect flux-data in all kinds of ecosystems, providing a database for synthesis and modeling. This dataset enables, for instance, comparisons across environmental gradients and across biomes. Results from this global project lead, on the one hand, to a better understanding of processes at the ecosystem level, on the other hand they can be used to validate and improve existing models. Both applications provide a basis for constraining the uncertainty in estimating carbon exchange of different compartments in the terrestrial carbon cycle (Friend et al., 2007).

However, datasets on carbon exchange are available primarily for more or less undisturbed terrestrial ecosystems (mostly forests or grasslands) so far (Bolin et al., 2000; Friend et al., 2007; Prentice et al., 2002). One reason for this is that disturbed ecosystems usually are very heterogeneous, which makes it difficult to conduct representative measurements for large areas. Another reason is that disturbed ecosystems often are located in very remote areas and therefore are hard to access. Though, especially in forest ecosystems, any kind of disturbance can lead to a fast release of its stored carbon to the atmosphere. The above mentioned large inter-annual variability, as well as the

high uncertainty of the terrestrial carbon balance, is mainly caused by variations in temperature, precipitation and radiation, in part arising from El Niño-Southern Oscillation variability (Heimann and Reichstein, 2008; Le Quéré, 2010; Sarmiento et al., 2010), but disturbances, like fires or wind-storms, are likely partly responsible for it (Lindroth et al., 2009; Magnani et al., 2007). Large scale disturbances can change not only the magnitude, but also the sign of carbon fluxes for extended time periods (Canadell et al., 2000). With respect to carbon exchange there is a need to increase the knowledge about the timing, location and magnitude of ecosystem disturbances for better understanding and reducing uncertainty of regional carbon cycles (Canadell et al., 2000; Potter et al., 2003).

1.2 Terrestrial carbon balance and ecosystem disturbances

Running (2008) stated that results from the FLUXNET community (Figure 5), showed that "disturbance was the primary mechanism that changes ecosystems from carbon sinks to carbon sources".

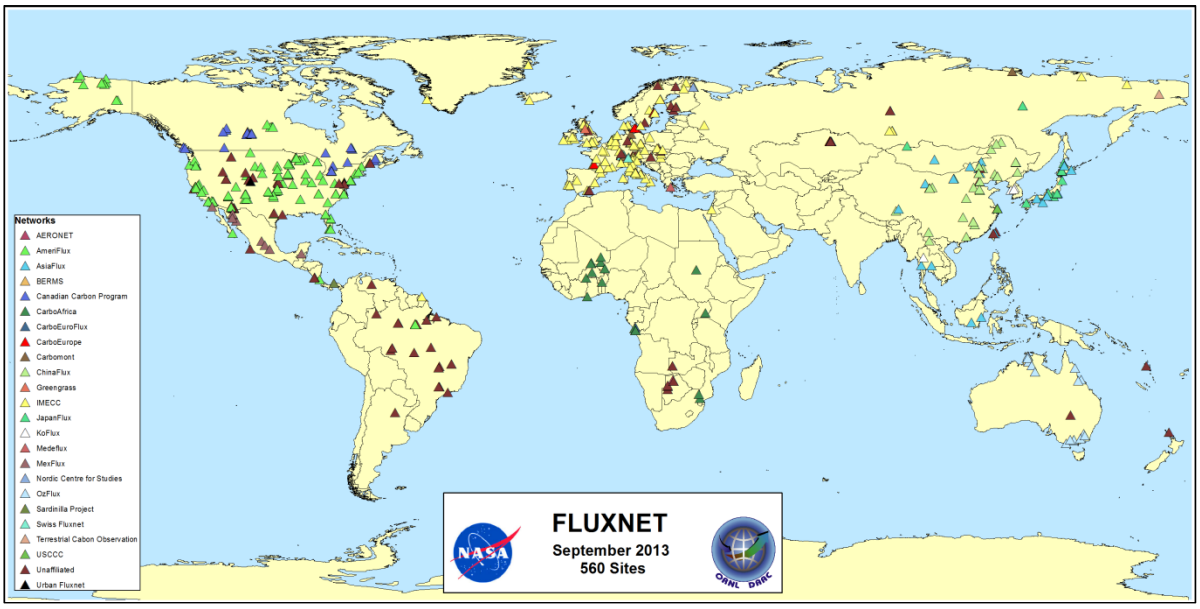

Figure 5: Location of the CO_2 flux observation sites that are part of the FLUXNET network (source: www.fluxnet.ornl.gov accessed: December 2013)

Areas with wind-throw events, for instance, where dead wood remains on the ground, may turn into a substantial carbon source for extended periods, in contrast to the general carbon sink behavior of even mature intact forest ecosystems (Knohl et al., 2002; Lindroth et al., 2009; Schulze et al., 1999). On the other hand, nutrients provided by dead wood may accelerate the process of re-growth, so the non-cleared wind-throw could become a net carbon sink again faster than a cleared wind-throw area. Ulanova (2000) stated that tree uprooting plays an important role in “maintaining stable tree and grass population structures in forest communities” and that “spruce regenerated better on mounds and fallen trees than on undisturbed surfaces”.

This would be of high importance for forest management in terms of carbon exchange (Kozlowski, 2002). Peters et al. (2012) stated that “moderate frequency disturbances are a relatively less important control on productivity than climate, soil, and species traits”. However, disturbance-caused damage of forest ecosystems, in particular from wind-storms, insect infestation, and wildfires is expected to increase in the future, due to climate change (Moore and Allard, 2011; Overpeck et al., 1990), and can have strong effects on terrestrial carbon exchange (Donat et al., 2011; Liu et al., 2011; Luyssaert et al., 2008; Running, 2008; Schelhaas et al., 2010; Seidl et al., 2011).

Thus, within the big picture of the carbon cycle, the importance of disturbance is far from negligible. Chen et al. (2004) write: “There is a critical need for predicting net carbon exchange under different disturbance regimes and at different stages of development”. In summary, there is still a lack of knowledge about carbon exchange in disturbed forest ecosystems, and in non-cleared wind-throw-disturbed forest ecosystem in particular, due to the scarcity of available datasets. To our knowledge, the only published reports to date refer to short time-period measurements in Siberia and Sweden (Knohl et al., 2002; Lindroth et al., 2009). As a result of this knowledge gap, most current models do not properly account for ecosystem disturbances and land management impacts.

1.3 What is a “disturbance”?

Because of its importance to the present work, the expression “ecological disturbance” will be shortly discussed and the terms defined here.

Ecological disturbance has been defined as “a temporary change in average environmental conditions that causes a pronounced change in an ecosystem. Outside disturbance forces often act quickly and with great effect, sometimes resulting in the removal of large amounts of biomass. Ecological disturbances include fires, flooding, wind-storm, insect outbreaks, as well as anthropogenic disturbances such as forest clearing and the introduction of exotic species” (Dale et al., 2001)“. Another definition describes disturbance as “a cause; a physical force, agent, or process, either abiotic or biotic, causing a perturbation (which includes stress) in an ecological component or system; relative to a specified reference state and system; defined by specific characteristics” (Rykiel, 1985). Pickett et al. (1999) and Picket and White (1985) defined environmental disturbance as a relatively discrete event in time and space that alters the structure of populations, communities, and ecosystems and causes changes in resource availability or the physical environment.

All these definitions are somewhat vague. What are average environmental conditions? How to specify a reference state or system? That is, what are the specific characteristics of the ecosystem? What makes a change pronounced? How long is temporary?

It is evidently not easy to find a precise and universal definition of disturbance. Stand-killing insect outbreaks, for instance, usually quantify as disturbance with these definitions, whereas low intensity herbivory is commonly treated as average condition or steady state of an ecosystem. However, there is a continuum of intensity ranging from infestation (clearly a disturbance) to herbivory (clearly not). The question is where to set the threshold for disturbance. Thus, a clear definition of disturbance can only be given in context of the average environmental conditions, and furthermore one has to keep in mind that "disturbance is clearly not an external event that happens to an ecosystem. Like other interactive controls, disturbance is an integral part of the functioning of all ecosystems that responds to and affects most ecosystem processes" (Chapin et al., 2002). The trigger of disturbance may be external (e.g., a wind-storm), but whether a given trigger causes a disturbance depends on the state and functioning of the ecosystem (see also: Angelstam and Kuulivainen, 2004).

Even if we cannot define ecosystem disturbances precisely, perhaps one can classify them in conceptual framework.

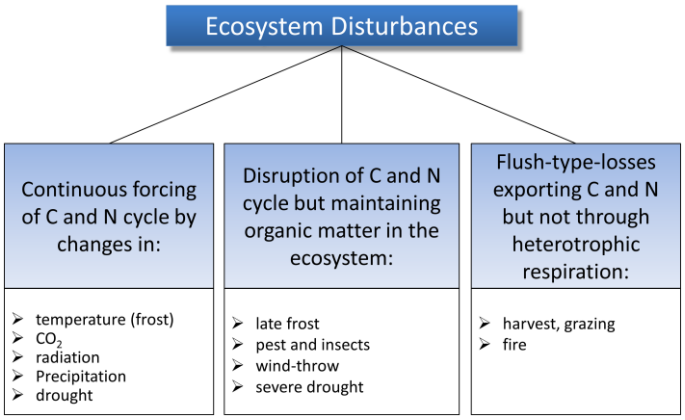

Figure 6: Classification of ecosystem disturbances with respect to effects on the carbon and nitrogen cycle. (modified from: Schulze et al., 1999)

Figure 6 shows ecosystem disturbance classified in terms of carbon and nitrogen exchange (Schulze et al., 1999). In the left box changes of, for instance, temperature, or radiation lead to a continuous forcing of the C and N cycle. In the right box disturbances like fire or harvest lead to a rapid export pulse of carbon and nitrogen out of the ecosystem, but not through comparatively slow heterotrophic respiration. The box in the middle refers to disturbances like insect outbreak or wind-throw. If an ecosystem has been hit by such a disturbance its carbon and nitrogen cycle is disrupted, but all biomass remains on site (although the carbon and nutrients contained in the dead biomass may not be available for re-growth for many years). As mentioned above, these boxes are maybe somewhat permeable and it is very difficult to define clear borders between them. For example, if it lasts too long or is too intense, a continuous forcing may lead to a severe stand replacing disturbance event, where C and N cycle are disrupted. Again, the difficulty is to define the border between forcing and disruption of C and N cycle. It becomes obvious that classification of ecosystem disturbance is very difficult also due to the lack of a clear and sharp border between biotic or abiotic forcing and severe ecosystem disturbance.

Globally, the most important ecosystem disturbances are caused by biotic forcings. In 2005 about 40 million hectares were affected by insects and diseases worldwide (FAO, 2010). Next to these biotic disturbances fire plays a major role and affected ca. 20 million hectares in 2005. About 8 million hectares were affected by other abiotic disturbances, like wind-throw (also see: Moore and Allard, 2011).

However, these values are mostly based on very sparse data. For Europe, where forestry is of high economic importance, severe wind-storms are seen to be at least as important as fire or insect-outbreaks (FAO, 2010; Gardiner et al., 2010).

1.4 Main processes of carbon exchange in ecosystems and related terms

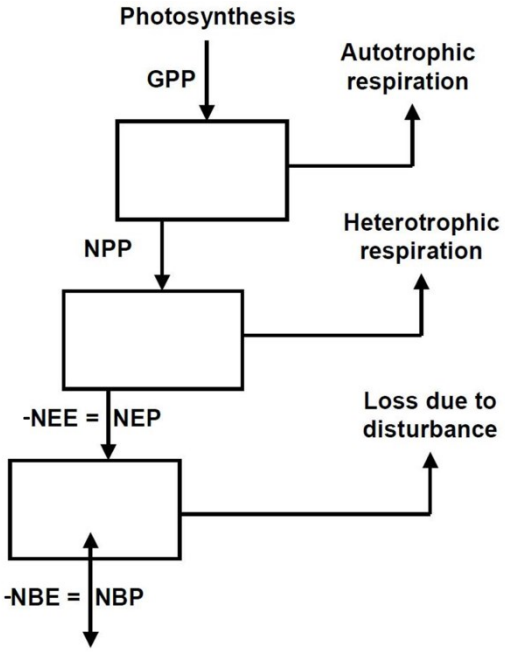

Figure 7: Flow-chart of ecological expressions in terms of carbon exchange within ecosystems. (Source: Kirschbaum et al., 2001)

In this section some ecological terms usually used in carbon accounting are defined (see Figure 7).

Gross primary production (GPP) stands for the amount of carbon in plants fixed by the process of photosynthesis at ecosystem scale (Chapin et al., 2002). Sometimes the term GEP (gross ecosystem production) is also used. GEP is defined as GPP minus plant respiration (Schmid et al., 2000). Autotrophic respiration (R_a) denotes the loss of carbon by internal plant metabolism. The difference between GPP and R_a results in the net primary production (NPP). Heterotrophic respiration (R_h) is the amount of carbon which is lost by other organisms than plants (primary producers) including carbon release through decomposition of dead trees, and coarse woody debris (CWD). The difference between NPP and R_h is the net ecosystem production (NEP) or net ecosystem exchange (NEE). NEE and NEP are different only in terms of the reference medium. For net ecosystem production the reference medium is the biosphere. Thus, positive NEP means net carbon gain to the ecosystem. For NEE the reference medium is the atmosphere. Thus, positive NEE means net carbon emission or upward directed flux. In other words: NEP = -NEE. Furthermore, NEE is usually used for describing fluxes on a half-hourly or hourly basis, while the integrated carbon exchange of one year or longer is expressed by NEP. Schulze and Heimann (1998) proposed another expression called net biome production/exchange (NBP/NBE) to take carbon losses through disturbance (L_D) also into account (NBP = NEP – L_D). In this context disturbance is related to so-called flush type disturbances (e.g., fire or harvest) where heterotrophic respiration is bypassed.

However, the expression NBE might not only be connected to these so called flush-type disturbances. “Biome is a general class of ecosystems” (Chapin et al., 2002) and is often identified with particular patterns of ecological succession and climax vegetation including natural mortality. A biome is therefore the quasi-equilibrium state of the local ecosystem and, as such, mainly a theoretical concept.

“An ecosystem consists of a biological community with its abiotic environment, interacting as a system” (Chapin et al., 2006). So with respect to the Bavarian Forest National Park there are several ecosystems at different successional stages. A recent wind-throw is next to an old growth forest ecosystem, and nearby there are ecosystems somewhere in between these classes. All these ecosystems differ in structure, flora and fauna, nutrient availability, but are within the same biome. In terms of carbon exchange this means that the NEE of an ecosystem generally represents only a single stone in the mosaic of the whole biome. To estimate NBE, one needs to measure either for a very long time, or in all ecosystems of the biome. So, to get information of NBP one has to measure either long enough or over sufficiently large areas. The question is how long is long enough, or how large is large enough?

1.5 Conceptual framework of the carbon balance development at ecosystem scale

Odum (1969) published a hypothesis of ecosystem development, where a forest is a strong carbon sink at the early stage of succession or growth. Then, after reaching a maximum, the sink strength of the forest decreases until the now old-growth mature forest reaches some sort of equilibrium where uptake through photosynthesis equals loss through respiration (see Figure 8).

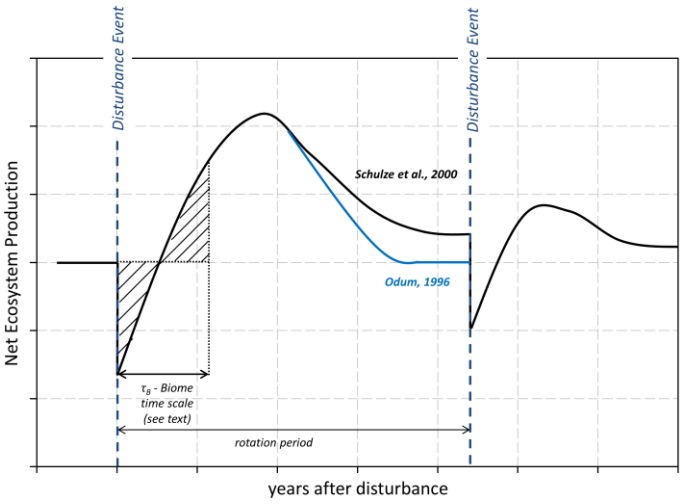

Figure 8: Conceptual framework of forest carbon balance development based on Odum (1969) and Schulze et al. (2000). The hashed area defines the biome time-scale used in the present work, but assumes that the initial disturbance is a stand-replacing disturbance (see text).

In contrast, Schulze et al. (2000) postulate that terrestrial forest ecosystems do not equilibrate (at least not in an instantaneous sense), but continue as small net carbon sinks over consecutive rotations of stages as sinks and sources over long periods of time. The relevant mechanism is that more and more carbon is transferred from intermediate pools (carbohydrates, leaves) to permanent pools (passive soil organic matter, black carbon) during every rotation period. A rotation period lasts from one disturbance event to the next. The longer the rotation period lasts, the more carbon is stored in permanent pools, as Schulze et al. (2000) further claim. However, the predicted increase of severe disturbance events due

to climate change could lead to an opposite situation. If the rotation periods are too short, maybe some ecosystems switch from long-term net carbon sinks to net carbon sources.

Actually, these two mentioned scenarios of carbon balance development after disturbance are not universal. As Goetz et al. (2012) notes, “the time of zero crossing, the peak uptake and its timing, and the time a new equilibrium is reached vary considerably for boreal, temperate conifer, temperate broadleaf and other forest types…”. In Addition, there can also be large differences in type and severity of disturbance (also see Thornton et al., 2002). This means, that the shape of the curve in Figure 8 likely looks different for different ecosystems which are hit by the same disturbance, and it also likely looks different for the same ecosystems that are hit by different types of disturbance.

Many researchers have therefore tried to test these hypotheses with estimated annual carbon exchange e.g., with inventory data or eddy covariance data. Mostly they used the chronosequence approach with data from roughly same ecosystems but different age and succession stage respectively (Bond-Lamberty et al., 2004; Gough et al., 2008; Howard et al., 2004; Janisch and Harmon, 2002; Law et al., 2003; Payeur-Poirier et al., 2012). Long-term Eddy Ccovariance measurements get more and more important in this respect (Baldocchi, 2003; Barford et al., 2001; Dragoni et al., 2011). As mentioned above, most of the available datasets of carbon exchange are from mature or old-growth more or less intact forests. With reference to Figure 8, there is much information about the middle and end of a rotation period, but we have only sparse knowledge about the behavior of an ecosystem immediately after disturbance. So, we have only little information about the beginning of a rotation period in Figure 8.

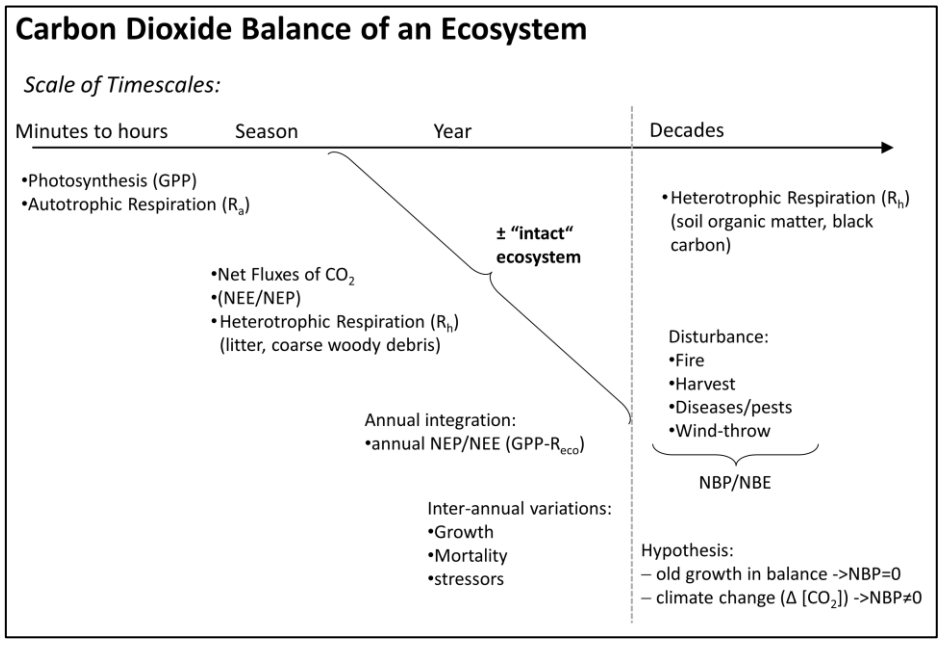

Figure 9: Processes affecting ecosystem/biome carbon balance over several timescales.

Figure 9 shows NEP regulating processes in terms of several time scales. Within the range of minutes to hours relevant processes are Photosynthesis (GPP), and autotrophic Respiration (R_a). Since the main procedure of calculating turbulent fluxes with eddy covariance usually contains block averaging, gap-filling also happens within this time interval. Considering longer time periods from season to year heterotrophic respiration of litter and CWD as well as the net flux (NEP/NEE) gets more important. Integrated net fluxes over such time periods can already reflect inter annual variations of an ecosystem like growth strength, mortality, stressors, and so on. After decades or so, the impact of disturbance events and of carbon pools with longer turnover times can be recognized wherefore the expression NBE/NBP has been proposed (Schulze and Heimann, 1998).

After the concept of Odum (1969) and Schulze et al. (2000), NBP of an ecosystem should be zero or even positive if time and space are large enough. However, if ecosystem disturbances occur more often, e.g., due to climate change, the next disturbance event may happen before the ecosystem is able to equilibrate. On the one hand, young emerging forests are usually large carbon sinks. But on the other hand, this does not necessarily compensate for carbon emissions from a disturbance that occurs too early. Thus, in ecosystems which are hit by disturbances more frequently, NBP would be no longer zero but negative (carbon source). Many ecosystems that are currently net carbon sinks, could therefore shift to net carbon sources within the next decades and remain like this for a very long time, depending on the frequency and intensity of disturbances. Similar illustrations of this conceptual framework can be found for example in Randerson et al. (2002), in IGBP Terrestrial Carbon Working Group (1998), in Ehman et al. (2002), in Nave et al. (2011), or in Schulze et al. (2000).

In this context we could think of another sort of timescale namely a “biome-timescale” τ_B (see Figure 8). The biome-timescale represents the period it takes for the ecosystem to re-gain the lost carbon due to a disturbance event. If disturbance events are spread shorter than τ_B, NBP is negative. In such cases the biome must change to a lower level over time.

Calculating exchange rates of CO_2 within time scales up to several years, we are often dealing with more or less intact ecosystems. However, disturbance history, as well as forest stand age, mainly influence the carbon exchange over longer time scales (Desai et al., 2005). It may take several decades, until an ecosystem is affected by episodic forcing like fire, harvest, wind-storm, and only by taking also such disturbance events into account one can get information of the overall Carbon Dioxide Balance of an ecosystem.

Therefore, up-scaling current available results of NEP and NBP respectively might not reflect long-term reality (Dragoni et al., 2011; Hommeltenberg et al., 2014) and could lead to an overestimation of global carbon sink strength (Dore et al., 2008; Körner, 2003).

There are several studies in the literature about eddy covariance measurements in disturbed forest ecosystems but only few about carbon exchange in wind-throw-disturbed forest ecosystems in particular. Amiro et al (2010) summarized results from more than 180 site years of EC measurements. Forest ecosystems were losses of Carbon following disturbance and shifted to carbon sinks after ten years in most cases, as they have found out. Fire disturbed coniferous forests in northern latitudes remain carbon sources for about 20-30 years, as hypothesized by Amiro et al. (2006) and confirmed by Dore et al. (2008). Results of a chronosequence of mixed deciduous forest in northern lower Michigan however (Gough et al., 2007) showed that the harvested and burned forest had become a net carbon sink even 6 years after disturbance event. Bond-Lamberty et al. (2004) estimated annual NEE using inventory data from a chronosequence of a boreal black spruce after wildfire. Their results implied that young stands are carbon sources of about 100 g C $m^{-2}yr^{-1}$, middle aged stands are carbon sinks with about -100 to -300 g C m^{-2} yr^{-1}, and old-growth stands are nearly carbon neutral. Lindroth et al. (2009) studied fluxes of CO_2 in two cleared wind-throw areas in Sweden after the Storm Gudrun and, after some modeling, stated that the wind-throws are large sources of carbon of about 897 to 1259 g C m^{-2} yr^{-1}. They mentioned that this efflux is mainly due to strong enhanced soil respiration caused by soil destruction through heavy machinery. This assumption could partly be confirmed by results from Knohl et al. (2002) who published results of 3-month eddy covariance measurements in a non-cleared wind-throw in the western Russian taiga. In this time period NEE was 180 g C m^{-2}, leading to an estimated annual NEE of about 400 g C m^{-2} yr^{-1}. Based on additional deadwood analysis, they projected that the non-cleared wind-throw will likely emit 100 g C m^{-2} yr^{-1} even 30 years after disturbance.

As can be seen, there is a strong demand for more, and particularly long-term, NEP measurements in disturbed forest ecosystems to adequately consider the impact of disturbance on regional carbon balance (Amiro, 2001; Law et al., 2002; Lindroth et al., 2009; Pregitzer and Euskirchen, 2004). According to non-cleared wind-throws the only available dataset of net ecosystem exchange is three months in duration (Knohl et al., 2002).

In summary, there is a high demand for CO_2-fluxdata of disturbed forests to better understand the source and sink relationship of different ecosystems (Canadell et al., 2010; Potter et al., 2003). Additionally extreme weather situations like wind-storms have increased since past years and will further increase in the future as a result of climate change (Dale et al., 2000; Moore and Allard, 2011; Schelhaas et al., 2003; Seidl et al., 2011). For these reasons this work investigates the ecosystem-atmosphere exchange over a wind-throw-disturbed upland spruce forest in the Bavarian Forest National Park.

1.6 Research questions

The overall objective of the study is to examine how the disturbance and the recovery from it affect the carbon cycling of this forest ecosystem. To this end CO_2 exchange (net ecosystem exchange – NEE) was measured by eddy covariance and combined with an ecosystem exchange model that includes dynamic vegetation.

The overall long-term question of this research is: How does this wind-throw-disturbed ecosystem behave after disturbance in terms of carbon exchange? Within this question it is also interesting, for instance, how long it will take the ecosystem to switch from carbon source to net carbon sink again.

Answering this overall long-term question is beyond the scope of this work. However, there are other important sub-questions which this study intends to address in this context:

- How large is the CO_2 efflux from the wind-throw area after the storm event?
- This net CO_2 exchange can be separated into gross ecosystem production (GEP) and ecosystem respiration (R_{eco}). How large are these component fluxes and…
- How do the dynamics of R_{eco} and GEP behave within the measurement period?
- What is the behavior of the carbon balance development predicted over the next 10 years and beyond by model simulations of a physical cohort model?

2 Site and Methods

2.1 Geography and ecological description

Measurements were taken within the Bavarian Forest National Park (BFNP) in the eastern part of Bavaria, Germany close to the border of the Czech Republic (see Figure 10 and Figure 11). Together with the adjacent Czech Sumava National Park it forms the biggest contiguous forest (approximately 1000 km²) within Europe. Its elevation ranges from 300 m up to over 1400 m a.s.l.

Figure 10: The study site in the Bavarian Forest National Park on the border between Germany and the Czech Republic (red arrow) modified, based on www.weltkarte.com.

On January 18th/19th, 2007, cyclonic storm Kyrill caused extensive damage over a broad swath of Europe. 62 million trees were uprooted or damaged respectively in central Europe during these two days (Fink et al., 2009). Within the BFNP storm Kyrill caused about 160 thousand m³ of deadwood (BFNP 2008, Jahresbericht 2007; www.nationalpark-bayerischer-wald.bayern.de). Figure 11 shows one extensive wind-throw area on Lackenberg before and after the event. At 1337m elevation, the Lackenberg is one of the highest mountains of the national park. In this area Kyrill has devastated about 30ha of forest and almost all trees were uprooted. Also shown in Figure 11 are aerial photographs of the study site from 2009 to 2011 where the impact of the storm can clearly be seen. Despite the policy of conservative forest management, the administration of the national park logged of a small zone around the wind-throw area in 2009, to protect the surrounding forest from bark-beetle infestation (also see Figure 11). Fortunately, this does not have any influence on the measurement quality at the study site (see section 2.4.2).

The terrain slopes from north to south (≈9◦). The pre-storm forest was about 150 years old (BFNP Administration, personal communication) with a tree density of approximately 1000 trees ha^{-1}. Average height was about 18 m and average girth was about 1.5 m (estimated from aerial photography and a survey of fallen trees). The number of new seedlings after the storm was estimated at about 2500 seedlings ha^{-1} (stem count in July 2010). The present vegetation mainly consists of Norway spruce (*Picea abies* (L.) H. Karst) even though at the Lackenberg site only few individuals of this species have survived the storm Kyrill. However, many new seedlings have since emerged almost everywhere between the fallen trees (see Figure 12). The other live vegetation is dominated by grasses (*Deschampsia flexuosa* (L.) Trin, *Luzula sylvatica* (Huds.) Gaudin, *Juncus effuses* (L.), fern (*Athyrium*

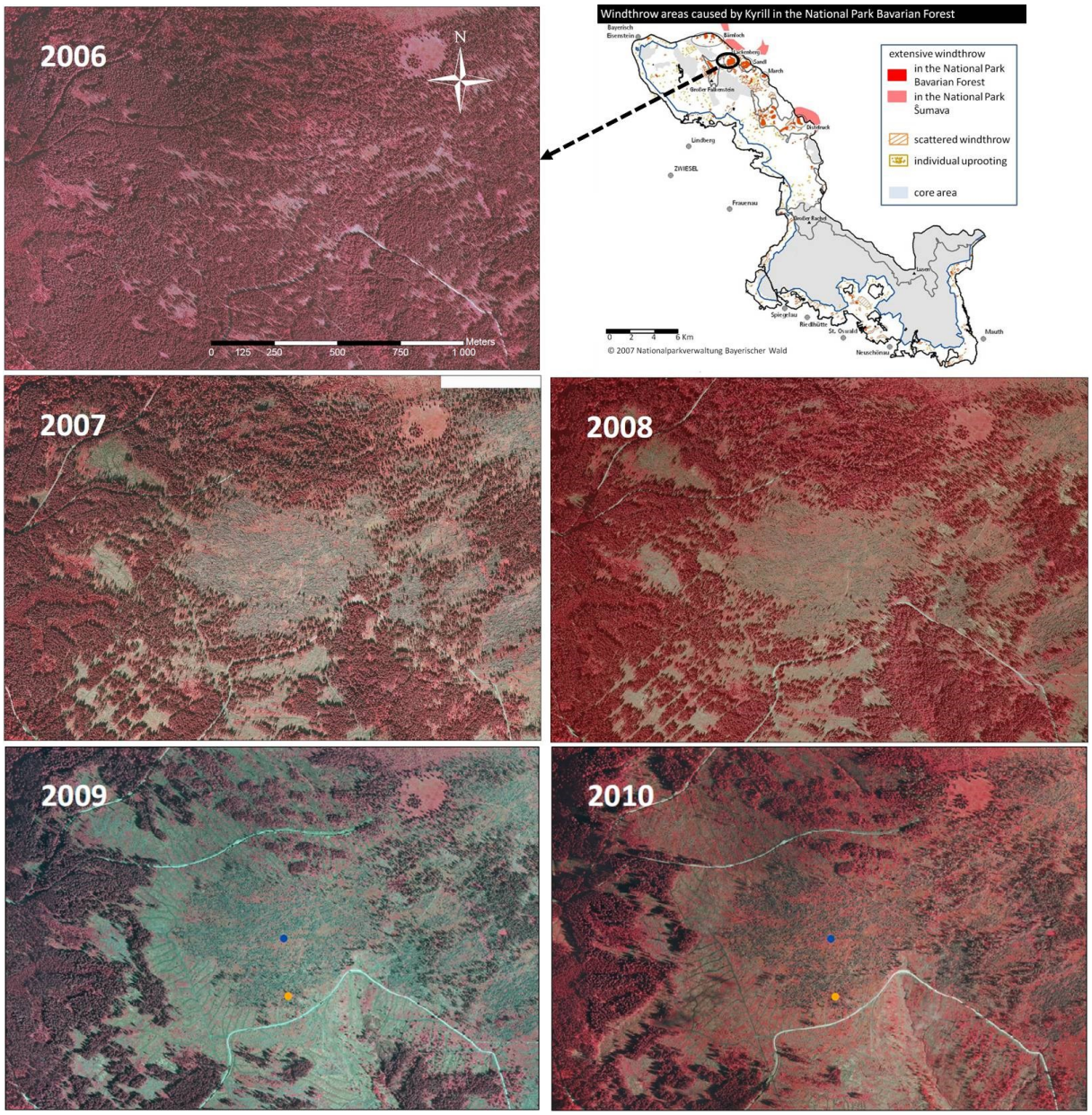

Figure 11: Chronosequence of the Lackenberg site from 2006 until 2010. Blue and orange point is the position of the main tower and satellite tower, respectively (red channel has been replaced by near-infrared). Upper right shows wind-throw areas caused by Kyrill in the Bavarian Forest National Park. (Source: Administration of the Bavarian Forest National Park)

disten-tifolium Tausch ex Opiz), few blue berries (*Vaccinium myrtillus* L.), and very few rowan berries (*Sorbus aucuparia* L.). The vegetation period roughly lasts from May to August. The snow cover period usually extends from November to March but can also last from September to May in some years. For a more detailed discussion of the vegetation period, see section 3.2.1.2. The Diameter of the root-plates from the uprooted trees, which is 2 m on average, was taken as the typical height of roughness elements, because most remaining and new emerging vegetation does not exceed this height yet. Predominant soil types in this region are Typic Dystrudepts (Dystric Cambisols),Andic Dystrudepts (Dystric Cambisols with low bulk density), and Entic Haplorthods (Entic Podzols) (Späth, 2010; Spielvogel et al., 2006). Soils at Lackenberg are well drained and not very deep, with the available root zone rarely exceeding 50–100 cm depth (also see section 3.1).

Figure 12: New emerging vegetation between fallen uprooted trees (Photo: M. Lindauer)

As explained in the introduction, this area is very well suited for conducting long-term measurements of carbon and energy exchange within a disturbed forest ecosystem. Thus, the measurement tower for this study was installed in the middle of this large wind-throw area (30 ha, 49.100°N, 13.305°O; 1308 m a.s.l.) at the beginning of 2009. For reference measurements of several parameters an additional tower (satellite tower) was installed ca. 200 m south of the main tower (49.098°N, 13.305°O; 1269 m a.s.l.). The positions of the main tower (blue dot) and the satellite tower (orange dot) are shown in Figure 11.

2.2 Climatological description

"Three-quarters of the year it is wet and one-quarter of the year it is cold!" This is how the vernacular describes the climate of the BFNP. Of course this is not the whole truth, as the climate of this region is quite varied and mainly depends on the altitude. Table 2 shows annual mean air temperatures, annual sums of precipitation and sunshine duration measured at two meteorological stations of the German Weather Service (DWD) in the vicinities, as well as temperature and rain amount at the Lackenberg site. Both DWD stations are located very close to the Bavarian Forest National Park and close to the measurement site but are at different altitudes. As expected, the climate at the lower station is warmer and drier than at the higher station. Measured precipitation at the Lackenberg site does not contain the amount of solid precipitation, because the type of precipitation gauge used is not able to gauge snowfall (see section 2.3).

Table 2: Climatic parameters of two German Weather Service (DWD) stations and at the Lackenberg site (sunshine duration was not measured at the study site)

	Großer Arber	Zwiesel	Lackenberg
latitude	49.114° N	49.029° N	49.100
longitude	13.135° O	13.240° O	13.305
altitude	1436 m	615 m	1308 m
distance to Lackenberg	ca. 12.2km	ca. 10.5km	-
air temperature (mean)			
2009	3.78°C	6.53°C	4.81
2010	2.52°C	6.41°C	3.43
2011	4.60°C	7.76°C	5.48
2012	3.73°C	7.34°C	4.73
2013	3.30°C	7.22°C	4.28
Precipitation (sum)			*only rain!*
2009	1538 mm	1166 mm	480 mm
2010	1493 mm	1003 mm	653 mm
2011	1315 mm	1036 mm	600 mm
2012	1439 mm	1245 mm	1001 mm
2013	1410 mm	1031 mm	729 mm
sunshine duration (sum)			
2009	1534 h	1724 h	-
2010	1412 h	1486 h	-
2011	1935 h	1939 h	-
2012	1736 h	1815 h	-
2013	1417 h	1371 h	-

The region is located within the transitional-zone from maritime to continental climate. Continental influence is reflected in dry and cold conditions in winter, with temperature minima often down to -25 °C or less in some locations (Elling et al., 1987). Summers are typically dry and warm, with occasional thunderstorms in the uplands. The Central German Uplands in the south-eastern part of Bavaria where the BFNP is located, are a barrier for the moist westerly air. Maritime influence leads to annual precipitation from 600-700 mm in the valleys and up to 1400-1800 mm or even more in the higher altitudes causing abundant snowfall in winter (ca. 30-40% of the annual precipitation is snow).

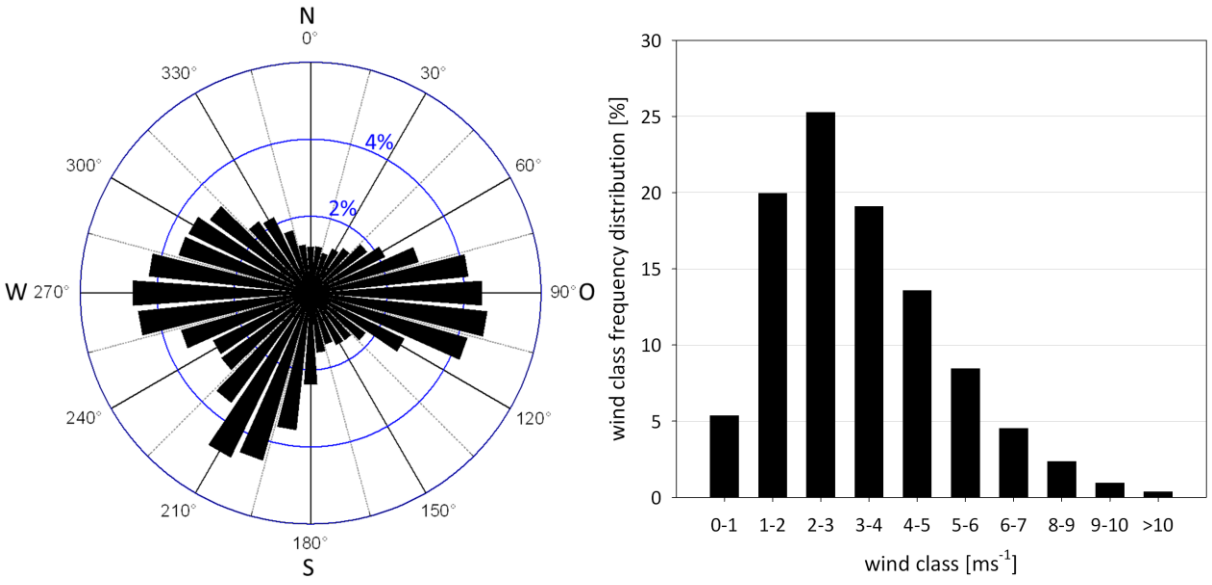

Figure 13: Distribution of wind direction (left) and wind class frequency distribution at the Lackenberg site (9m) estimated from measured half-hourly values 2009 – 2011.

Snow depths of 2 m or higher are not unusual, and hence, the region is very popular for its richness in snow - in these uplands the snow cover period can last seven months and more. Annual average temperatures of the region are 3 to 4 °C in the uplands, and 6.5 to 8°C in the lower parts. Regional cold-air-pools causing temperatures below 0°C in the morning of even early summer days are characteristic for the BFNP in the lower regions (Elling et al., 1987). An evaluation of wind measurements at the Lackenberg site from 2009-2011, show that prevailing wind directions are west to south-west, except for continental weather conditions when wind is blowing from easterly directions. Wind speeds mainly range from 1 to 5 m s^{-1} (half-hourly averages) but gusts of up to 60 m s^{-1} were detected within the measured 10-minute averages (Figure 13).

Figure 14 shows time series plots of measured air temperature, net radiation and rain amount from the Lackenberg site from 2009 to 2013. Missing values (blue) of air temperature were filled either with data from the satellite tower or with data from a meteorological station on top of the nearby hill Großer Falkenstein (49.086 °N, 13.282 °E, 1307 m a.s.l. distance to Lackenberg ca. 2 km, data provided by BFNP Administration). Temperatures fell beneath -20 °C and less in winter and went up to 25°C or more in summer within the measurement period. Measured rain amount only shows liquid precipitation, as the sensor used is not able to measure snowfall adequately (Section 2.3). Missing values of rain amount were filled with data from the satellite station. Unfortunately there is no

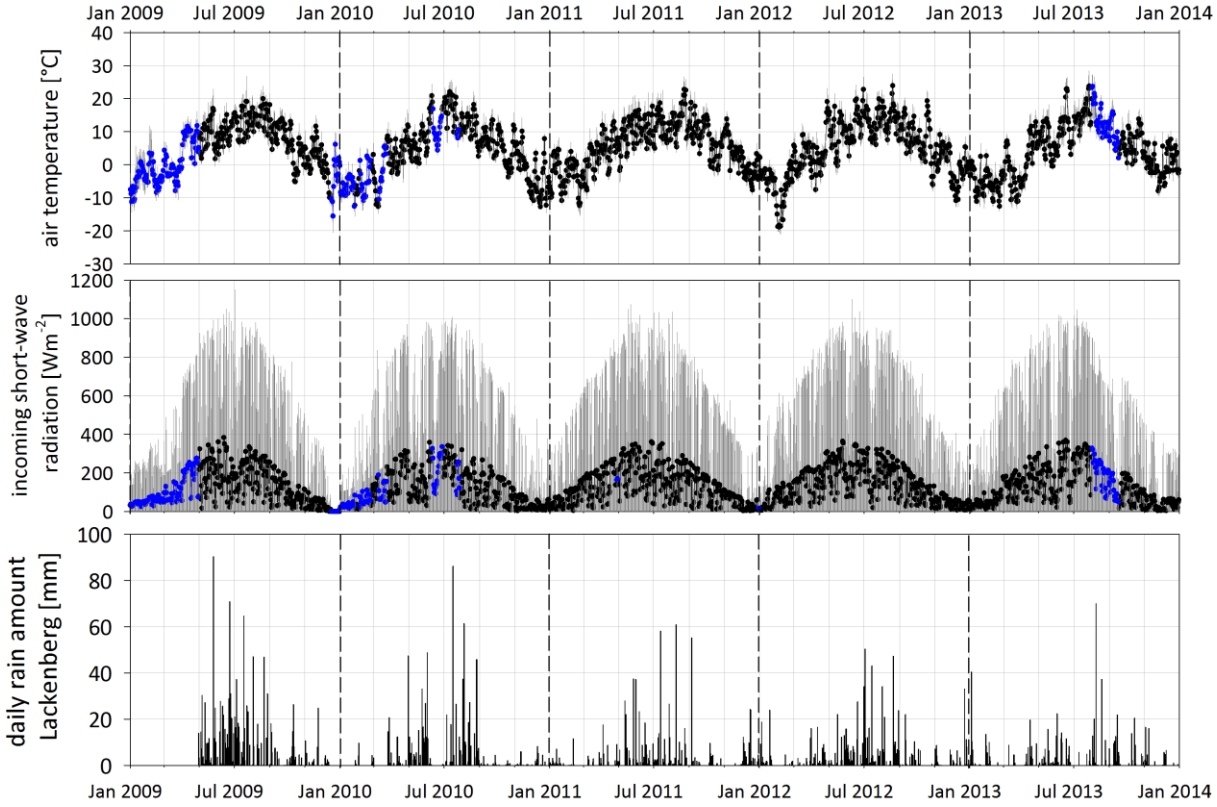

Figure 14: Daily mean values of air temperature (6m) and incoming short-wave radiation. Gray bars indicate range of values (max/min). The lower graph shows daily rain amount (solid precipitation could not be detected by the used sensor). Blue color indicates missing values substituted with data from nearby weather station or modeled values (see text).

sensor for incoming short-wave radiation installed at the satellite tower or at meteorological stations in the surrounding area. Thus, the incoming short-wave radiation was modeled based on calculated extra-atmospheric radiation and using an empirical relationship between atmospheric turbidity and relative humidity. The procedure is described in detail in Section 3.1.

2.3 Instrumentation

The main Tower at the Lackenberg site is shown in Figure 15. It is 9 m high and is made of hot-dip galvanized steel. The eddy covariance (EC) system consists of a CSAT3 sonic anemometer (Campbell Scientific, Logan, UT, USA) for measuring three dimensional wind components and sonic temperature and an open path infra-red gas analyzer (IRGA) LI-7500 (Li-Cor, Lincoln, NE, USA) for measuring volumetric concentrations of CO_2 and water vapor. LI7500 IRGA was calibrated regularly every 4 to 8 weeks by the zero and span calibration procedure recommended by the manufacturer. Zero CO_2 and H_2O concentration was calibrated with a standard mixture of synthetic dry air from Air Liquide Paris, France). CO_2 span was calibrated with a CO_2 standard (delivered from Deuste Steiniger GmbH, Mühlhausen, Germany), containing 381 ppm CO_2 ± 0.5%. H_2O span was determined using a dew point generator Li610 (Li-Cor), which was referenced to an optical dew point sensor Hygro-M3 (General Eastern, Woburn, MA, USA). The EC sensors were mounted on top of the 9 m tower, together with an HMP45 (Vaisala, Vantaa, Finland) for measuring relative humidity and air temperature in a passively ventilated shield. Wind profile measurements (wind speed and direction) were performed by three two-dimensional sonic anemometers at 0.8 m (WMT52), 2.5 m (WMT52), and 6 m (WXT520) height (all three sensors are from Vaisala). The WXT520 at 6 m also contains integrated sensors for air temperature, relative humidity, rain intensity, and air pressure. A four component net radiometer CNR 1 (Kipp&Zonen, Delft, The Netherlands) was also installed at 9 m height together with a Li-190 (Li-Cor) for measuring photosynthetically active photon flux density (PPFD). Surface radiation temperature was measured with an infra-red remote temperature sensor IR120 (Campbell Scientific), mounted at about 6 m height. Instruments for soil measurements included TCAV-L averaging Soil Temperature Probes, CS616 Water Content Reflectometer (both from Campbell Scientific), and two HFP01SC Soil Heat Flux Plates (Hukseflux, Delft, The Netherlands). Sensors for soil temperature and soil volumetric water content were installed at 4 cm depth, and the soil heat flux plates were installed at 8 cm depth. A Garmin 16-HVS GPS Receiver (Garmin, Olathe, KS, USA) was used for exact time synchronization of all measurements. Data logging was done by a CR3000 micro logger (Campbell) and data were additionally stored on a MSEP800/L minicomputer (Kontron, Eching/München, Germany). Power was supplied by 12V batteries which were charged either by solar panels or by fuel cells (Udomi, Neuenstein, Germany).

As mentioned above, for reference meteorological measurements a satellite tower (49.098°N, 13.305°O, 1269m a.s.l.) was installed ca. 200 m south of the main tower. Another WXT520 (Vaisala) sensor, measuring air temperature, relative humidity, air pressure, wind speed, wind direction, and rain intensity was mounted on top of this 9 m high satellite tower. All instruments, the measured parameters, and their temporal resolution are summarized in Table 3

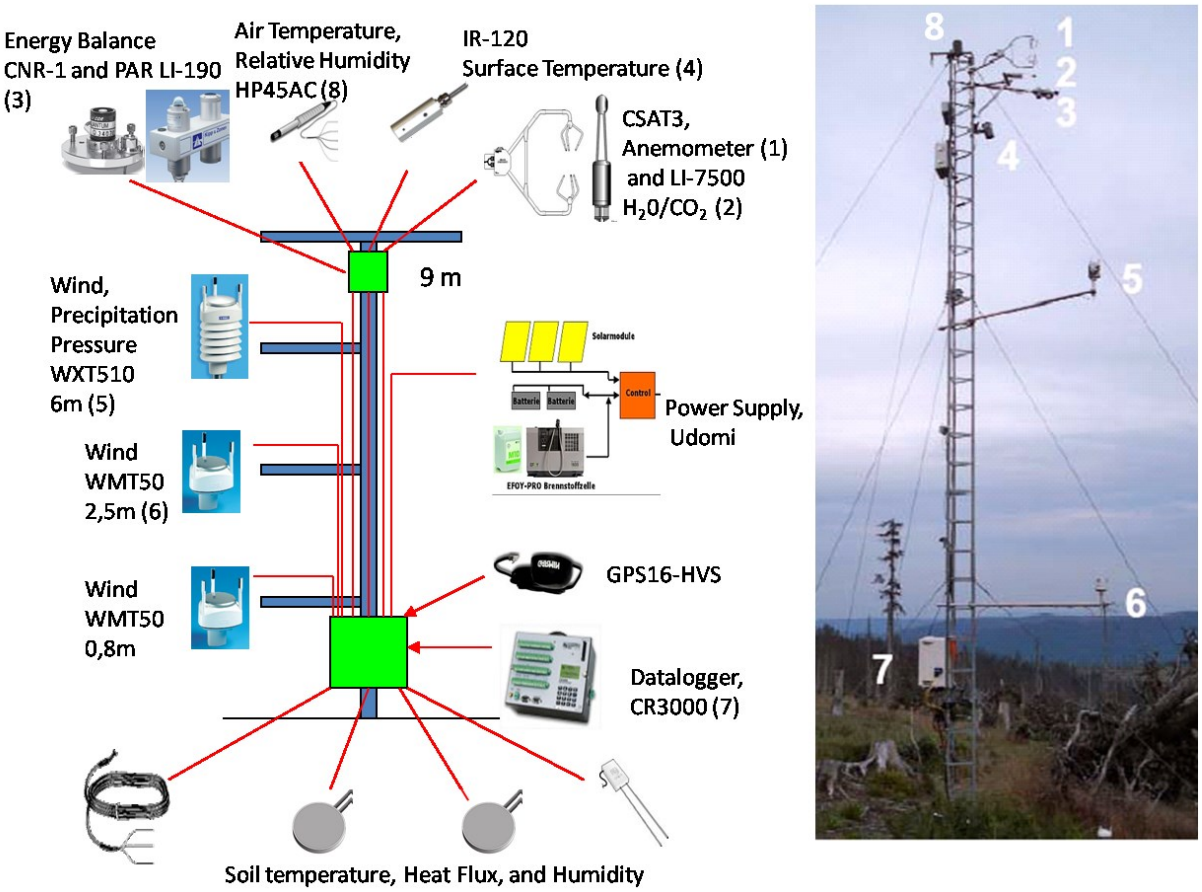

Figure 15: Measurement tower at the Lackenberg site (main tower) with instrumentation. (Photo: B. Wolpert). For Details of the instruments see Table 3

Table 3: Measured parameters with unit, temporal resolution, height, notation, and manufacturer

Parameter	Unit	Temporal resolution	Sensor height	Instrument	Company
3-d wind components	$m\ s^{-1}$	10 Hz	9m	CSAT-3	Campbell
H_2O	$g\ m^{-3}$	10 Hz	9m	LI-7500	LI-COR
CO_2	$mg\ m^{-3}$	10 Hz	9m	LI-7500	LI-COR
air temperature	°C	10 Hz	9m	HMP 45 C	Vaisala
relative air humidity	%	10 Hz	9m	HMP 45 C	Vaisala
radiation	$W\ m^{-2}$	10 min	9m	CNR 1	Kipp&Zonen
photosynthetically active radiation	$\mu mol\ m^{-2}s^{-1}$	10 min	6m	LI-190	LI-COR
surface radiation temperature	°C	10 min	6m	IR 120	Campbell
air temperature	°C	10 min	6m	WXT 520	Vaisala
relative air humidity	%	10 min	6m	WXT 520	Vaisala
precipitation	mmh^{-1}	10 min	6m	WXT 520	Vaisala
air pressure	mbar	10 min	6m	WXT 520	Vaisala
wind direction	°	10 min	6m	WXT 520	Vaisala
wind speed	$m\ s^{-1}$	10 min	6m	WXT 520	Vaisala
2x wind direction	°	10 min	2.5m/0.8m	WMT 50	Vaisala
2x wind speed	$m\ s^{-1}$	10 min	2.5m/0.8m	WMT 50	Vaisala
soil temperature	°C	10 min	-0.04m	TCAV-L	Campbell
soil heat flux	$W\ m^{-2}$	10 min	-0.08m	HFP 01 SC	Hukseflux
soil volumetric water content	%	10 min	-0.04m	CS 616-L	Campbell
time leveling /coordinates				GPS 16HVS	Garmin
data acquisition				CR3000	Campbell
Satellite tower:					
air temperature	°C	10 min	9m	WXT 520	Vaisala
relative air humidity	%	10 min	9m	WXT 520	Vaisala
precipitation	mmh^{-1}	10 min	9m	WXT 520	Vaisala
air pressure	mbar	10 min	9m	WXT 520	Vaisala
wind direction	°	10 min	9m	WXT 520	Vaisala
wind speed	$m\ s^{-1}$	10 min	9m	WXT 520	Vaisala

2.4 Eddy covariance

The eddy covariance (EC) technique uses fast measurements (10-50Hz) of vertical wind velocity and mixing ratios of trace gases (e.g., CO_2) to calculate the net exchange of such trace gases between the atmosphere and the biosphere on an ecosystem scale (Kaimal and Finnigan, 1994). The usual average period for the calculated covariance is half an hour or an hour. In this work we used half an hour as averaging period. Ideally, summing up such half-hourly values over one year yields the net carbon dioxide balance of the ecosystem or net ecosystem productivity (see Section 1.4). Thus, with measurements at a single point, one can – with some assumptions – estimate the net exchange at the ecosystem scale. As already explained in Section 1.1, the eddy covariance method has gained more and more attention for estimating trace gas exchange over various ecosystems and has become a

useful and a popular tool not only for micrometeorologists by now. However, there are lots of things to consider before getting from high frequency measurements of vertical wind velocity and CO_2 concentration to CO_2 fluxes, and finally to the annual net ecosystem exchange of CO_2. As the theory, requirements, and limitations of the EC method are described in detail and comprehensively in the literature (e.g., Aubinet et al., 2012; Burba and Anderson, 2010; Foken, 2008; Kaimal and Finnigan, 1994), this section only briefly discusses the major assumptions that the EC method is based on, and summarizes the necessary flux corrections that have to be applied. A short summary of the most important gap-filling methods follows. At the end of the section the semi-empirical models namely the non-linear regression model is described in detail as it is the probably most used one for filling missing CO_2 flux-data and as it is also used in this work.

2.4.1 Major assumptions for applying EC method

To explain the use of the eddy covariance method for estimating trace gas exchange we start with the complete budget equation of the component *s* with its mixing ratio χ_s (from: Aubinet et al., 2012).

$$\underbrace{F_S}_{V} = \frac{1}{4L^2}\int_{-L}^{L}\int_{-L}^{L}\int_{0}^{h_m}\left[\underbrace{\overline{\rho_d}\frac{\partial\overline{\chi_s}}{\partial t}}_{I} + \underbrace{\overline{\rho_d}\overline{u}\frac{\partial\overline{\chi_s}}{\partial x} + \overline{\rho_d}\overline{v}\frac{\partial\overline{\chi_s}}{\partial y} + \overline{\rho_d}\overline{w}\frac{\partial\overline{\chi_s}}{\partial z}}_{II} + \underbrace{\frac{\partial\overline{\rho_d}\overline{u'\chi'_s}}{\partial x} + \frac{\partial\overline{\rho_d}\overline{v'\chi'_s}}{\partial y}}_{III} + \underbrace{\frac{\partial\overline{\rho_d}\overline{w'\chi'_s}}{\partial z}}_{IV}\right]dzdxdy \quad (1)$$

Where F_s (term V) is the flux of the component between the atmosphere and the ecosystem; h_m is the measurement height; ρ_d is the density of dry air; u, v, and w are the wind speeds in x, y, and z direction, respectively. Term I describes the storage of the component below the measurement height, term II describes the transport by advection, and term III as well as term IV describe the turbulent transport (horizontal and vertical, respectively).

Using some assumptions, equation (1) can be very much simplified. The most important assumption is that the measurements are conducted in homogeneous and flat terrain. Thus, all horizontal gradients in (1) can be neglected. Therefore, the one-point measurement can be assumed representative for the whole volume. Furthermore, assuming vertical advection to be zero, the rest of term II ($\overline{\rho_d}\overline{w}\frac{\partial\overline{\chi_s}}{\partial z}$) can generally be neglected as well. If we additionally assume high turbulence intensity, meaning good mixing of the air below the measurement height, we can also neglect the storage term (term I). Thus, if these major assumptions are fulfilled sufficiently F_s can be calculated simply as

$$F_S = \overline{\rho_d w'X'_S} \quad (2)$$

This net flux (usually in units of µmol $m^{-2} s^{-1}$) between the biosphere and the atmosphere can be directly estimated as the covariance between the vertical wind speed and the mixing ratio of the substance of interest, for instance, CO_2 by the eddy covariance method. Furthermore, it is equal to the net ecosystem exchange: $F_s = NEE_C$ (see section 0).

Whether or not the assumptions leading from eq. (1) to (2) are valid needs to be examined for each site and flux-averaging period. Procedures to perform such tests, and criteria to accept or reject measured fluxes as compliant with (2) are included in the data quality assurance and quality control methods described in the Sections following below.

2.4.2 Data post processing

To satisfy some of these assumptions there are corrections, for others there are not. Therefore, the location where the measurements are conducted should be chosen very carefully. As mentioned above, ideally the terrain should be homogeneous and flat, which is often not the case. One example for such a non-ideal site in 'complex terrain' is the Lackenberg site. There is a large (30 ha) contiguous wind-throw area which is very homogeneous. However, the terrain is not perfectly flat, but is inclined (see Section 2.1). Thus, one has to look more carefully at the measured fluxes and the corrections that have to be applied. One correction which is necessary to make $\overline{w}=0$ (no vertical advection, which is one of the above mentioned major assumptions), is the rotation of the coordinate system of the 3D wind sensor.

There are several methods for this coordinate rotation. One is the double rotation (e.g., Kaimal and Finnigan, 1994) where the coordinate system is first rotated into the mean wind direction ($\overline{v}=0$). The second turn is through the new y-axis to make $\overline{w}=0$. These rotations are done for every half-hourly or hourly value. Another method is the so called Planar-Fit regression (Paw U et al., 2000; Wilczak et al., 2001) where a hypothetical plane is estimated from measured 30-min averages of $\overline{u}$, $\overline{v}$, and $\overline{w}$ data. Therefore, a long measurement period (at least a month) is needed. The coordinate system is then aligned with this average stream-plane. The main problem with the double rotation is that the resulting angles can be

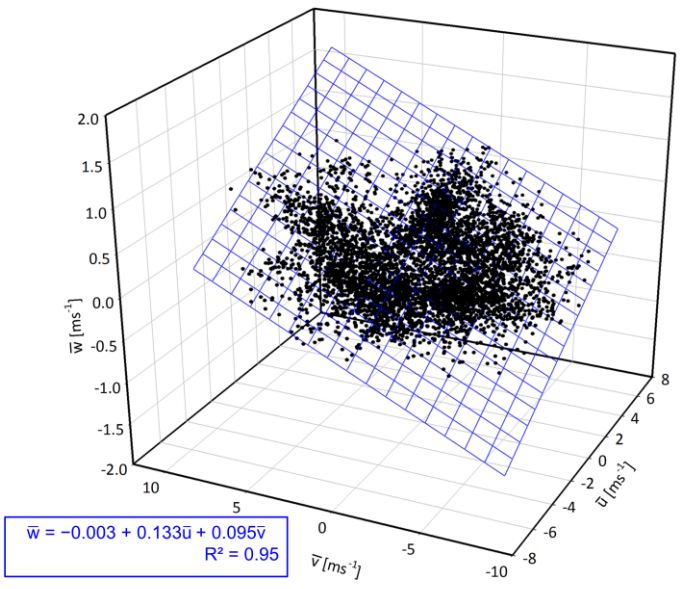

Figure 16: 3D plane (blue) fitted to $\overline{u}$, $\overline{v}$, and $\overline{w}$ values of the sonic anemometer in spring and summer 2011. Time period is from end of snowmelt till the sensor has been replaced (21.03 – 02.08.)

very high, which often makes no physical sense. By contrast the Planar Fit method fits the coordinate system to the average wind field. In this method, the 30-min average of $\overline{w}$ is not necessarily zero anymore, only over longer time periods, e.g., one month. Today, the Planar Fit method is the accepted standard for EC applications and has also been applied in this work. The regression periods for calculating the coefficients of the plane were subdivided into non-snow-covered period and snow-covered period every year. In summer 2011 the sonic anemometer had to be calibrated and was therefore replaced by another one. Thus, the coefficients had to be estimated also for the time period of the replacement unit. An example of such a plane is shown in Figure 16 for spring and summer 2011.

Term I of Equation (1) describes the change of storage within the control volume. If there is no closed canopy and if we can assume well-mixed air (high turbulence intensity), which is mainly the case at daytime, this storage term may also be negligible. However, at nighttime this is hardly the case anymore. At night there are usually stable conditions with low mixing of the air. Under such conditions neglecting the storage term is no longer valid. Then the emitted CO_2 from the ecosystem is likely stored at the ground and cannot be detected by the EC system anymore. This change in storage can be estimated using profile measurements of CO_2 concentration below the EC sensors (e.g., Schmid et al., 2003)). Measuring in complex (not totally flat) terrain, CO_2 might even be transported laterally down the slope (drainage flows) and bypass the sensor. In such cases, also profile measurements of CO_2 concentration would not be sufficient for estimating the change in CO_2 storage. This is one of the most important problems of measuring CO_2 exchange via the EC method during nighttime. A more detailed explanation of this problem and how it is commonly handled is given in section 2.4.4. Although the major assumptions are fulfilled there are some additional corrections which have to be applied to the calculated covariance that is to the estimated flux.

Especially with closed-path infra-red gas analyzers (IRGA) but also with open-path IRGAs there could be a time lag between the 3D-sonic measurement and the IRGA measurement. To account for this, a lagged correlation analysis is applied to find the maximum covariance, which is supposed to be the “real” value. For each half-hour the time lag is estimated that maximizes the covariance between IRGA and sonic measurements to correct for the time which it takes for an eddy to get from one sensor to the other.

Another important adjustment is the WPL-conversion (Webb et al., 1980) which compensates for density fluctuations that affect the measured fluctuations in CO_2, CH_4, and other gases. In other words, an instrument would measure a flux just because of volume expansion. The WPL-correction compensates for these fluctuations by converting measured absolute concentrations (mole m^{-3}) into

mixing ratios relative to dry air (mole $mole^{-1}$). This is not necessary if the used IRGA measures already mixing ratios (e.g., LI7200).

Also important is the correction to adopt the spectral resolution of the measurement system to the actual turbulence spectrum. This was done via transfer functions after Moore (1986) using spectral models by Kaimal et al. (1972) and Højstrup (1981).

There are quite a lot so-called post processing software packages available by now, e.g., EddyPro (LI-COR), TK3 (Mauder et al., 2013), EDDYSOFT (Kolle and Rebmann, 2007), and others. These software packages promise a better and easier handling of the huge raw-data-sets and usually include all common post-processing steps like despiking of high frequency data, coordinate rotation, buoyancy correction, correction for spectral loss, etc. All of the packages are very flexible, i.e. users can decide whether they want to activate a given correction or not. The main reason for this flexibility is that there is no universal best procedure for the post-processing which is applicable for all sites. There is no standard procedure to get from high frequency data to high quality half-hourly or hourly fluxes. To name only one example, the Planar-Fit correction is the commonly used method, though in some cases the double rotation might be more useful (e.g., when the measurement period is very short). Some of the corrections are still under debate (e.g., Lee and Massman, 2011).

Data Post Processing in this work, including all the steps, was done with the software package TK3 (Turbulence Knight) developed at the University of Bayreuth (Mauder et al., 2013).

Below all applied corrections and post-processing adjustments for this work are summarized in sequential order:

1. Despiking of high frequency data after Vickers and Mahrt (1997) based on Højstrup (1993)
2. Time-lag-correction by maximizing covariances
3. Planar Fit coordinate rotation (Wilczak et al., 2001)
4. Corrections for spectral deficiencies after Moore (1986) via transfer functions using spectral models by Kaimal et al. (1972) and Højstrup (1981)
5. Accounting for effects of density fluctuations, and conversion of CO_2 and H_2O fluxes to mass-conserving units, after Webb et al. (1980)
6. Iteration of correction steps (2-5) because of their interdependence until heat fluxes and CO_2 fluxes do not change more than 0.01 % from one step to the next one

Also implemented in the software package is a Quality Assurance and Quality Control QA/AC method according to Foken and Wichura (1996) where each flux-value is flagged regarding to its quality in terms of fulfilling particular EC conditions (flags range from 1 - good data quality to 9 - bad data qual-

ity). According to Foken et a. (2004) all half hourly values with an overall flag > 6 were rejected. For the gap-filling models (see section 2.4.4 and 3.2) we only used values with flag < 4.

Another quality criterion would be that the footprint (upwind area where the atmospheric flux measured by an instrument is generated) during the average period has to be adequate, i.e. that the measured flux preferably completely represents the area of interest. This might be not the case in very stable conditions as it is usually at night or when measuring in a very heterogeneous and patchy terrain including different types of land-use. There are many suitable footprint models published by now, e.g., Kljun et al. (2004), Kormann and Meixner (2001), or Schmid (1997). These models describe the source area of the estimated flux and give information about the percentage of the estimated flux coming from / going to the area of interest. In this work the footprint model after Kormann and Meixner (2001), which is also implemented in the software package TK3, was used. The footprint was divided into target area (wind-throw) and non-target area (wind-throw or forest, respectively). If less than 75% of the measured flux could be assigned to the target area, the respective half-hourly flux value was rejected. A circle with approximately 250 m radius around the measurement tower roughly represents the estimated annual mean footprint area (80% of the estimated flux can be attributed to this area) for the EC measurements.

As have been shown above not every measured CO_2-flux value is of high quality fulfilling all major assumptions of the EC method. Furthermore, even the high-quality flux-data-set after data-post-processing can still contain some outliers. These outliers probably do not affect the annual sum of NEE but they can have a drastically influence on the gap-filling quality. However, it is quite difficult to find an objective method to detect such spikes in the flux-time-series. Papale et al., (2006), for instance, used the median absolute deviation about the median (MAD) for outlier detection in the flux time-series, while Kochendorfer et al. (2011) consider all values outside a certain range (mean ± 3σ) as outliers. Anthoni et al. (1999) define all values as outliers if $|F_C| > 25$ µmol m^{-2} s^{-1}. Similar borders for outliers can be found e.g., in Elbers et al. (2011). In this work we used a little different method to detect spikes within the raw fluxes.

CO_2-fluxes were sorted into time-windows of 3 consecutive half-hourly values during 25 days (for example 00:00 – 01:30 of 25 consecutive days; see Figure 17). Values within each time-window were considered to be normal distributed. Therefore, any CO_2 flux was considered as outlier if it

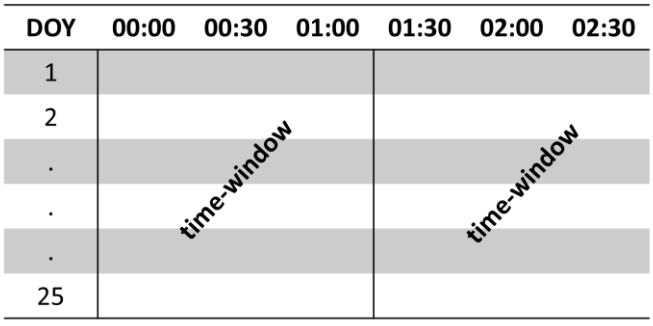

Figure 17: Scheme of the time-windows for which the outlier test was performed

exceeded mean ± 2.5σ of the respective time-window.

2.4.3 Annual sums of NEE – how to do gap-filling

Bad weather conditions, instrument failure, technical problems, or rejected values lead to a more or less patchy annual CO_2 flux-dataset with many gaps depending on the used instruments and the climate or weather at the measurement site. To get information whether the study site is a net source of carbon or a net sink of carbon and how big the source or sink is on an annual timescale, all the missing values i.e. all the gaps have to be filled. There are many gap-filling methods described in the literature to get annual carbon balances from hourly or half-hourly flux-values. Here we give a short overview of the most common gap-filling methods. As used in this work the non-linear regression method is described in more detail at the end of this section as well as in the results (section 3.2).

Gap-filling methods can roughly be divided into non-parametric and parametric methods.

Non-parametric methods:

Linear interpolation as the simplest way to fill gaps should only be used for short gaps (not more than 3 missing observations). Another empirical method is for instance ensemble mean diurnal variation where missing values are replaced by the average of a data ensemble that is similar to the missing one. A missing value at 10 a.m. would for example be replaced by the average of the 10 a.m. values from the last 10 days and the next ten days. Choosing the length of the time window is somehow subjective at this. More based on meteorological conditions are look-up-tables. For predefined time periods classes of temperature and photosynthetically active radiation (PAR) are created. Intervals for these classes could be for instance 2°C (temperature) and 100 µmol m^{-2} s^{-1} (PAR) depending on the site characteristics and the local climate. Missing CO_2 flux values are replaced with the average value from all measured values within the corresponding class.

Parametric methods (non-linear regression models)

The non-linear regressions use non-linear equations which express relationships between the NEE flux and environmental variables such as temperature and light. Usually, there is one equation used for R_{eco} and one for GEP. The parameterized equations are fit to the observed data and then used to fill missing NEE values. As we used such non-linear regressions in this work, the method is explained in more detail in the following section (see section 2.4.4 and 3.2).

Generally, important gap-filling procedures are explained and discussed in more detail, for instance in Falge et al. (2001) or in Moffat et al. (2007).

2.4.4 Local gap-filling procedure

Equation (3) shows the budget equation of carbon on ecosystem scale:

$$NEE_C = F_{VOC}\text{-}GEP+R_h+R_a+\Delta F_{C_{lat}} \quad , \tag{3}$$

where NEE_C is the net carbon exchange of the ecosystem, F_{VOC} is the carbon flux contribution from volatile organic compounds. GEP is the carbon assimilated by the process of photosynthesis, R_h and R_a are the carbon emitted through heterotrophic and autotrophic respiration, respectively which can be summarized as ecosystem respiration (R_{eco}). ΔF_{lat} is the net lateral transport of carbon e.g., advection or leaching, as well. This has already been explained partially in the introduction. The EC method only accounts for the vertical turbulent net flux of CO_2 which can be divided into R_{eco} and GEP

$$NEE_C = -GEP+R_{eco} \approx F_{EC} \tag{4}$$

F_{EC} is the CO_2 flux measured by the EC method. Due to no photosynthetic activity at night we can define

$$F_{EC_{night}} = R_{eco} \tag{5}$$

Respiration is a microbiological process, thus it is mainly driven by temperature and this relationship is somehow exponentially. Therefore, with a simple two-parametric Arrhenius-type function of temperature we can express ecosystem respiration as:

$$R_{eco} = a*e^{bT} \quad , \tag{6}$$

where a and b are free parameters and T is either air or soil temperature. The equation of Lloyd and Taylor (1994) as a special form of an Arrhenius-type function is also often used in modeling R_{eco} by now

$$R_{eco} = R_{ref}e^{\left(\frac{1}{T_{ref}\text{-}T_0}\text{-}\frac{1}{T_K\text{-}T_0}\right)} \tag{7}$$

R_{ref} is the respiration at T_{ref}; E_0 is 309K; T_K is air or soil temperature, T_{ref} is 298,16K. R_{ref} and T_0 were fitted to the respective dataset (Falge et al., 2001; Lloyd and Taylor, 1994). In this work we used equation (6) to model ecosystem respiration (see section 3.2.1.1).

At nighttime there are often very stable conditions with very low wind speed. Under such conditions turbulent mixing is suppressed. As turbulent transport is one of the major assumptions of the EC application, measured fluxes in calm nights are not reliable. The respired carbon from the ecosystem will likely be accumulated close to the ground and will therefore not or just partly be detected by the EC sensors. Additionally depending on the terrain the emitted CO_2 will be “flushed” away by drainage flows. At the Lackenberg site the terrain is very rough enhancing turbulent mixing but the terrain also

slopes abetting such drainage flows. Thus, EC based calculated nighttime CO_2 fluxes during such conditions do not reflect actual CO_2 exchange processes and lead to an underestimation of nighttime CO_2 emissions due to low mixing conditions. Accounting for this problem is one of the biggest challenges concerning nighttime EC measurements (Aubinet, 2008; Mahrt, 2010; van Gorsel et al., 2009; Vickers et al., 2012). As an example, despite lots of effort it was not possible so far to measure horizontal advection even not by using several EC towers within one fetch (Aubinet et al., 2010). The most common method to solve the problem is still to reject every flux-value during such 'low-mixing' conditions and replace it with modeled values. Usually friction velocity (u_*), that is friction in scale of a speed, is used as a scale for turbulence or for mixing intensity, respectively

$$u_* = \left[\left(\overline{u'w'}\right)^2+\left(\overline{v'w'}\right)^2\right]^{\frac{1}{4}} \quad (8)$$

Plotting R_{eco} against u_*, R_{eco} normally first increases with increasing friction velocity but at a certain threshold Reco becomes independent of u_*. The usual way is to reject all measured flux values below this u_*-threshold (this procedure is explained in detail in section 3.2.1.1). It is to say that this u_*-threshold strongly depends on the ecosystem and in some cases the expected independence could not be determined with the desired reliability (Ruppert et al., 2006). As u_* only accounts for the mechanical generated turbulence it is not the best parameter describing turbulence. Suggestions for other parameters which can describe in some way how well the air is mixed can be found, for instance, in Gu et al. (2005), Wharton et al. (2009), or in Acevedo et al. (2009). However, the discussion concerning this problem in the scientific community has not been finished, therefore, we decided to use the usual u_*-filter to separate well-mixed and not well-mixed conditions (section 3.2.1.1)

Assuming that the model for nighttime ecosystem respiration can reasonable represent also daytime respiration we can calculate GEP by subtracting the modeled daytime respiration from the measured daytime net CO_2 flux (9)

$$GEP \approx -F_{EC_{daytime}}+R_{eco\ (modelled)} \quad (9)$$

As GEP stands for 'Productivity' we arranged (9) in a way that GEP is positive.

Photosynthesis is an enzymatic process thus usually a hyperbolic Michaelis-Menten-type function is used to model this process (Michaelis and Menten, 1913). The main driver for this enzymatic reaction is light that is photosynthetically active flux density (PPFD). Although happening at the leaf-level this can also be applied to the ecosystem level (see e.g., Falge et al., 2001; Schmid et al., 2003)

$$GEP = \frac{\alpha GEP_{sat} PPFD}{GEP_{sat} + \alpha PPFD} \quad (10)$$

Here α is the initial slope of the curve (quantum yield efficiency) and GEP_{sat} is the saturated (potential) rate of ecosystem uptake. If this model can be applied for the whole growing-season or must be applied to several time periods is very site specific.

Using these two models every missing CO_2-flux value can be filled and the annual carbon budget can be calculated. As one advantage of this gap-filling method also the annual sums of the component fluxes can be estimated while other gap-filling methods are mostly not able to account for this flux partitioning.

Exemplarily for 2011 out of 17520 half hourly values of the year 10281 (59%) could be estimated using EC measurements. 169 flux values have been rejected due to any rain event during the half-hour average period. Another 564 flux values have been rejected due to quality criteria (CO_2 Flag after Foken and Wichura (1996) was bigger than 6. Applying the footprint criterion led do the rejection of only 42 values during the whole year. 372 values have been considered to be outliers and therefore have been removed. Most values had to be rejected due to the u_*-threshold. 3589 values (35% of all measured values) had a u_* value beneath 0.3 ms^{-1} and therefore were additionally rejected. All the rejected values had to be replaced by modeled fluxes (see section 3.2.1.1 for details).

2.5 Quality Control – Daily Plot

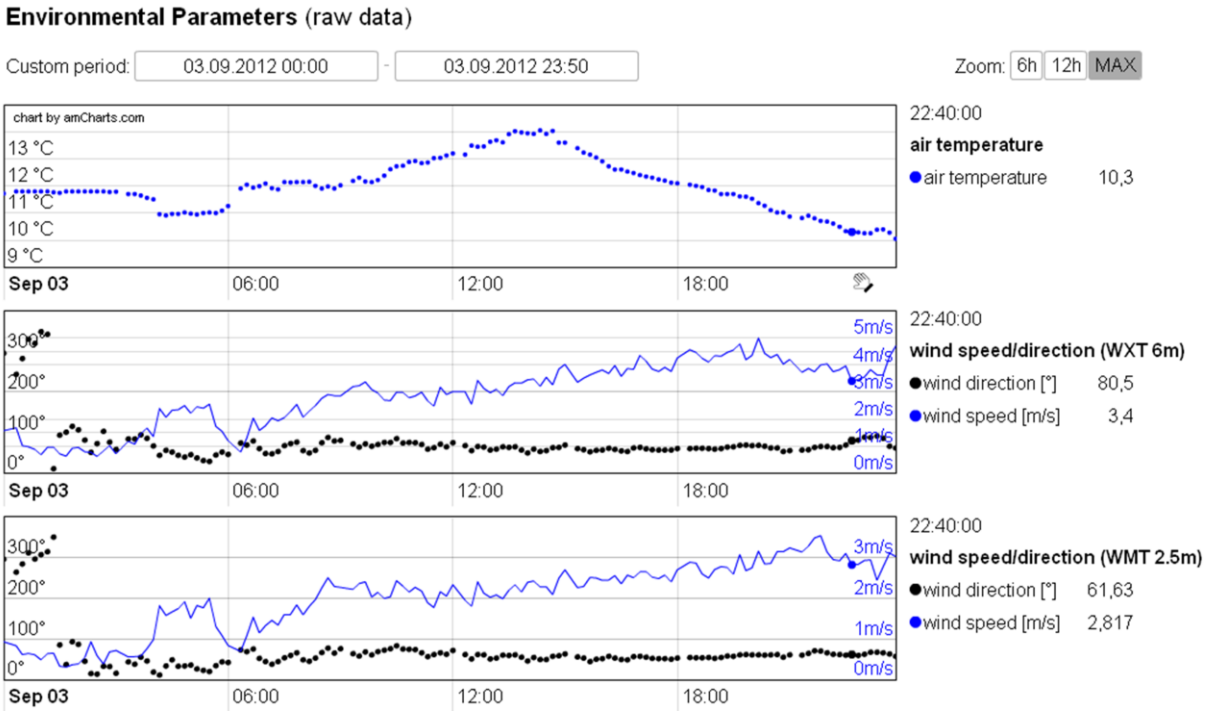

Figure 18: Daily Plot from the 03.09.2012 of meteorological parameters. Exemplarily for air temperature, wind speed and direction in 6 and 2.5 m height

As already mentioned, the measurements were made on a very remote site. Thus, problems with the measurement system or with the energy supply might be recognized very late after they have occurred, leading to potentially large data gaps. For this reason, remote access was established to the minicomputer via GPRS connection (Router C1500, TDT, Essenbach, Germany) at the site and all meteorological parameters each of the last day were copied to a web server. By examining the time series plots of the last day for a suite of important variables, the status of measurements could be checked quite easily in this way. In consequence, most problems could be detected and responded to very quickly and larger data gaps could be avoided by this method. This link was implemented in summer 2010 and large (technically caused) data gaps like at the end of 2009 or the middle of 2010 did not occur anymore since then. The eddy covariance system is now running since the end of May in 2009. Longer contiguous periods of missing data usually occur in winter when temperatures are very low and the instruments are frozen (Figure 19). These periods can last up to several months in this region. There has been another long time period with missing data in spring and summer 2010 due to technical problems. These large data gaps in 2010 led to an

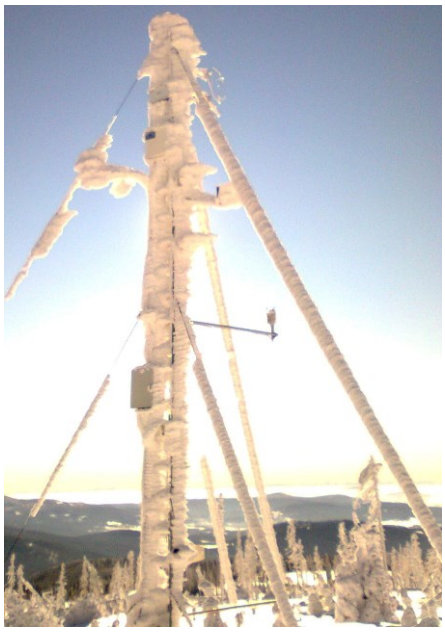

Figure 19: Measurement tower in January 2012. Most time of the winter instruments are frozen. (Photo: B. Wolpert)

increased uncertainty of the estimated annual NEE (see also section 3.2.1.7).

2.6 Carbon balance model LandscapeDNDC

To estimate the relative contribution grass, trees and soil to ecosystem fluxes, we applied a combination of models that were coupled within the modeling framework LandscapeDNDC (Haas et al., 2013). This framework is a new implementation of the ecosystem model MoBiLE (Modular Biosphere simuLation Environment; Grote et al., 2009a; Grote et al., 2009b; Holst et al., 2010). The model runs were done in close cooperation with Dr. Rüdiger Grote from KIT IMK/IFU.

2.6.1 Model description

The central parts of LandscapeDNDC are the physiologically-based vegetation model PSIM (Physiological SImulation Model; Grote, 2007) and the biogeochemical soil process model DNDC (De-Nitrification-De-Composition; Li et al., 1992). These were complemented with models that describe micro-environmental conditions within the biosphere (e.g., light distribution, soil temperature development, water availability). The PSIM model was designed for the parallel use of various vegetation types or plant species. It has been evaluated for grasslands (Grote et al., 2009b) and various homogeneous forests (Grote et al., 2011a). It has also been applied at a mixed forest, simulating several tree species simultaneously (Grote et al., 2011b). The present study, however, is the first application of LandscapeDNDC where trees and grasslands are simulated simultaneously, with special focus on their mutual interactions that change dynamically with time.

The model framework calculates environmental conditions for a number of canopy- and soil layers, depending on meteorological parameters and ecosystem layer properties (e.g., leaf area for above ground, and water holding capacity for below ground layers). The exposure conditions of a specific vegetation type (group of plants with homogeneous properties) are defined by the layers it is occupying, according to its height, canopy architecture, and rooting depth. Foliage and fine root biomass are explicitly distributed across the occupied layers, which are shared with other vegetation types that occupy the same layers. On the other hand, vegetation types affect the ecosystems by resource use (nitrogen, water) and shading. Thus, above ground competition is dominated by shading from other cohorts, which concentrate their foliage in higher canopy layers (asymmetric competition), while below ground competition only depends on the presence of fine roots in a particular soil layer and the species-specific uptake capacity. Since the model considers all processes as 'one-dimensional', the emerging ecosystem is horizontally homogeneous, implying an even distribution of plants. Ground coverage of each plant type or species is updated at the beginning of each year, based on net biomass growth in the previous year. This is done either by assuming a constant size of an individual (in case of ground vegetation) or a constant number of individuals that expand by in-

creasing their average crown diameter (in case of trees). These assumptions also allow a decrease in coverage for ground vegetation if net growth is negative. Negative net growth in trees would lead to less assimilating tissue but does not decrease coverage.

Meteorological data (air temperature and global radiation) are driving a common photosynthesis model that calculates the carbon uptake depending on light, temperature, and enzyme activity based on Farquhar et al. (1980) and the water constraint according to Ball et al. (1987). This approach determines carbon gain (GEP) by iteratively adjusting stomatal conductivity and thus transpiration demand, which in turn is limited by water availability. The light saturated carboxylation rate is reduced when (a) nitrogen concentration in the leaf tissue is below optimum, and (b) the seasonal phenology. The latter impact is assumed to occur in deciduous species in parallel with bud burst and senescence and is calculated for evergreen species with the sigmoidal approach presented in Mäkelä et al. (2004). Further, vegetation modules simulate phenology (Grote, 2007; Lehning et al., 2001), plant respiration (Thornley and Cannell, 2000), senescence and allocation of carbon and nitrogen (Grote, 1998), as well as nitrogen uptake (ammonia and nitrate separately accounting for). Total plant uptake capacity is determined by demand according to a defined optimum nitrogen concentration within the plant, fine root biomass and specific uptake capacity (per root biomass). Similarly, water uptake is simulated using potential transpiration as the demand term that is defined by assimilation and water use efficiency of the plant species. Uptake thus depends on the seasonal biomass development as well as the spatial distribution of fine roots throughout the root profile. Additional plant model procedures describe mortality and increase of diameter and height in trees using the taper functions presented in Zianis et al. (2005). The model is based on a set of physiological processes that are assumed universal for all plant species but are steered by species-specific parameters, the most important of which are presented in Table 4.

Ecosystem respiration (R_{eco}) is modeled as the composite of total plant respiration (or autotrophic respiration), including growth- and maintenance respiration as well as carbon usage for transporting and transforming nitrogen (Thornley and Cannell, 2000), and heterotrophic respiration. Heterotrophic respiration, in turn, is the sum of numerous energy consuming processes related to microbial activities such as decomposition, nitrification and denitrification, the majority of which take place in the soil, including litter layer and CWD. These processes are calculated as dependent on temperature, acidity, water-, carbon- and nitrogen contents separately for each soil layer (Li et al., 2000; Li et al., 1992). Heterotrophic respiration, fine root respiration and the fraction of wood respiration that is attributed to coarse roots together are termed ‘soil respiration’ here, for simplicity.

Table 4: Important species-specific parameters

Description	Unit	Spruce	Source	Grass	Source
maximum RubP saturated rate of carboxylation at 25 °C for sun leaves	µmol m^{-2} s^{-1}	39.5	Wang et al. (2003)	33.50	adjusted (Urban et al. 2007)
maintenance respiration coefficient at reference temperature	-	0.25	Grote et al. (2011a)	0.9	adjusted
activation energy for photosynthesis	J mol^{-1}	75750	Falge et al. (1997)	55125	Wohlfahrt et al. (2001)
activation energy for dark respiration	J mol^{-1}	63500	Falge et al. (1997)	49942	Wohlfahrt et al. (2001)
activation energy for Michaelis-Menten constant for CO_2	J mol^{-1}	65000	Falge et al. (1997)	59356	Farquahr et al. (1980)
activation energy for Michaelis-Menten constant for O_2	J mol^{-1}	36000	Falge et al. (1997)	35948	Farquahr et al. (1980)
activation energy for electron transport	J mol^{-1}	37000	Farquhar et al. (1980)	46270	Wohlfahrt et al. (2001)
ratio between maximum electron transport rate and RubP saturated rate of carboxylation	--	2.47	Grassi et al. (2001)	2.98	Urban et al. (2007)
ratio between dark respiration rate and carboxylation capacity at 25 °C	--	0.011	Farquhar et al. (1980)	0.045	Urban et al. (2007)
slope of foliage conductivity in response to assimilation in BERRY-BALL model	--	6.4	Medlyn et al. (2001)	10.4	Baldocchi and Xu (2005)
maximum water use efficiency	$mgCO_2$ gH_2O^{-1}	4.8	Cienciala et al. (1994)	6	Urban et al. (2007)
minimum water use efficiency	$mgCO_2$ gH_2O^{-1}	4.8	(assumed constant)	2	Urban et al. (2007)
maximum stomata conductivity	mmol H_2O $m^{-2}s^{-1}$	125	Sellin and Kupper (2004)	588	Tjoelker et al. (2005)
minimum stomata conductivity	mmol H_2O $m^{-2}s^{-1}$	10.4	Medlyn and Jarvis (1999)	21.9	Wohlfahrt et al. (2001)
max. spec. NH_4-uptake rate	$kgNH_4$-N kg^{-1} DWfine root day^{-1}	0.0001	McFarlane and Yanai (2006)	0.012	Osone and Tateno (2005)
max. spec. NO_3-uptake rate	$kgNO_3$-N kg^{-1} DW fine root day^{-1}	3.36E-05	McFarlane and Yanai (2006)	0.006	Osone and Tateno (2005)
time interval necessary to complete growth of new foliage	Days	90	Bergh et al. (1998)	20	Durand et al. (1999)
total leaf longevity from the first day of the emergend year on	Days	1825	Gower et al. (1993)	300	Li et al. (2005a)
time interval necessary to complete litterfall of foliage	Days	590	Grote et al. (2011b)	60	Li et al. (2005a)
minimum temperature sum for foliage activity onset	°C	350	Andersson et al. (2002)	0	Li et al. (2005a)
foliage biomass under optimal, closed canopy condition	kgDW m^{-2} ground	1.1	Bergholm et al. (2007)	0.35	Hussain et al. (2011)
maximum fraction of nitrogen retranslocated before tissue loss	--	0.3	Berger et al. (2009)	0.54	Aerts (1996)
fraction of dying fine root biomass	1 day^{-1}	0.003	Brunner et al (2013)	0.002	Tjoelker et al. (2005)
fraction of dying sapwood biomass	1 day^{-1}	0.0007	Longuetaud et al. (2006)	--	
optimum nitrogen concentration of foliage	kgN $kgDW^{-1}$	0.015	Wang et al. (2003)	0.019	Tjoelker et al. (2005)
optimum nitrogen concentration of fine roots	kgN $kgDW^{-1}$	0.01	Withington et al. (2006)	0.011	Tjoelker et al. (2005)
optimum nitrogen concentration of sapwood	kgN $kgDW^{-1}$	0.001	Ukonmaanho et al. (2008)	--	
specific leaf area under full light	m^2 $kgDW^{-1}$	6.3	Meir et al. (2002)	9.9	Tjoelker et al. (2005)
specific leaf area in the shade	m^2 $kgDW^{-1}$	4.2	Meir et al. (2002)	9.9	(assumed constant)
optimum ratio between fine root- and foliage biomass	--	0.33	Borken et al. (2007)	2.7	Jackson et al. (1997)

2.6.2 Model set up

The model was run with the two plant types 'Norway spruce' and 'Perennial grass', assuming an even grass distribution and a random distribution of trees. Soil properties are derived from soil samples, assuming that soil properties were not significantly affected by the storm event. The first spin-up simulation year was 2005 (4 years before measurements started), and we introduced a disturbance at the beginning of year 2007 (the date of the storm event). By this disturbance, tree biomass was transferred to the litter compartment of the model and the 'Norway spruce' plant type was re-initialized. No change in biomass of the 'Perennial grass' type was assumed. This spin-up ensures that the effects of uncertainties in the carbon pool initialization of the soil are minimized.

The initialization of the 'undisturbed' forest was done according to the number (app. 1000 trees per ha) and average size (18 m height) of fallen trees, making sure that the amount of debris at the site is correctly represented. After the storm event, the 'Norway spruce' compartment was re-filled with 2500 young trees (initialized with 0.4 m height) based on a stem count in year 2010. The parameterization of spruces is derived from previous studies (i.e. Grote et al., 2011a; Grote et al., 2011b) and the parameters for grasses are mostly derived from literature. It should be noted that a literature-based parameterization is bound to have relatively large uncertainty, because grassland is always heterogeneous. In order to get as close as possible to the site specific ground vegetation properties, model parameters from gramminoids at other mountainous sites were used to supply reference parameters (e.g., Urban et al., 2007; Wohlfahrt et al., 2000; Wohlfahrt et al., 2001). The parameterization was completed with parameters used for other grassland sites (see Table 4).

The only data-tuning adjustments applied were on two parameters for grasslands: 1) maximum RubP saturated rate of carboxylation and 2) the coefficient for maintenance respiration. These two parameters are affecting photosynthesis and plant respiration. The adjustment procedure was to start with the lowest values available from literature (33.5 and 0.1, respectively; see Table 1) and increase iteratively by steps of 0.05 until daily values for measurements and simulations over the total investigation period gave a 1:1 slope.

Measured daily meteorological data (average air temperature and humidity, sum of precipitation and global radiation) are used to drive the model. Including the spin-up period, the model was run over the years 2005 – 2017 and for the long-term run from 2005 - 2025 (section 0).

3 Results and discussion

3.1 Seasonal course of ecosystem characteristics

In this section some more measured environmental parameters like soil temperature, soil heat flux, and photosynthetically active radiation in addition to those already shown in the methods are presented. Further, the models to fill missing values of short-wave incoming solar radiation and soil temperature are described followed by estimated energy fluxes.

Some meteorological and climatological parameters have already been described in section 2.2. In this section, seasonal courses of soil temperature, soil heat flux, and photosynthetically active radiation (PAR) or photosynthetically active photon flux density (PPFD), respectively are described. As temperature and PPFD are the main drivers for carbon exchange processes (Falge et al., 2001), and are therefore used for the gap-fill modeling (see section 2.4.3), missing values of these "drivers" have to be filled.

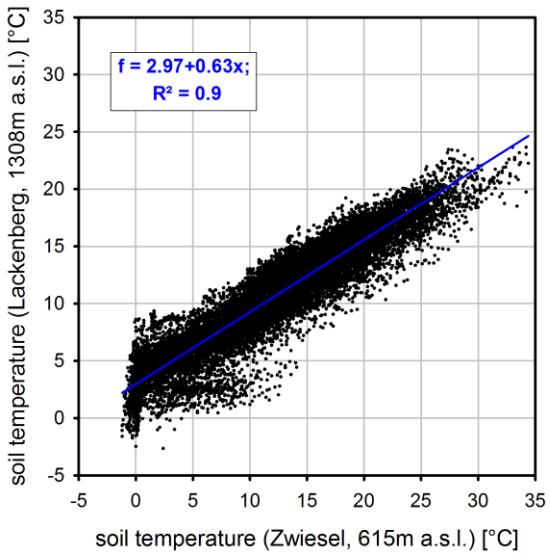

Figure 20: Soil temperature at the DWD station Zwiesel vs. soil temperature at the Lackenberg site during the measurement period. Missing values were filled with the blue equation.

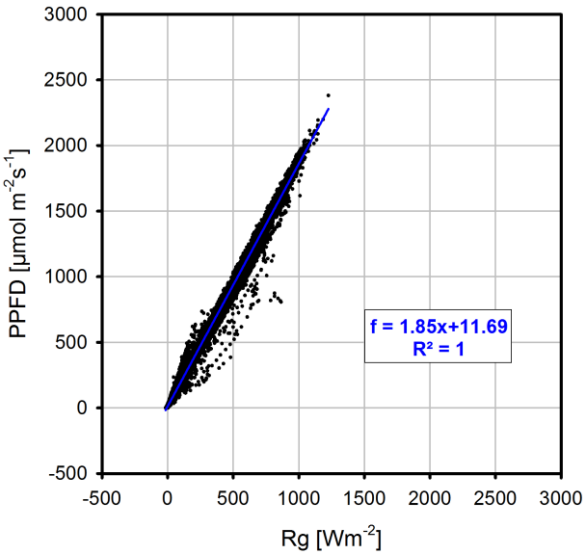

Figure 21: Relationship between incoming short-wave radiation (R_g) and photosynthetically active photon flux density (PPFD) at the Lackenberg site

Missing values for soil temperature were modeled with the relationship between soil temperature from the nearby weather station of the German weather service (DWD) in Zwiesel (49.03°N; 13.24°E; 615m a.s.l.) and soil temperature at the Lackenberg site (see Figure 20).

PPFD (Figure 21) is highly correlated with incoming short-wave radiation (global radiation: R_g) which in turn was modeled using the relationship between extraterrestrial incoming short-wave radiation and relative humidity. Therefore, this extraterrestrial radiation (R_E) was calculated as described, for instance, in Stull (2000):

$$R_E = -S * T_r * \sin \Psi \quad (11)$$

S is the solar constant, Tr is a net sky transmissivity (depending on path length through the atmosphere, atmospheric absorption characteristics, and cloudiness) which can be approximated by: Tr = 0.6+0.2*sinΨ. Ψ is the local elevation angle of the sun. Then, measured values of R_g were divided by R_E to get the fraction of expected incoming short-wave radiation which is somehow the same as the actual transmissivity of the atmosphere. This fraction was plotted against binned values of relative humidity (see Figure 22). In this way missing half hourly values of global radiation for each relative humidity class could be modeled.

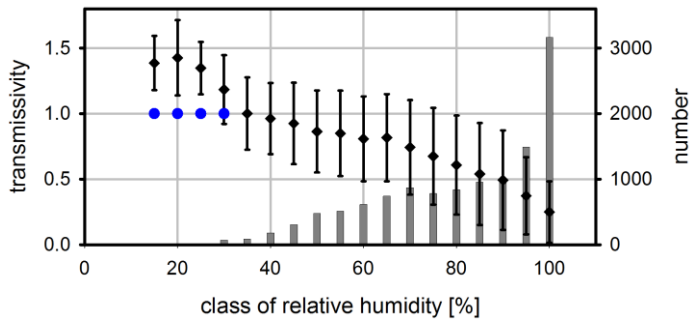

Figure 22: transmissivity (fraction of expected incoming short-wave radiation) against binned values of relative air humidity (black diamonds). Only sparse data (grey bars show frequency) was available for relative humidity from 0 to 30%. Thus, the transmissivity for these values was set to 1 (blue circles).

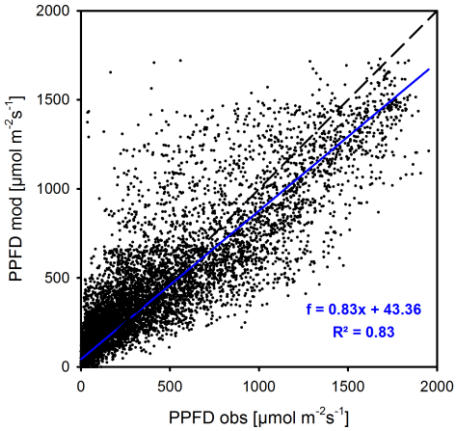

Figure 23: Observed vs. modelled values of PPFD - exemplarily for 2013.

Considering the sparse parameter input of this model (astronomical information, time, and relative humidity) the applicability for modelling short-wave incoming radiation and on that way PPFD is exceptionally good, at least for the study site (Figure 23).

Therefore, the relationship in Figure 22 was further developed and tested at different sites (see Appendix).

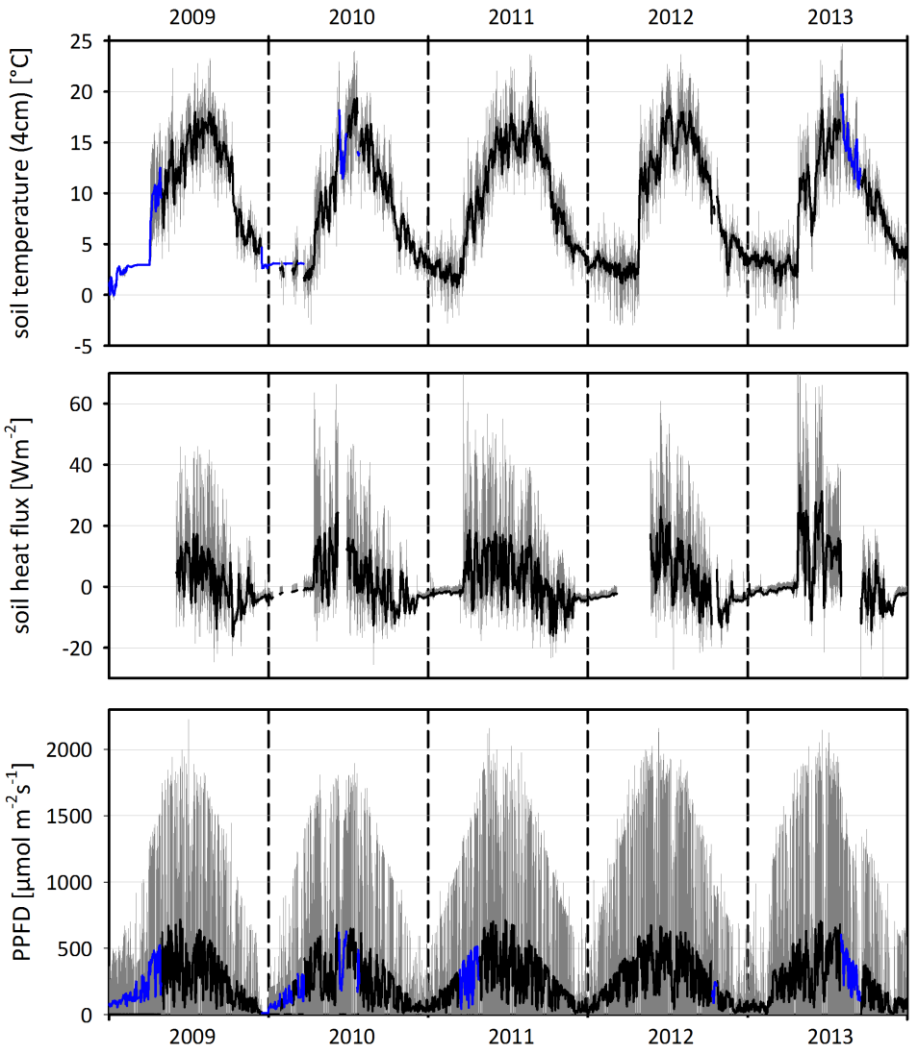

Figure 24: Daily averages of soil temperature, soil heat flux, and photosynthetically active radiation at the Lackenberg site. Grey bars show range of values during the day (maximum and minimum). Blue dots indicate gap-filled values.

Figure 24 shows daily averages of soil temperature, soil heat flux, and PPFD. Daily PPFD roughly ranges between 5 and 700 µmol $m^{-2} s^{-1}$ with maximum 10-min averages of over 2000 µmol $m^{-2} s^{-1}$. Daily integrated PPFD was highest in June of each year with 61.8 (2009), 58.2 (2010), 61.3 (2011), 58.2 (2012), and 60.7 mol $m^{-2}d^{-1}$ (2013). Lowest values of daily PPFD were observed in winter and range between 0.1 and 0.5 mol $m^{-2}d^{-1}$ (2012). The daily variation was much higher in summer than in winter. Monthly integrated PPFD ranged from about 57 mol $m^{-2}month^{-1}$ (December 2009) up to about 1200 mol $m^{-2}month^{-1}$ (May 2011). Average daily soil temperature was highest in the end of summer with values up to 20 °C while single values in summer sometimes reached almost 25 °C. It can be clearly seen, that even in winter soil temperature in 4 cm depth only rarely goes beneath 0 °C. This is due to the isolating effect of the snow cover in the winter months. Soil heat flux is also very constant during the snow-covered periods. Considering these two parameters, the snow covered periods can be estimated. In winter 2009/2010 the site was snow covered from approximately 25.11.2009 - 07.04.2010, in winter 2010/2011 the site was snow covered from 01.12.2010 -

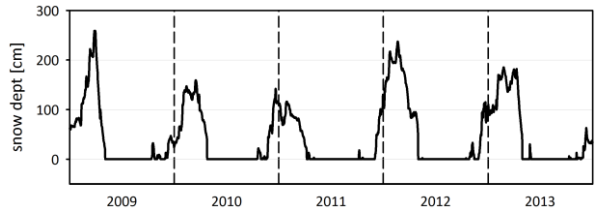

Figure 25: Snow depth at the DWD weather station Großer Arber from 01.01.2009 to 01.01.2014.

20.03.2011, in winter 2011/2012 from 30.11.2011 - 28.04.2012, and in winter 2012/2013 from 30.11.2012 - 27.04.2013. Pictures from a web cam that was also installed on the measurement tower support this result. Unfortunately the web cam was installed not before spring 2010. Additional information about the snow cover at the Lackenberg site was derived from the snow height measurements at the DWD weather station Großer Arber already mentioned in section 2.2. Since this weather station is at a similar elevation and is with about 12 km distance not far away from the study site, the snow covered periods are assumed to be quite similar between the two locations. Figure 25 shows the time series of the snow depth at Großer Arber. There the surface was continuous covered with snow from 01.12.2009 - 25.04.2010, 24.11.2010 - 08.04.2011, 04.12.2011 - 01.05.2012, and from 29.11.2012 - 30.04.2013. These periods matches quite well with the above mentioned ones.

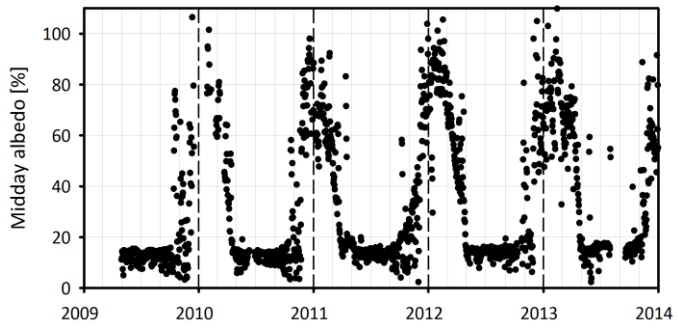

Figure 26: Daily averages of midday albedo (12:00 – 14:00).

Midday albedo did not show any marked variations outside the snow-covered periods in all three years. In winter with rising snow cover midday albedo values sharply increase up to about 100% (Figure 26). Excluding snow covered periods average albedo of this site was about 14%.

Soil volumetric water content (SVWC) showed only little variation during the year. After strong rain events SVWC sometimes rose up to 50% but never reached values above. On the other hand SVWC almost never fell beneath 20% during the measurement period. 88% of measured SWC values were between 30 and 40% (Figure 27).

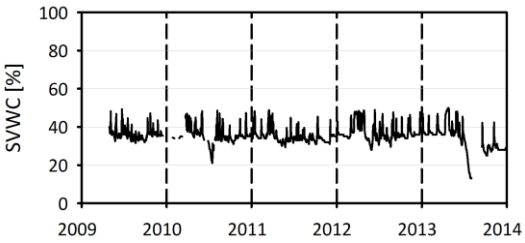

Figure 27: Soil volumetric water content (SVWC)

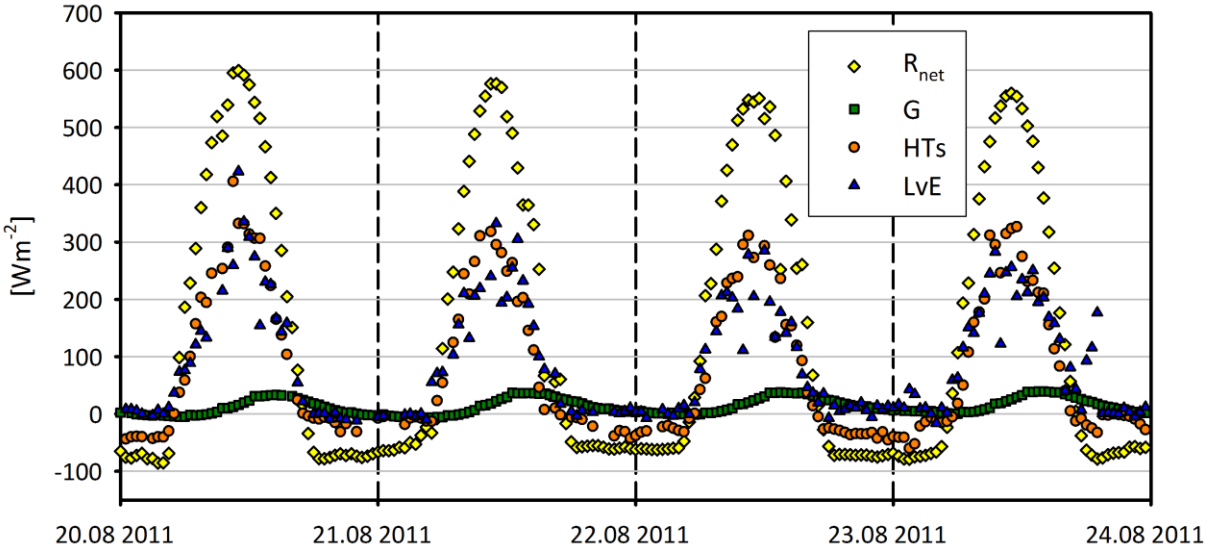

Figure 28: Net Radiation (R_{net}), soil heat flux (G), sensible heat flux (HTs), and latent heat flux (LvE) during four golden days in August 2011 (half-hourly averages).

Figure 28 shows net radiation (R_{net}), soil heat flux (G), sensible heat flux (HTs), and latent heat flux (LvE) from 20th till 23rd of August in 2011.

During these cloudless "golden days" energy input at noon was about 600 Wm^{-2} but reached (half-hourly avg.) maximum values of over 800 Wm^{-2} during summer time within the 5-years measurement period. During nighttime, depending on the weather situation, net radiation fell down to -100 Wm^{-2}. The soil heat flux is comparably small with maximum daily means not beyond -20 to 20 Wm^{-2} during the measurement period (see Figure 24). Fluxes of sensible and latent heat are quite similar within these "golden days" and in average during the whole measurement period, as well (Figure 29). Bowen-ratio (Bo - ratio between sensible and latent heat) was in average 1.05, 1.14, 1.46, 1.19, and 1.15 for 2009 to 2013. That means the residual available energy after subtracting soil heat flux is almost equally split into heating of the surface and evapotranspiration. These values are higher compared to intact spruce forests but are much lower than, for instance, in clear-cuts where Bo values up to 5 can be found (Schulze et al., 1999).

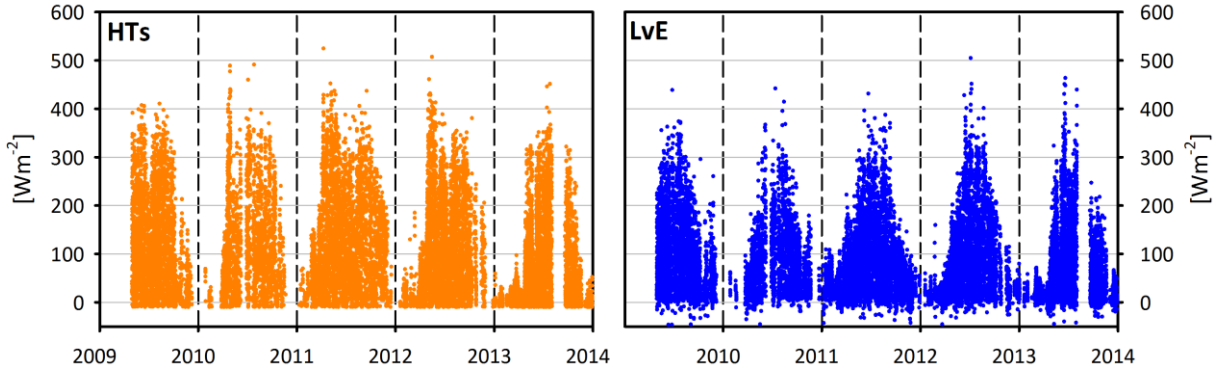

Figure 29: Time series plots of measured sensible heat flux (HTs) and latent heat flux (LvE) from 2009 to 2013.

The portion of daytime available convective energy used for evapotranspiration can be estimated via: LvE/(HTs+LvE). On average 49%, 47%, 43%, 55%, and 50% of the available convective energy was used for evapotranspiration in 2009, 2010, 2011, 2012, and 2013.

3.2 CO_2 exchange (NEE)

In this section, the CO_2 exchange estimated via eddy covariance and via the LandscapeDNDC model framework is shown. Main aspects concerning the eddy covariance measurements include the gap-filling procedure, and diurnal and seasonal courses, as well as, annual sums of NEE, GEP, and R_{eco}. After a discussion of uncertainty, a short discussion of the CO_2 exchange during snow covered periods is following.

Main results from the LandscapeDNDC model simulations are the relative contributions of grass, trees, and soil to ecosystem fluxes, as well as the prediction of the carbon balance development of the Lackenberg site during the next years (mid-term and long-term). The most important results of this section are published in *Agricultural and Forest Meteorology* (Lindauer et al., 2014)

3.2.1 CO_2 exchange via eddy covariance

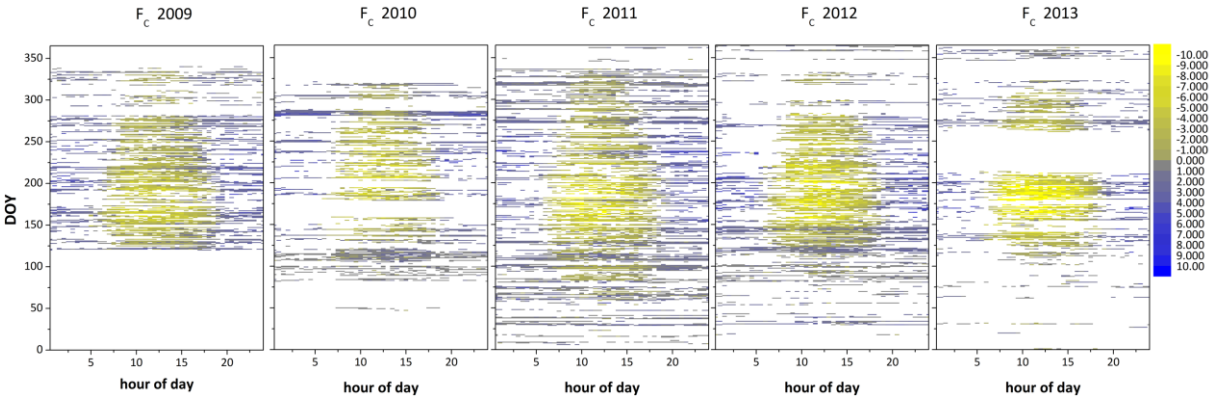

Figure 30: Fingerprints of measured CO_2 fluxes. X-axis shows half-hour of day. Y-axis shows day of year. Each "pixel" represents one half-hourly value. Scale is from blue (net carbon emission) to yellow (net carbon uptake)

Figure 30 shows fingerprints of measured CO_2 fluxes. The measurement period started in the beginning of May 2009. Measured values roughly range from about -15 µmol $m^{-2} s^{-1}$ (net carbon gain) at daytimes in summer to 7 µmol $m^{-2} s^{-1}$ (net carbon emission) at nighttime. White space indicates missing values caused by, for instance, bad weather conditions, technical problems, or quality criteria (see section 2.4.4). Despite the missing values, it is obvious that summertime day-time net fluxes are negative, indicating that GEP exceeds ecosystem respiration during such time periods. Considering the substantial amount of dead-wood of about 4 kg C m^{-2} (Wolpert, 2012) lying on the ground and the short time-period after the storm event, this result was somewhat surprising. In fact, we assumed the area to be a net source of carbon at daytime in summer, as well. Relatively cold tem-

peratures and the fact that much of the coarse woody debris (CWD) is not yet in direct contact with the soil, and thus stays relatively dry, are likely causes for reduced decay processes in this disturbed ecosystem. In addition the remaining and new emerging vegetation (see section 2.1) leads to an already strong GEP.

For calculating annual sums of NEE and its component fluxes R_{eco} as well as GEP all gaps in Figure 30 have to be filled. Hence gap-filling of missing values is very important. For this gap-fill-modeling we use a standard method with site specific biophysical information (section 2.4.4.). As the measured net flux consists of two opposing/different (R_{eco}/GEP) processes they were modeled separately.

3.2.1.1 Nighttime CO_2 Fluxes - R_{eco}

R_{eco} can be directly derived from nighttime CO_2 measurements. At the Lackenberg site there is only sparse vegetation and a high amount of dead-wood is lying on the ground hence most of the respired CO_2 is assumed to come from the soil or the surface. Thus, the model for ecosystem respiration was derived by plotting nighttime CO_2 fluxes against soil temperature in 4 cm depth. Higher R^2 values

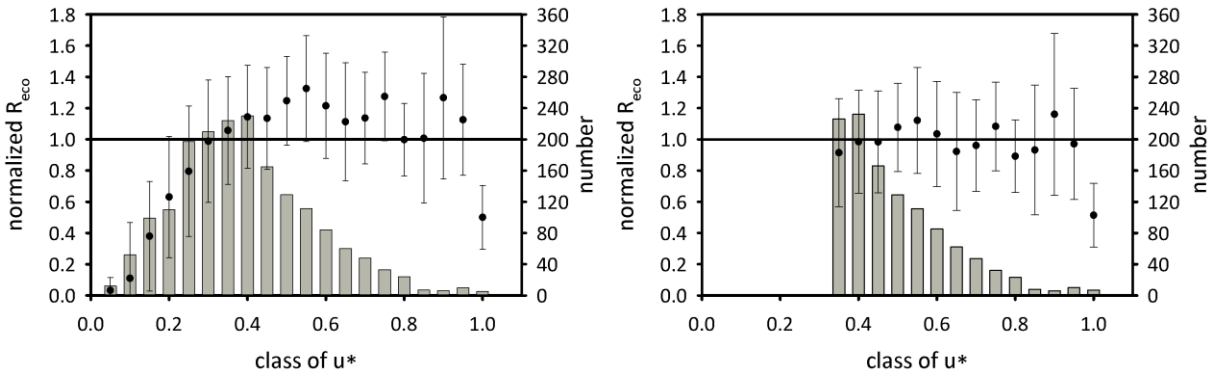

Figure 31: Normalized R_{eco} – i.e. ratio between measured and modeled values – against binned values of u_*. Black circles denote the average within the u_*-bins; error bars show one standard deviation; grey bars show number of values within the u_*-bins. Left: model was derived using all values. Right: model was derived only using flux values with $u_* > 0.3 ms^{-1}$ (exemplarily for 2009).

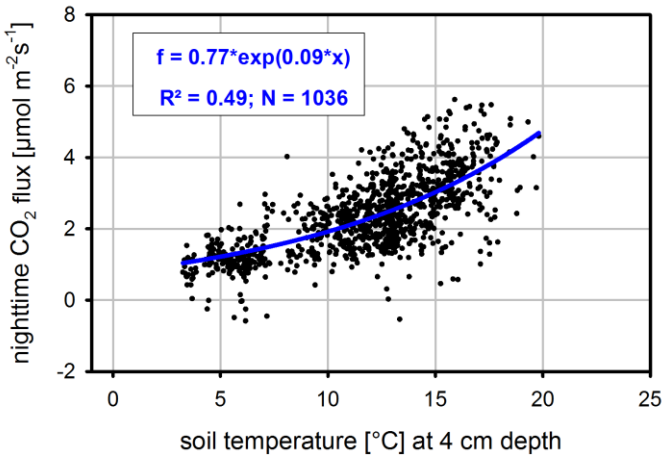

Figure 32: Nighttime CO_2-fluxes against soil temperature. u_*>0.3 ms^{-1}; exemplarily shown for 2009 (all year).

compared to plotting nighttime respiration against air temperature or surface radiation temperature confirmed this assumption. Values were defined as nighttime values if global incoming shortwave radiation (R_g) < 20 Wm^{-2}. Missing values of soil temperature were modeled according to Figure 20. As already explained in the methods (section 2.4.4) it is very likely to underestimate respiration during calm nights using the EC method.

Therefore, we rejected every flux value where there was not enough turbulent mixing using a u_*-filter. To derive a threshold for distinguishing between non-turbulent and turbulent conditions we plotted normalized R_{eco} (i.e. the ratio between measured values and modeled values of nighttime respiration) against binned values of u_* (Exemplarily shown for 2009 in Figure 31). It is obvious that at about a u_* value of 0.3 ms^{-1} fluxes became independent of u_*. Therefore, if u_* was below 0.3 ms^{-1} the estimated CO_2 flux was rejected and replaced by a modeled value. In Figure 31 left, the plateau is at about 1.2 of normalized R_{eco} because all values were used to estimate this first model. After rejecting all flux values with $u_* < 0.3$ m s^{-1}, normalized R_{eco} is at about 1.0 as it should be by definition (Figure 31 right). The final model for ecosystem respiration was derived by plotting measured nighttime fluxes which have a u_* value bigger than 0.3 m s^{-1} against soil temperature (see Figure 32). This u_*-threshold of 0.3 m s^{-1} was also applied to derive R_{eco} models for the other years.

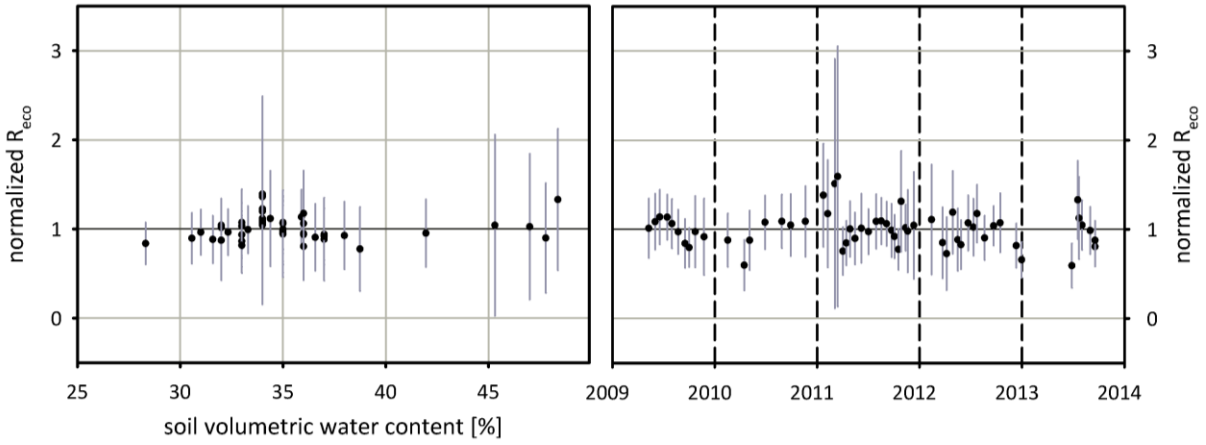

Figure 33: Binned values (n=100) of normalized ecosystem respiration plotted against volumetric soil water content (left) and against time (right). Error bars show one standard deviation.

As can be seen in Figure 33 no marked relationship could be recognized between normalized R_{eco} and volumetric soil moisture or season. Therefore, the model for ecosystem respiration was derived from measurements over one whole year and without adopting for different soil moisture conditions or seasonal aspects.

Coefficients for the respiration model in 2009, 2010, 2011, 2012, and 2013 are shown in Table 5.

In contrast to the nighttime model, the model for daytime values has to be adapted to the seasonal stage of plant development. In deciduous forests, for instance, this is mostly not a big problem. At this the model

Table 5: Model parameters for the R_{eco} model (equation (6), uncertainty estimates in brackets)

	a (R_0)	b	Q_{10}	R^2	n
2009	0.77 (0.04)	0.09 (0.003)	2.48	0.49	1036
2010	0.63 (0.03)	0.11 (0.003)	2.88	0.69	643
2011	0.58 (0.02)	0.11 (0.002)	2.97	0.71	1923
2012	0.78 (0.03)	0.10 (0.002)	2.59	0.65	1337
2013	0.93 (0.04)	0.09 (0.003)	2.46	0.54	656

periods can be divided into growing season and non-growing season while the growing season lasts from bud-burst until leaf-fall. However, at the Lackenberg site with its young and mixed vegetation it is not easy to define sharp borders of the growing season.

3.2.1.2 Growing season – vegetation period

There are several methods to estimate the length of the growing season of an ecosystem. One way is to estimate the beginning of bud burst of the predominant species of the ecosystem. Menzel (1997) and Menzel & Fabian (1999) developed a model for estimating the beginning of bud burst considering the number of cold days in the recent winter. According to this model the beginning of spruce bud burst at the Lackenberg site would have been at about 14.05.2009, 29.05.2010, 18.05.2011, and 10.05.2012, respectively. Another model has been developed by Rötzer et al. (2004), where bud burst starts if a critical temperature sum is reached until DOY = 140. Applying this method to the Lackenberg site, the critical temperature sum was not reached in any year of the measurement period. Therefore, the burst would have been on DOY 140 (20.05) at all five years for the Lackenberg site based on this model. However, at the Lackenberg site there are only few spruces remaining which are still very young. Thus, beginning of the growing season is most probably not equal to the beginning of spruce bud burst.

Knohl et al. (2003), for instance, define the growing season from the first day when daily NEE was negative until the last day when it was negative. As there were few days during the measurement period with no missing value it is not possible to estimate the growing season based on daily NEE. Dragoni et al. (2011) define start of growing season not only if daily NEE is negative but on the first day when NEE during daytime goes down. Applied to the Lackenberg site, growing season would have been started on 08.05.2009, 17.05.2010, 25.03.2011, 28.04.2012, and 26.04.2013, respectively.

The end of the growing season can, for instance, be estimated after Wilpert (1990), saying that the growth of xylem ends if the running mean air temperature on 5 consecutive days is below 10°C but not later than October 5th. Based on this method end of xylem growth at the Lackenberg site would have been on 03.10.2009, 31.08.2010, 22.09.2011, 14.09.2012, and 05.10.2013.

A general method is to define the growing season when daily mean air temperature exceeds 5°C (Kolari et al., 2009). Accordingly at the Lackenberg site growing season would be roughly from 02.04.2009 – 11.10.2009 (192 days), 18.04.2010 – 13.10.2010 (178 days), 18.04.2011 – 18.10.2011 (183 days), 10.04.2012 – 14.09.2012 (157 days), and 14.04.2013 – 29.09.2013 (168 days).

It has become clear that it is not possible estimating sharp borders of the growing season at the Lackenberg site. All methods yield several dates resulting in different length of the growing season.

Therefore, the model for GEP was estimated for every month, to account for seasonal differences but keep available data for each model as high as possible. Also this classification according to months is very subjective it is widely used if no sharp borders of the vegetation period could be found (e.g., Morgenstern et al., 2004; Zha et al., 2004).

3.2.1.3 Daytime CO_2 fluxes - GEP

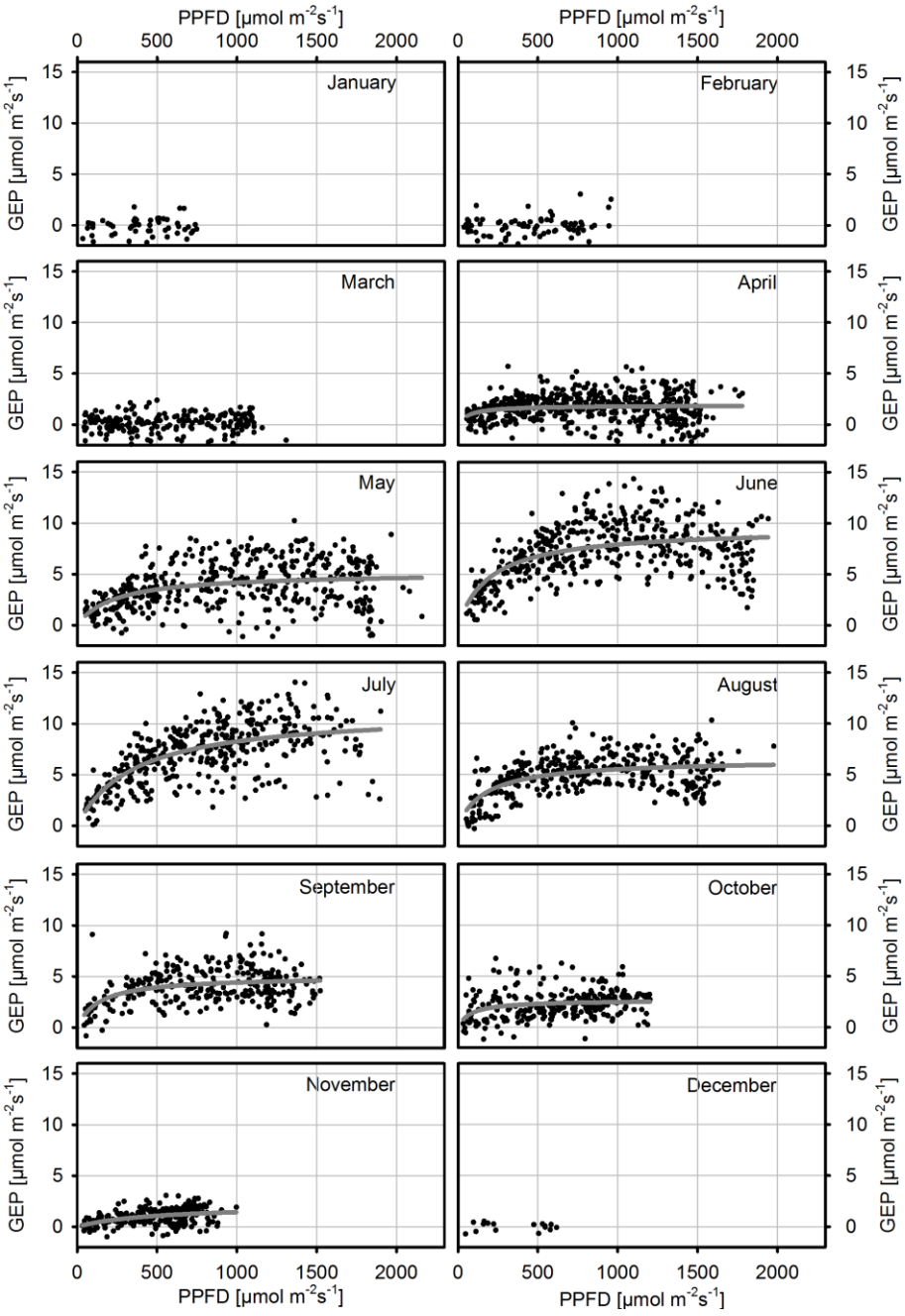

Figure 34: GEP against photosynthetically active photon flux density (PPFD) with hyperbolic regression lines. Exemplarily shown for 2011.

With the relationship shown in Figure 32 R_{eco} could be modeled. With modeling daytime values of R_{eco} it is possible to calculate GEP via GEP ≈ -NEE + $R_{eco_{modelled}}$ (see section 2.4.4). These calculated GEP values were plotted against photosynthetically active radiation or photon flux density (PPFD), respec-

tively (see Figure 34). A hyperbolic Michaelis-Menten-type function was used to model GEP (Equation 10). Before the model could be derived, also all daytime values with $u_* < 0.3$ ms^{-1} were rejected. As GEP is highly variable during the year the parameters for this model were estimated for every month. A clear hyperbolic relationship was generally found not before May. However, in the beginning or at the end of the growing season, it makes no difference whether the model or the average of all measured values of the respective month is used for gap-filling (Figure 34). Therefore, the average was used in April and November. As already mentioned above, no measurements were available before beginning of May in 2009. During this large data-gap from 01.01.2009 to 01.05.2009 GEP was also assumed to be zero because the surface was most probably covered with snow up to this date (see section 3.1). December to March, GEP was set to zero (average of estimated values is zero). Model parameters for the measurement period are shown in Table 6.

Measured GEP values (Figure 34) show high scatter compared to their magnitude leading to the small R^2 values in Table 6 which do not exceed 0.52. The main reason for this high scatter is that GEP or carbon assimilation by photosynthesis is influenced also by environmental factors other than PPFD, including temperature, water or nutrient availability. However, at least in summer months there is a marked hyperbolic relationship visible. Therefore, we decided to use these ecophysiologically-based gap-fill models instead of non-parametric gap-filling methods (Falge et al., 2001).

Table 6: Model parameters for hyperbolic Michaelis-Menten-type GEP model (equation (10), uncertainty estimates in brackets). Due to technical problems no
August 2013. Parameters for July were therefore used for August, as well. Units for α and GEP_{sat} are in [µmol CO_2 $m^{-2}s^{-1}$.

	2009				2010				2011				2012					
	α	GEP_{sat}	R^2	n	α	GEP_{sat}	R^2	n	α	GEP_{sat}	R^2	n	α	GEP_{sat}	R^2	n	α	G
May	0.014	5.10	0.15	408	0.018	3.62	0.15	299	0.022	5.16	0.15	444	0.033	4.09	0.11	545	0.029	
	(0.004)	(0.40)			(0.006)	(0.32)			(0.005)	(0.29)			(0.008)	(0.17)			(0.009)	(
Jun	0.025	8.43	0.41	413	0.028	6.67	0.14	95	0.047	9.55	0.30	421	0.033	11.44	0.51	443	0.042	1
	(0.004)	(0.34)			(0.014)	(0.75)			(0.01)	(0.31)			(0.004)	(0.37)			(0.008)	(
Jul	0.027	9.19	0.40	372	0.036	10.11	0.35	288	0.031	11.21	0.45	385	0.037	11.67	0.52	376	0.041	1
	(0.004)	(0.40)			(0.007)	(0.45)			(0.010)	(0.47)			(0.005)	(0.42)			(0.006)	(
Aug	0.029	6.66	0.32	420	0.026	9.67	0.43	285	0.037	6.49	0.31	354	0.059	8.51	0.15	351		
	(0.005)	(0.23)			(0.005)	(0.54)			(0.008)	(0.22)			(0.012)	(0.28)				
Sep	0.031	5.03	0.19	290	0.044	5.29	0.18	278	0.036	5.01	0.19	280	0.034	6.91	0.23	293	0.046	
	(0.007)	(0.24)			(0.011)	(0.24)			(0.006)	(0.24)			(0.007)	(0.31)			(0.011)	(
Oct	0.033	3.62	0.14	127	0.006	3.83	0.27	189	0.033	2.67	0.07	273	0.090	3.72	0.02	114	0.027	
	(0.012)	(0.32)			(0.003)	(0.79)			(0.007)	(0.17)			(0.107)	(0.43)			(0.007)	(

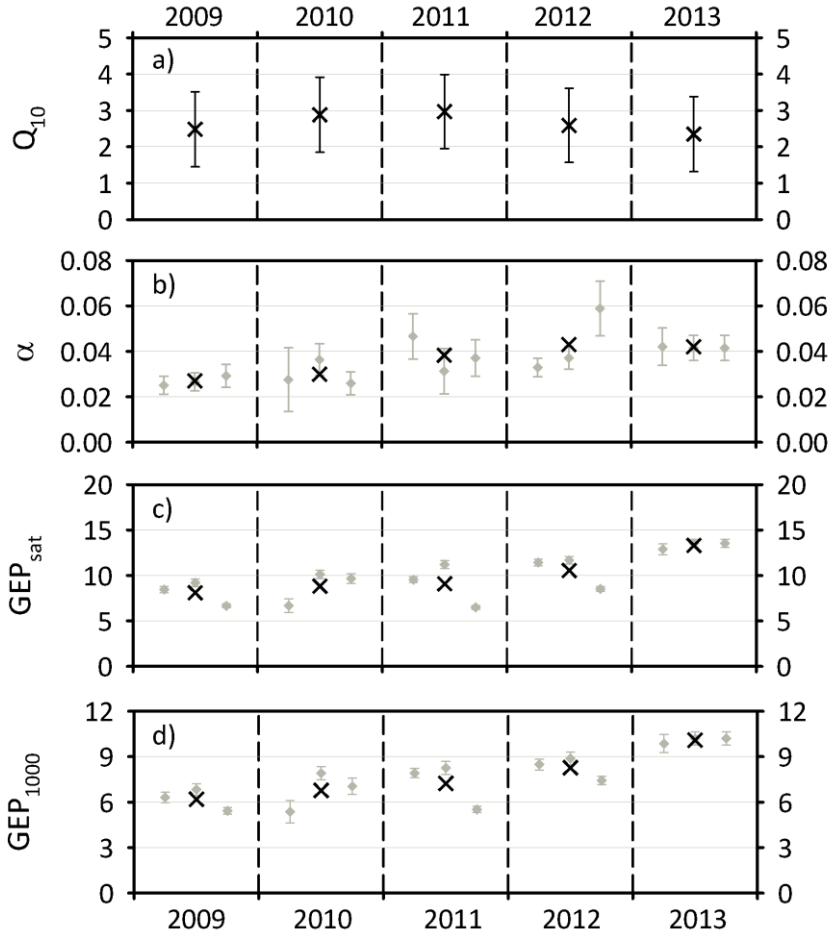

Figure 35: a) Q_{10}; black cross donates the annual value. **b), c), and d)** α, GEP_{sat}, and GEP_{1000}, respectively. Grey diamonds are the values for June, July, and August. Black cross denotes the average of the 3 months. Units for α, GEP_{sat}, and GEP_{1000} are in µmol CO_2 $m^{-2}s^{-1}$.

Figure 35 shows parameters of the data-derived parametric models for flux partitioning and gap-filling from Table 5 and Table 6 as well as GEP_{1000}. Q_{10} generally serves as a measure describing the rate of change of a biological or chemical system after increasing the temperature by 10 °C. Q_{10} values (calculated as $Q_{10} = e^{10b}$) denotes the increase of the respiration rate when temperature is increased by 10◦C. The variations in Q_{10}were small, and it is inconclusive whether the initial increase and later decline is due to offsetting trends in autotrophic and heterotrophic respiration, or whether this simply reflects inter-annual variability. Nevertheless, estimated Q_{10} values are in the range of other comparable European forests (e.g., Van Dijk and Dolman, 2004).

The quantum yield efficiency α (Figure 35b), describes the efficiency of the ecosystem to convert light into fixed carbon. This parameter, as well as GEP_{sat} (GEP at light saturation, Figure 35c), and GEP_{1000}, (GEP at PPFD = 1000 µmol m^{-2} s^{-1}, Figure 35d), steadily increased during the measurement period. α was 0.027 (2009), 0.030 (2010), 0.038 (2011), 0.043 (2012), and 0.042 (2013). GEP_{sat} averaged at 8.09 (2009), 8.82 (2010), 9.08 (2011), 10.54 (2012), and 13.31 (2013) µmol m^{-2} s^{-1}. GEP_{1000} was 6.19 (2009), 6.77(2010), 7.23 (2011), 8.27(2012), and 10.09 (2013) µmol m^{-2} s^{-1}. The compara-

tively low (e.g., Buchmann and Schulze, 1999) but increasing values of α, GEP_{sat}, and GEP_{1000} are a marked indication for the resilience of the ecosystem.

3.2.1.4 Daily and seasonal course of CO_2 fluxes

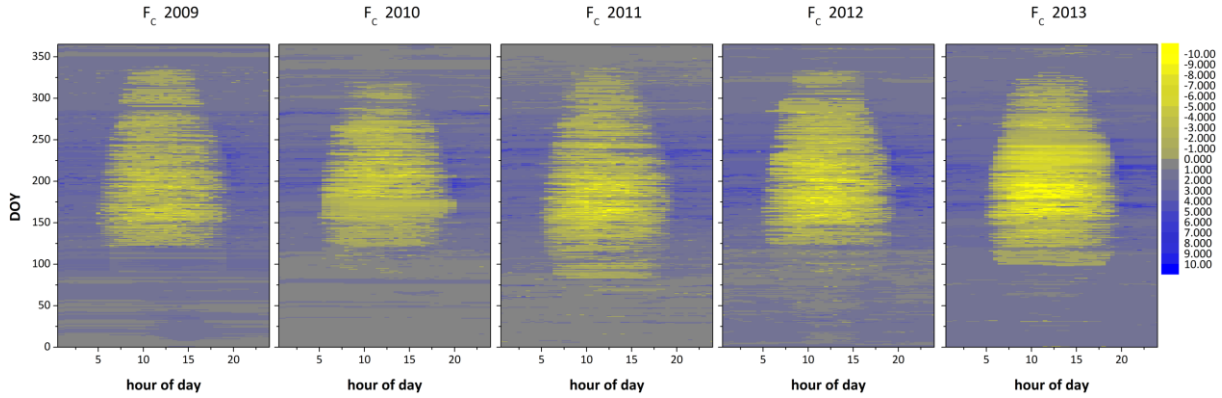

Figure 36: Fingerprints of measured and gap-filled CO_2 fluxes. X-axis shows half-hour of day. Y-axis shows day of year. Each "pixel" represents one half-hourly value. Scale is from blue (positive - net carbon emission) to yellow (negative - net carbon uptake). Values in the legend are in µmol m^{-2} s^{-1}

With the now derived models for R_{eco} and GEP every missing CO_2 flux value can be filled leading to the complete fingerprints in Figure 36. Here one can see the typical "egg-shape" of the negative (yellow) daytime net fluxes in between the positive (blue) nighttime net fluxes. Additionally the start of the growing season is indicated with the relatively sharp border from grey/blue colors to yellow colors in the midday flux values at about DOY 125 (2009), 125 (2010), 80 (2011), 125 (2012), and 100 (2013). However, this could mainly be caused by the gap-filling procedure for GEP (section 3.2.1.3). Time periods with large data-gaps become also apparent in Figure 36. Gap-filling of these periods leads to quite blurred sections in the fingerprints especially in the winter months and for example from DOY 155 – 180 in 2010.

Table 7: Estimated maximum and minimum values of daily carbon fluxes after gap-filling in g C $m^{-2}d^{-1}$. Date is in brackets.

	2009	2010	2011	2012	2013
NEE_{max}	2.6 *(27.04.)*	2.7 *(09.10.)*	2.9 *(27.08.)*	2.2 *(28.04.)*	1.9 *(11.11.)*
NEE_{min}	-1.5 *(05.06.)*	-1.8 *(26.07.)*	-1.9 *(16.07.)*	-2.1 *(18.07.)*	-3.3 *(15.07.)*
GEP_{max}	4.4 *(12.07.)*	5.1 *(01.07.)*	5.0 *(15.06.)*	5.7 (*06.07.*)	7.0 *(21.06.)*
$Reco_{max}$	4.3 *(17.07.)*	5.1 *(16.07.)*	5.1 *(25.08.)*	4.9 (*06.07.*)	5.9 *(03.08.)*
$Reco_{min}$	0.8 *(12.01.)*	0.6 *(07.04)*	0.6 *(06.03.)*	0.7 *(29.03.)*	0.7 *(31.01.)*

From the now available full dataset of CO_2-fluxes, daily, as well as the diurnal courses of CO_2 exchange can be seen. Daily sums of carbon fluxes ranged between -1.5 and 2.6 in 2009, between -1.8 and 2.7 in 2010, between -1.9 and 2.9 in 2011, between -2.1 and 2.2 in 2012, and between -3.3 and 1.9 g C $m^{-2}d^{-1}$ in 2013 (see Table 7 and Figure 37). Thus, the difference between maximum and minimum daily values exhibited an increasing trend during the measurement period, and both maximum R_{eco}, as well as GEP were increasing over these years. GEP increase is attributable to the recovery of the ecosystem, and R_{eco} most likely increased due to the progressive mobilization of

carbon as fallen trees and other CWD continued to collapse and come into contact with the soil and also due to increases in autotrophic respiration as a result of increased GEP.

Daily ecosystem respiration was highest in the summer months and lowest in winter, driven by soil temperature. Daily gross ecosystem production was also highest in early summer, when vegetation was fully established and temperature, as well as PPFD were high (see also Table 7).

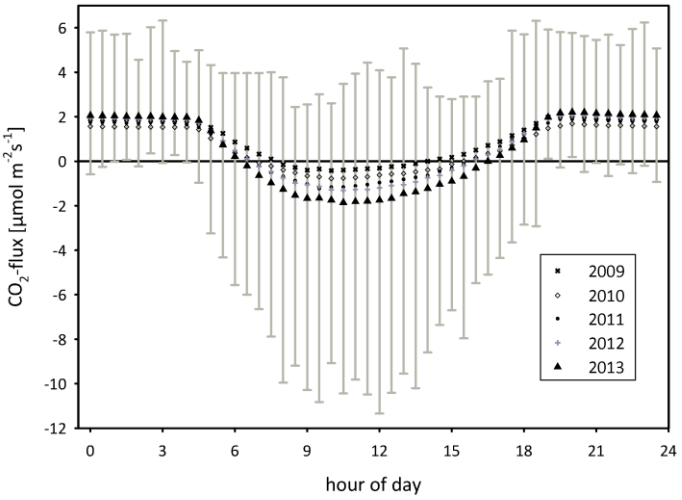

Figure 37: Ensemble half-hourly averages of NEE 2009, 2010, 2011, 2012, and 2013. Error bars indicate the range of values (MIN/MAX) exemplarily for 2011

However, compared to similar intact forest ecosystems the minimum (summed) daily NEE values are quite small. In a mature intact spruce forest, (Tharandt: 50°57'49" N, 13°34'01" E, 380 m a.s.l., distance to Lackenberg ca. 210 km) daily sums of NEE reach values down to -10 g C m^{-2}d^{-1} (Gruenwald and Bernhofer, 2007). Even considering the roughly 1000 m lower elevation of Tharandt, this indicates that the Lackenberg site is still at an early recovery stage.

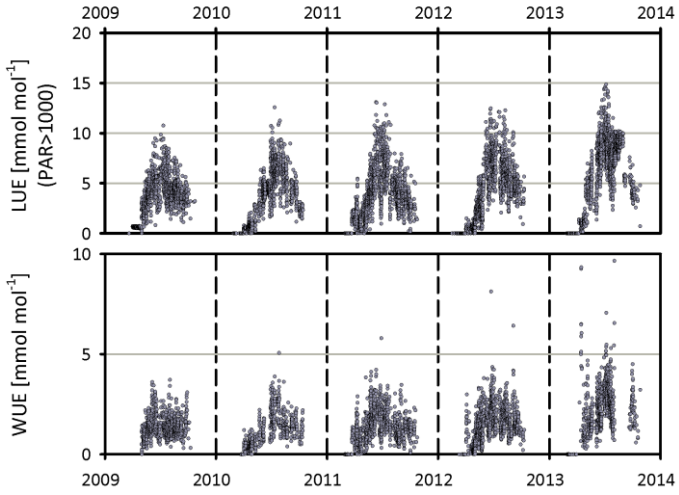

Figure 38: Light-use-efficiency (LUE) and water use efficiency (WUE) at the Lackenberg in 2009, 2010, 2011, 2012, and 2013. Only values with PPFD > 1000 µmol m^{-2} s^{-1} have been used.

Light-use-efficiency (LUE) can now be calculated as $\frac{GEP}{PPFD}$ if PPFD > 1000 µmol m^{-2} s^{-1} and averaged at 3.5 (2009), 3.7 (2010), 3.7 (2011), 3.9 (2012), and 6.0 (2013) mmol mol^{-1}, respectively. Maximum half-hourly values of LUE reached about 15 mmol mol^{-1} (Figure 38). Water-use-efficiency (WUE) was calculated as $\frac{GEP}{F_a}$ where F_a is the water vapor flux in mol m^{-2}s^{-1} estimated by EC method. WUE averaged at 1.4 (2009), 1.3 (2010), 1.4 (2011), 1.5 (2012), and 2.4 (2013) mmol mol^{-1} (Figure 38). LUE, as well as WUE tend to increase during the measurement period, again suggesting an increase of plant biomass and therefore indicating the expected recovery of the upland forest ecosystem.

3.2.1.5 Annual sums of NEE

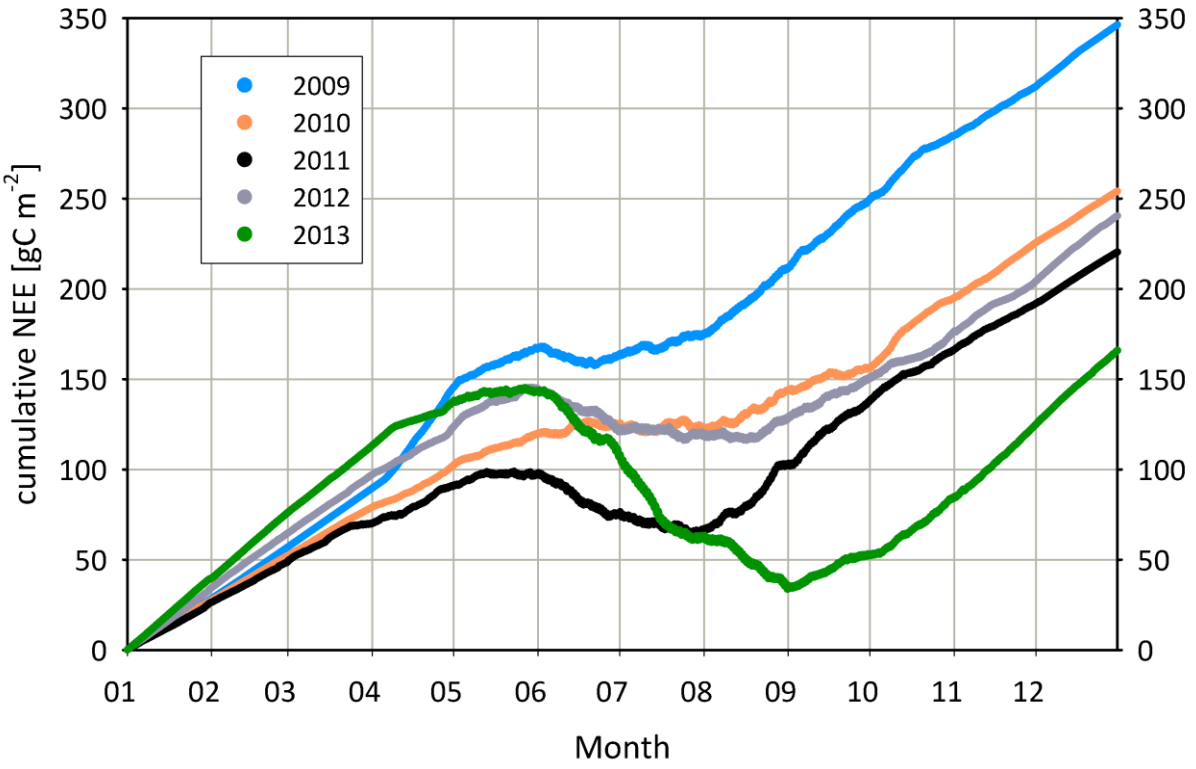

Figure 39: Cumulative NEE for 2009, 2010, 2011, 2012, and 2013.

Annual patterns of cumulative NEE (see Figure 39) at the Lackenberg site showed an almost constant carbon emission rate from about October to March or April. In the summer months there is a short time period of net carbon gain (slope of the curve is negative), which is highly variable in length and intensity over the five-year measurement period. Annual NEE was estimated at 347, 255, 221, 240, and 167 g C $m^{-2}yr^{-1}$ from 2009 to 2013. Therefore, the wind-throw-disturbed ecosystem was overall still a marked source of carbon two to six years after Kyrill. It is to say that no NEE measurements were available before May 2009, thus the time period from January till May 2009 is completely modeled, making uncertainty high. The cumulative patterns of NEE show similar behavior during autumn and winter. During this time period CO_2 is lost to the atmosphere with almost the same intensity in all five years. The length of the time period with net carbon uptake was varying during the 5 years as well as the month with maximum carbon uptake or maximum carbon emission (Table 7), respectively. Main differences between the annual patterns of NEE within the five years can only be found during spring and summer.

3.2.1.6 Flux partitioning

In Figure 39 we can see a reduction of the ecosystem's source strength from 2009 to 2011 while in 2012 annual NEE was little higher again. The question is whether this development can be fully ac-

credited to either R_{eco} or GEP. To answer this question annual NEE was separated in annual sums of ecosystem respiration and gross ecosystem production. If the decreasing annual NEE would clearly show the recovery of the ecosystem, as it would be expected from the classical theories (see section 1.5), we would see an equivalent increase in GEP, while ecosystem respiration would either be constant or gradually declining during the measurement period. Annual sums of net ecosystem exchange (NEE), ecosystem respiration (R_{eco}), and gross ecosystem production (GEP) are shown in Figure 40 for 2009, 2010, 2011, 2012, and 2013.

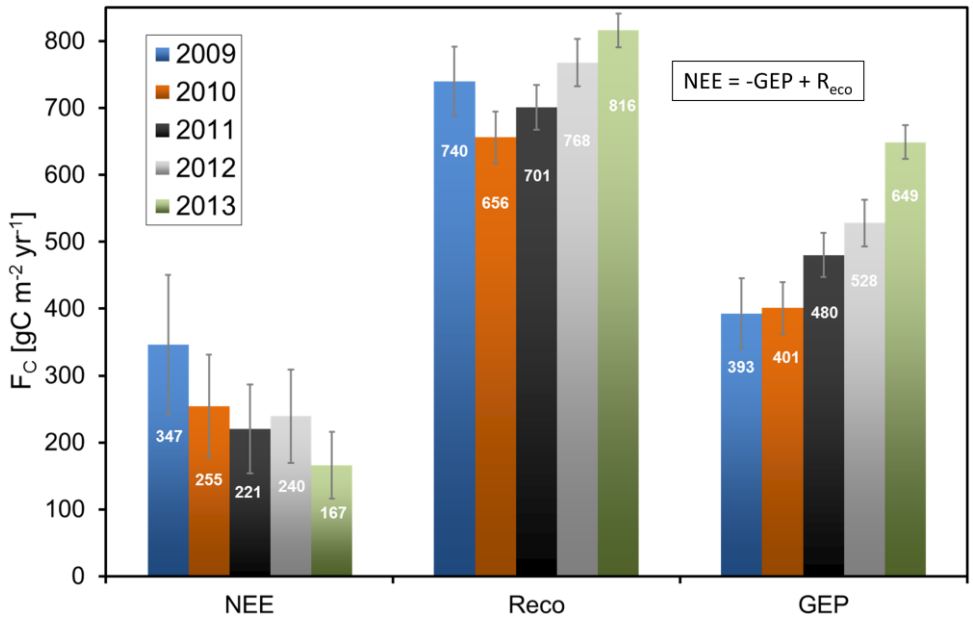

Figure 40: Estimated annual sums for net ecosystem exchange, ecosystem respiration, and gross ecosystem production. Uncertainty estimates are derived from an ad-hoc Monte Carlo simulation (see section 3.2.1.7)

Looking at Figure 40 one can see a marked increase in GEP during the measurement period from 393 (2009) to 649 g C $m^{-2}yr^{-1}$ (2013). The increase in GEP shows that the ecosystem is already able to fix a considerable amount of atmospheric carbon during the vegetative season. At the same time ecosystem respiration ranges between 656 and 816 g C $m^{-2}yr^{-1}$ and therefore clearly exceeds GEP.

To conclude, despite a clear trend to higher carbon uptake in annual GEP the annual R_{eco} and thus, also NEE values are quite variable. This maybe confirms the assumptions of other studies. Harmon et al. (2011), for instance, stated that post-disturbance R_{eco} does not always follow the monotonic decline assumed in the theory (also see: Janssens et al., 2001). The downward trend in annual NEE as we would expect it, deriving from the successional development of the ecosystem is most likely still masked by environmental drivers e.g., substrate availability, annual weather conditions, or length of growing season.

3.2.1.7 Uncertainty of annual NEE

With equation (3) the budget equation of carbon on ecosystem scale was shown. As mentioned in 2.4.4 all chemical forms of carbon should be considered when estimating annual sums of carbon exchange (Lovett et al., 2006; Randerson et al., 2002). The contribution of chemical compounds other than CO_2 is assumed to be negligible (e.g., Schmid et al., 2003). Furthermore, the coniferous vegetation is still sparse at the Lackenberg site. Lateral carbon fluxes, for example, dissolved organic carbon (DOC) were assumed to be negligible, as well. Runoff DOC estimates adjacent to the study site of less than 5 g C $m^{-2}yr^{-1}$ (Beudert B., personal communication) confirm this assumption.

Although the EC method has been used for many years now to estimate carbon exchange in different ecosystems there is still an intensive debate about the uncertainties related to this method. While the uncertainty of single half-hourly or hourly values is usually estimated to be about 10-20% (Foken, 2008), stating the uncertainty of annual sums of net ecosystem exchange is not trivial and the "universal best method" has not been found yet. An extensive description and discussion of all errors and uncertainties regarding to eddy covariance measurements can be found, for instance, in Richardson et al. (2012). Generally uncertainties can be divided into random errors and systematic errors. Random errors include variability among averaging periods, inadequate sample size, varying flux footprint, or random noise in the signal. Systematic errors might be for example inadequate height above the surface, incorrect application of the used corrections, or calibration errors. A more detailed explanation and discussion of systematic and random errors is given, for instance, in Loescher et al. (2006), or in Moncrieff et al. (1996). Even if we can distinguish between random and systematic errors in theory, the uncertainty of every measured flux is most likely a combination of both (Moncrieff et al., 1996). The resulting uncertainty due to random error is generally assumed to have a very small influence on the annual NEE (Baldocchi, 2008). Moncrieff et al. (1996) estimated that the annual random error is reduced to $1/\sqrt{N}$. However, Schmid et al. (2003) reported that this would only be the case if assuming statistically independent samples which is questionable regarding to EC measurements.

Derived from several studies Elbers et al. (2011) set the measurement error of annual NEE to ±5%. Hagen et al. (2006) found the uncertainty of annual NEE to be in the order of about 10%. However, if annual values of NEE are very small these relative values likely would lead to a underestimation of the uncertainty. Dragoni et al. (2007) investigated the cumulative effect of random errors on annual sums of NEE. They found out that the uncertainty of annual NEE mainly depends on the contribution of the gap-filling model. Furthermore, their results show that the impact of random errors to annual NEE was very small compared to potential systematic errors. Systematic errors can contribute much

more to the uncertainty of annual NEE than random errors (Lee et al., 2004; Massman and Clement, 2004).

Generally, there are three methods to estimate the random uncertainty for annual NEE (Richardson et al., 2012). The paired tower approach (Finkelstein and Sims, 2001; Hollinger and Richardson, 2005; Rannik et al., 2006), the 24h differencing approach (Hollinger and Richardson, 2005; Richardson et al., 2008), and the model residual approach (Lasslop et al., 2008; Richardson and Hollinger, 2005; Stauch et al., 2008). With the paired tower approach another tower with EC instrumentation is used as reference for calculating the random error. By contrast, the 24h approach uses the flux measured exactly 24h later at the same place under similar environmental conditions as reference. Differences between modeled and observed values are used to estimate the random uncertainty via the model residual approach. Using this approach it is assumed that the model error is negligible and all residuals derive from the random error.

Estimating the uncertainty via the model residual approach is described, for instance, in Moffat et al. (2007), or in Aurela et al. (2002).

Estimating the effect of random errors on annual integrated NEE Kochendorfer et al. (2011) assume a typical daytime NEE random error NEE_{growth} of 20 µmol $m^{-2} s^{-1}$ and calculated the annual random error ΔNEE_{rand} via:

$$\Delta NEE_{rand} = \sqrt{\sum_{i}^{17520} (NEE_{growth} \Delta t)^2} \qquad (12)$$

This worst-case scenario yields an annual random uncertainty of about ±57 g C $m^{-2} yr^{-1}$ At the Lackenberg site, even in summer measured daytime fluxes did not fall below -15 µmol $m^{-2} s^{-1}$ during the measurement period and the random error of each half-hourly value is therefore assumed to be much below 20 µmol $m^{-2} s^{-1}$ (Figure 41). Furthermore, it is most unlikely, that the random error accumulates in one direction only. Thus, the above mentioned uncertainty of ±57 g C $m^{-2} yr^{-1}$ is most probably too high for the Lackenberg site.

In this work the 24h approach (Richardson et al., 2006) was therefore applied to estimate the distribution of random errors during one year. As suggested by Hollinger and Richardson (2005) environmental conditions are similar if PPFD is within 75 µmol $m^{-2} s^{-1}$, T_{air} is between 3 °C, wind speed is within 1 m s^{-1}, and vapor pressure deficit is within 0.2 kPa. The random error ε was defined as

$$\varepsilon = \frac{(\sigma_t - \sigma_{t+24h})}{\sqrt{2}} \quad (13)$$

where σ_t is an estimated flux at time t and σ_{t+24} an estimated flux 24 hours later. 174, 150, 314, 180, and 94 observations in 2009 to 2013 could be found were the environmental conditions were similar with random error averages of 0.16, 0.06, -0.09, -0.01, and -0.15 µmol $m^{-2} s^{-1}$, respectively. The distribution of errors is shown in Figure 41. Assuming a random error of ±2 µmol $m^{-2} s^{-1}$ (over 95% of all estimated errors are within these borders) and applying equation (12) would yield an annual random error of ± 6 g C $m^{-2} yr^{-1}$. However, by comparing the 24h approach with the paired observations approach, Dragoni et al. (2007) found out that the 24h approach likely overestimates annual random error by as much as a factor of two.

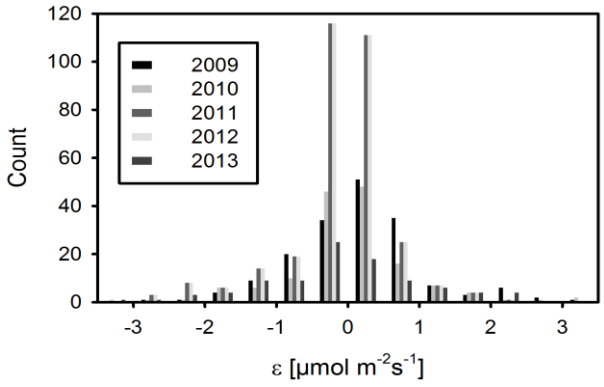

Figure 41: Distribution of ε estimated with 24h approach for 2009, 2010, 2011, 2012, and 2013.

However, it should be kept in mind that the potential magnitude of an unknown systematic bias could markedly exceed these uncertainties (Dragoni et al., 2007; Loescher et al., 2006).

By contrast to the random uncertainty the systematic uncertainty is much more difficult to constrain when calculating annual sums of NEE with the eddy covariance method (see beginning of this section). The best example for that is probably the correction for advection which has not been achieved yet (Aubinet et al., 2010). A careful selection of the measurement site, appropriate measurement set up, regularly instrument calibrations, and strict quality control of the measurements can keep the uncertainty related to the systematic error small. Baldocchi (2003), for example, stated that if measuring in nearly ideal sites uncertainty of annual NEE estimates is less than ±50 g C m^{-2}

However, often used for indicating systematic error of eddy covariance measurements is the surface energy balance closure, i.e. the regression between net radiation minus soil heat flux against fluxes of sensible and latent heat. Ideally the slope of this regression should be 1. Usually the residual in this closure of the energy balance is about 30% depending mainly on the measurement site and time of the day. Although measured with the same instrument the closure of the energy balance does not allow any sound statement about the uncertainty of NEE as it is by no means sure, that the residual can be fully accredited to the EC measurement (Schmid et al., 2003). Additionally it is by no means clear whether the residual is a result of inadequate measurement or, for instance, other atmospheric phenomena which cannot be detected by the EC method, like large scale transport mechanisms

(large eddies with time-scales longer than an averaging interval of 30 or 60min), or non-propagating circulations (eddies that are not transported by the mean wind) (Mahrt, 2010; Mauder et al., 2010; Mauder et al., 2013). Foken et al. (2012) therefore suggested to correct fluxes of water vapor and sensible heat to close the energy budget but not to apply this correction for fluxes of carbon dioxide or other trace gases.

By contrast, Mauder et al. (2013) suggested to indirectly correct for a systematic error of the measured CO_2-fluxes resulting from non-propagating circulations using the residual of the surface energy balance closure. As these non-propagating circulations only can occur in a convective boundary layer (Mauder et al., 2010), this method is only applicable to daytime fluxes (selective systematic error). Applied to the present study, the selective systematic error of CO_2-fluxes attributed to the energy balance closure would be -2, -13, -7, -18, and -32 g C $m^{-2}yr^{-1}$. However, since the correction of systematic and selective systematic errors is still under debate annual sums of NEE of this study were not corrected for this selective systematic error.

A detailed discussion concerning the energy-balance-closure-problem can be found in Foken et al. (2011) or in Mauder et al. (2007). Nevertheless, even if the closure of the energy balance should not be used for estimating uncertainty of EC measurements it can still serve as an indicator whether the EC method is applicable at a particular site. As can be seen in Figure 42 with a residual of 15% the energy balance closure at the Lackenberg site is in the range of most eddy covariance sites (Li et al., 2005b; Wilson et al., 2002).

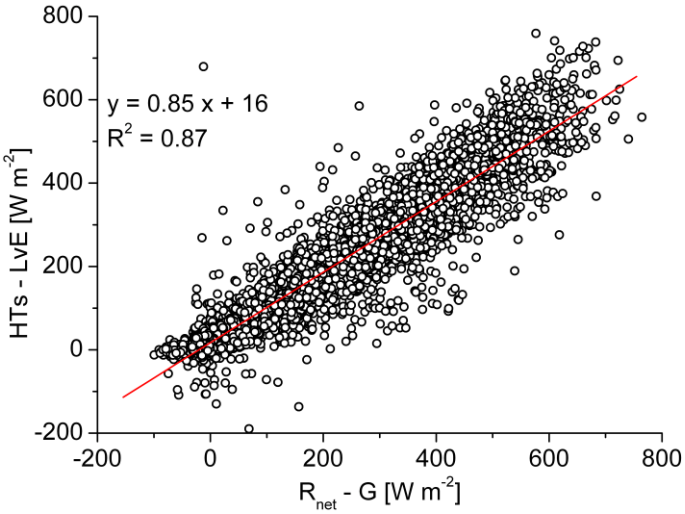

Figure 42: Energy balance closure – exemplarily shown for data from 2009 and 2010. X-axis shows net radiation (R_{net}) minus soil heat flux (G). Y-axis shows turbulent fluxes of sensible (HTs) and latent heat (LvE). Graph from Wolpert (2012).

Defining an adequate u_*-threshold (see section 3.2.1.1) is also a marked source of uncertainty regarding to gap-filled annual sums of NEE. Abdicating the u_*-filter, for instance, would lead to a marked underestimation of annual NEE of 70 g C $m^{-2}yr^{-1}$, exemplarily for 2011. This large difference again demonstrates why the u_*-filter is that important and why it is still that highly debated in the literature (see 2.4.4).

Due to missing values, caused by this u_*-filter but also caused by bad weather conditions or technical problems, the gap-filling procedure has the biggest impact on uncertainty of annual NEE estimates

(Dragoni et al., 2007). To get information about the overall impact of the used gap-filling procedure on the uncertainty of annual NEE we compared our results with some other gap-filling models. The gap-fill modeling after Reichstein et al. (2005), as well as the gap-fill modeling after Lasslop et al. (2010) were used to fill missing values of our dataset. This was done using an online flux partitioning and gap-filling tool from the Max Planck Institute for Biogeochemistry in Jena, Germany (http://www.bgc-jena.mpg.de/~MDIwork/eddyproc/). A comparison of all respective results is shown in Table 8.

Table 8: Estimates of annual NEE (in g C m^{-2}) at the Lackenberg site using different gap-filling methods; u_*-filter is set to 0.3 ms^{-1}.

	local gap-fill modeling	Reichstein et al. (2005)	Lasslop et al. (2010)
2009	**347**	342	433
2010	**255**	219	223
2011	**221**	241	240
2012	**240**	226	318
2013	**167**	129	n.a.

The algorithm of Reichstein et al (2005) did not gap-fill the first months of 2009 as there are no measurements available. However, the R_{eco} values derived from the flux-partitioning sequence were available for this time period. We therefore added the sum of all these R_{eco} values from 01.01.2009 - 01.05.2009 to the integrated NEE values derived by the online-tool for the rest of the year to get the annual NEE.

Results of Table 8 demonstrate that estimated annual NEE values derived by different gap-filling models are in good agreement (also see: Stoy et al., 2006) with maximum differences in annual NEE ranging from 20 to 86 g C m^{-2}. Although such a comparison can give a kind of feeling how the estimated annual NEE results should be classified, it cannot provide definite and absolute information about the uncertainty.

The models for the gap-filling, used in this study, both have a certain range of uncertainty. Using a Monte Carlo simulation the distribution of all possible NEE results can be obtained by running the models with every possible parameter value (bootstrapping) within its uncertainty range (usually 95% confidence). For estimating the gap-filling uncertainty in annual NEE estimates such an ad hoc Monte Carlo simulation (Zeeman et al., 2010) for 2012 yields an uncertainty of annual NEE in the order of ±70 g C m^{-2} (95% confidence) which corresponds to about 30% of annual NEE. Due to limitation of time this could not be conducted to the other years. Since the random error is very small compared the error deriving from the gap-filling procedure (e.g., Dragoni et al., 2007) the ±30% serve as total uncertainty of the estimated annual NEE values in this work.

Therefore, the absolute uncertainty of annual NEE in this study is 347 ±104, 255 ±77, 221 ±66, 240 ±70, and 167 ±50 g C m^{-2} for 2009, 2010, 2011, 2012, and 2013. Anyway, for the upcoming years the uncertainty should be calculated by Monte Carlo simulation for each single year, because NEE values get more and more small, thus, requiring an absolute value of uncertainty.

3.2.1.8 R_{eco} during snow covered periods

Estimating and understanding properly gas-exchange processes beneath, or within a closed snow cover is still an ongoing process due to lack of data especially in mid-latitudes with seasonal snow cover (Liptzin et al., 2009; Massman, 2006; Mast et al., 1998; Williams et al., 2009). Methods to estimate CO_2 exchange beneath, through, or above a closed snow cover include among others eddy covariance, soil cambers, or gradient technique (Ilvesniemi et al., 2005; Liptzin et al., 2009; Monson et al., 2006a).

However, it is clear that winter is by no means a period of low activity regarding to CO_2 exchange processes (Brooks et al., 2005; Wang et al., 2011). Monson et al. (2006a) reported that wintertime CO_2 efflux in a subalpine forest in the Rocky Mountains made up 7-10% of annual NEE. Liptzin et al. (2009) estimated that at their site at Niwot Ridge, Colorado, wintertime CO_2 efflux contributed about 30% to the annual NEE. They also stated that their measured flux values were with about 0.71 to 0.86 µmol $m^{-2} s^{-1}$ among the highest reported in the literature for snow covered ecosystems. Ilvesniemi et al. (2005) estimated wintertime CO_2 efflux in a boreal Scots pine stand, Finland, to be in the order of 28 – 39 g C m^{-2} (soil chamber measurements) and 66 - 90 g C m^{-2} (eddy covariance measurements). Their reported wintertime fluxes ranged from 0.95 - 2.21 µmol $m^{-2} s^{-1}$ in early November to < 0.13 µmol $m^{-2} s^{-1}$ in January and February. Schindlbacher et al. (2007) reported wintertime carbon fluxes from a mountain forest in Tyrol, Austria, of about 0.64 µmol $m^{-2} s^{-1}$. Their estimated accumulated carbon efflux during snow covered period was 62 g C m^{-2} (12% of total annual soil respiration).

The thickness of the snowpack significantly influences beneath snow microbiological activity (and thus the magnitude of respiration) because insulation effect of snow can keep soil temperature high even all winter long (Groffman et al., 2001; Mast et al., 1998; Monson et al., 2006b). Zimov et al. (1996) stated, that global warming, could release large amounts of carbon that are presently stored in permafrost. However, there is also much discussion to what extend other factors like substrate availability/quality or soil moisture contributes to controlling wintertime CO_2-efflux.

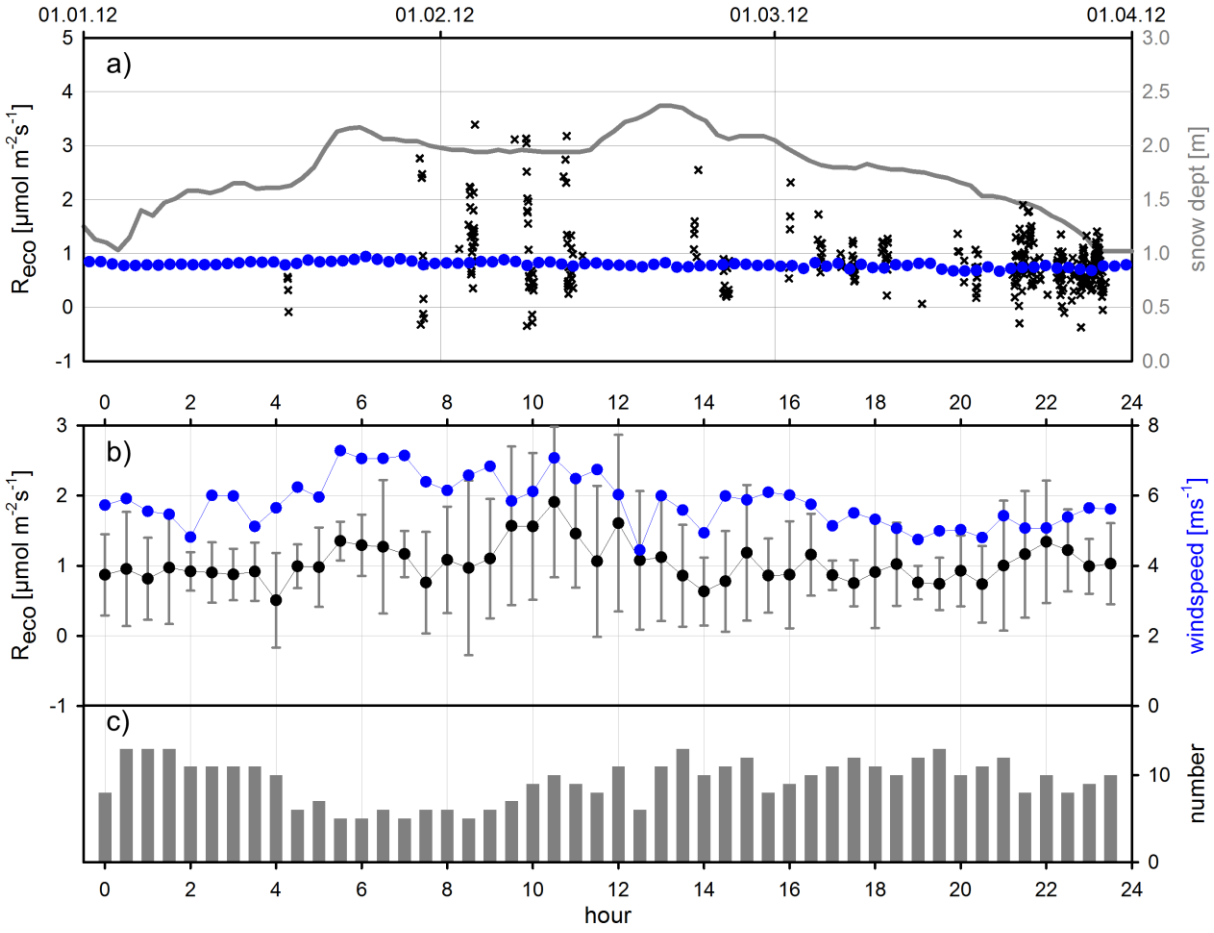

Figure 43: Respiration under snow covered conditions exemplarily shown for beginning of 2012. **a):** snow depth from the German weather service (DWD) station at Großer Arber (light blue line); measured high quality flux values (black x); **b):** ensemble mean of measured half hourly CO_2-flux values (black dots - error bars show 1σ) and ensemble half-hourly wind speed (blue dots) for the time period of the upper graph; **c:** grey bars show number of measurements in each half hour.

The five year measurement period of this study also includes numerous EC-measurements during snow-covered periods. Thanks to frequent fair weather conditions, over 400 measured half-hourly quality controlled CO_2-flux values were available during times when snow depth was more than 1 m, in winter 2012. This is more than in all three previous winters (2009, 2010, and 2011) together. An example time series plot of measured CO_2-flux values is shown in Figure 43 for January to March 2012. Measured CO_2-flux values show high scatter and range from -0.4 to 3.4 µmol m^{-2} s^{-1} during this time. No dependency on snow depth can be seen. The lower graph in Figure 43 shows that ensemble average efflux is about 0.5 to 1.5 µmol m^{-2} s^{-1}, which is quite high considering the high snow depth (Figure 44). This relatively high CO_2-efflux, despite the high snow-depth, shows a weak correlation with mean wind-speed (R = 0.46), and thus may point to gas exchange mechanisms such as pressure pumping, as described in Massman (2006)

Figure 44: Picture from webcam at the Lackenberg main tower on 27.12.2011. Snow depth can be estimated visually from the depth marker (pole - blue arrow) which is 2 m. Division marks are 20 cm. Therefore, snow-dept on this day was about 1 m.

or Bowling and Massman (2011), where pressure fluctuations can significantly enhance diffusive fluxes through snowpack. However, currently available data are insufficient to draw a conclusion here. Estimated flux-values during the snow-covered periods are shown in Table 9.

Table 9: Estimated CO_2-fluxes during snow-covered (> 1 m) periods.

	2009/2010 31.01.2010 - 31.03.2010	**2010/2011** 13.12.2010 - 05.02.2011	**2011/2012** 21.12.2011 - 19.04.2012	**2012/2013** 29.11.2012 - 24.04.2013
maximum measured NEE [µmol $m^{-2} s^{-1}$]	1.76	3.80	3.40	3.38
maximum daily avg after gap-filling [µmol $m^{-2} s^{-1}$]	0.90	1.06	1.03	1.36
avg measured	0.60 (n=118)	0.94 (n=225)	1.10 (n=470)	0.65 (n=299)
daily-sum after gap-filling [g C m^{-2} day^{-1}]	0.87	0.87	0.84	1.24
Total R_{eco} per period [g C m^{-2}]	52	48	125	182

3.2.2 CO_2-exchange via Landscape DNDC

In conditions where storage-change or advective transport can be neglected, eddy-covariance measurements represent the net carbon flux from the ecosystem to the atmosphere. From such measurements alone it is not possible to distinguish between various R_{eco} components or the contribution of grass and spruce trees to GEP. Due to the remoteness of the site and the size of the CWD and the quickly growing young spruce trees, it was impractical to measure carbon fluxes from individual ecosystem components. Therefore, we used the LandscapeDNDC model framework for simulations of the carbon budget, to evaluate the relative contributions of different ecosystem components to NEE, and to assess their evolution through time. The EC based estimated daily carbon fluxes (derived after gap-filling) were compared with the modeled daily carbon fluxes in this section to test the model. Additionally with this model the carbon balance development of the near future can be simulated.

3.2.2.1 Comparison between measured and simulated NEE

The ecosystem model PSIM within LandscapeDNDC simulated the carbon exchange of the windthrow area during the period of 2009 to 2013. Figure 45 shows simulated vs. measurement derived values of daily GEP, R_{eco}, and NEE. The linear regression models (blue lines) underpin the generally good performance of the model simulation. The values around zero in the GEP column mainly derive from measurements in autumn. When temperatures are low there is no carbon exchange according to the model while the measurements indicate very little carbon fluxes.

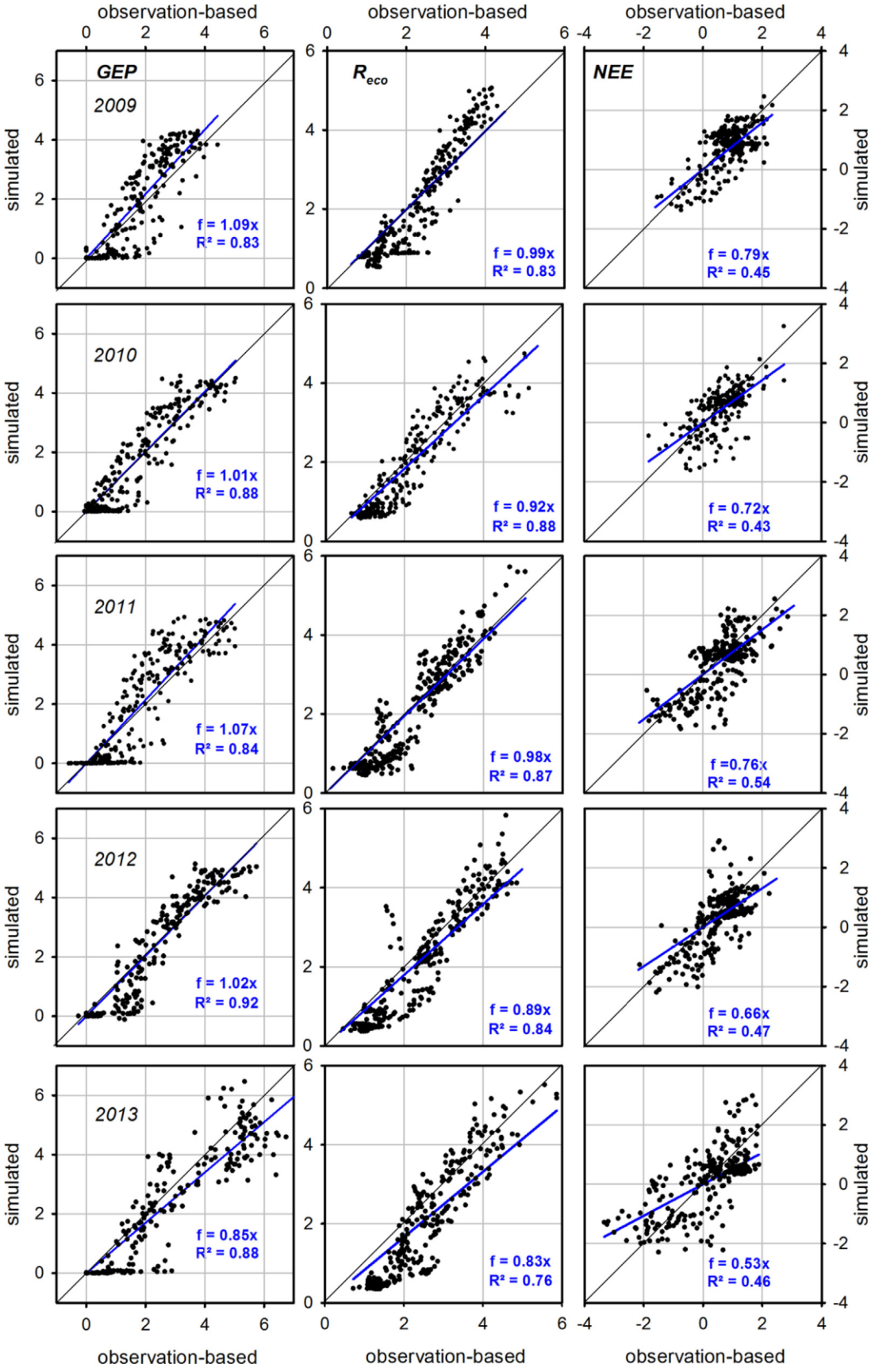

Figure 45: Simulated vs. observation-based estimates of daily CO_2-flux components – units are in g C m^{-2}. GEP (left column), R_{eco} (middle), and NEE (right) in 2009, 2010, 2011, 2012, and 2013 (rows). Observation-based daily sums may be derived from a combination of observations and gap-filled values.

Annual patterns of GEP, R_{eco}, and NEE are shown in Figure 46 for simulated and observation-based estimates, respectively.

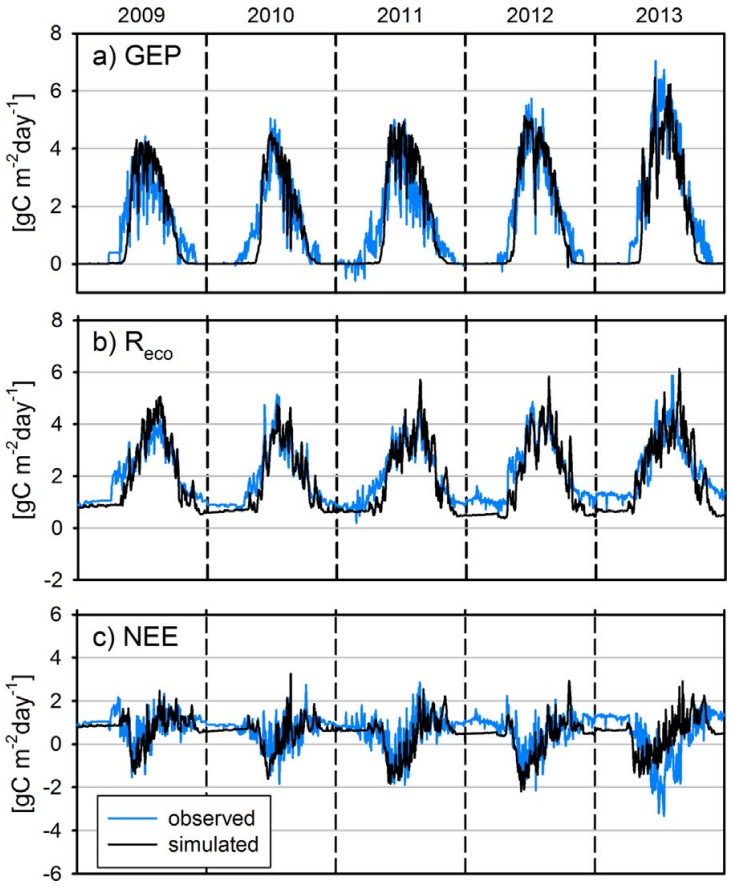

Figure 46: Annual patterns of simulated and observation-based (gap-filled) daily CO_2-fluxes.

Simulated and measured carbon fluxes show a very good agreement in GEP while there appears a marked underestimation in the simulation of R_{eco}, leading to an equivalent underestimation in annual NEE. This difference between measurements and simulations in R_{eco} mainly derives from the winter-months. It is not clear at this time whether this difference originates from an underestimation of the simulation or an overestimation of the measurements. Maybe it is a combination of both. Overall the model corresponds well to total ecosystem fluxes. The role of the model simulations is on the one hand to evaluate relative contributions of grass, trees, and soil to ecosystem fluxes. On the other hand they offer a view at a probable past and future development of the ecosystem's carbon budget. Therefore, a mid-term (2006-2017) as well as a long-term (2006-2025) simulation were conducted. Measured climate data was used for projecting the respective climate variables for the model runs.

3.2.2.2 Mid-term simulation:

The simulated relative contributions of grasses, spruce trees and soil (including debris) to the carbon exchange can be seen in Figure 47. The relative contribution of spruce trees to GEP is increasing, but is still rather small (10–30% at the end of the investigation period). Two to six years after the disturb-

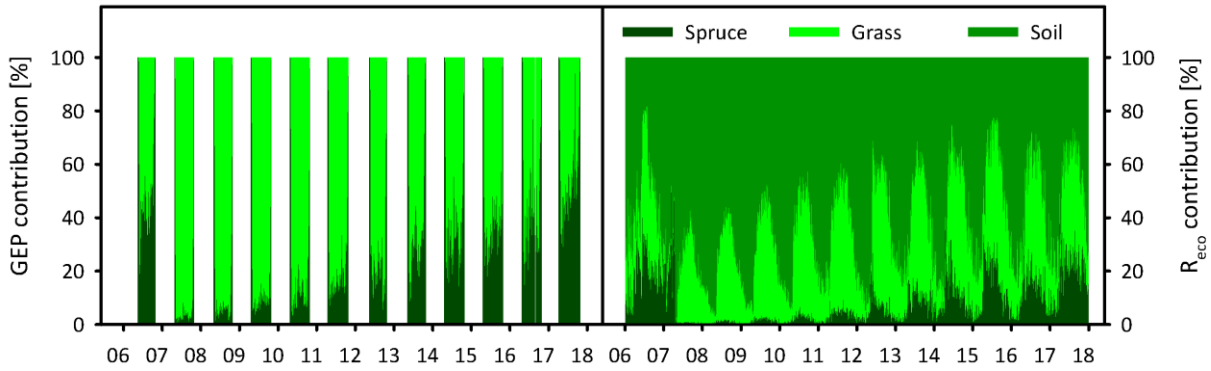

Figure 47: Relative contribution of simulated CO_2-flux to GEP (left) and R_{eco} (right). X-axis shows the year (20XX).

ance, soil respiration has the highest contribution to R_{eco} (about 50% in summer and 90% in winter). The contribution of spruce to R_{eco} is still very small but tends to increase more strongly than that by grass.

Concerning annual NEE, the simulations indicate that the ecosystem switched from a slight carbon source even before the storm in 2006 (NEE ≈ +50 g C $m^{-2}yr^{-1}$) to a strong carbon source in 2007 (NEE ≈ +500 g C $m^{-2}yr^{-1}$) due to Kyrill. Annual NEE decreases quite fast in the following years to about -50 g C m^{-2} in 2017 indicating that about 10 years after disturbance the ecosystem might switch from a net carbon source to a net carbon sink (Figure 48).

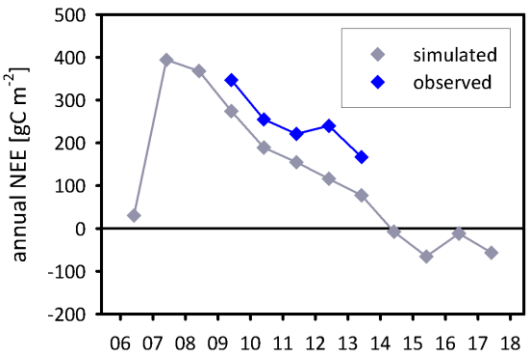

Figure 48: Mid-term simulated and observation-based annual NEE. X-axis shows the year (20XX).

The fact that NEE was positive even in 2006 has not been expected, however, there are some things which can explain it: first thing is the cold climate and a very short vegetation period which constrains the period of net carbon uptake to only a few months. Second, the age of the forest was about 150 years and therefore a high mortality probably led to near equilibrium between carbon gain and carbon loss. Maybe also the storm event in 2007 has hit the ecosystem in the middle of a recovering from earlier disturbance events. The vegetation coverage most likely was very sparse even before the storm (Wolpert, 2012). Although to our knowledge except of 2007 no severs disturbance events are reported at this site in the near past but probably many little stressors (rough climate, occasional thinning) kept the carbon sink strength of this ecosystem rather small in the past.

The simulations of the carbon balance development at the Lackenberg site show that the ecosystem likely will switch from net carbon source to net carbon sink within the next ten years. It also shows the gradual transition in GEP which is mainly dominated by grass-vegetation immediately after the

storm but gets more and more dominated by spruce trees. A matter of uncertainty is the expected tree mortality during ecosystem succession. Simulated biomass fits quite well to estimated biomass but the model tends to overestimate the dimensions of the new growing trees. The relatively high elevation of the study site and thus a cold and rough climate could probably explain the higher mortality or slower growth rate of spruces in this high elevated region compared to forest ecosystems in other regions. Additionally, the above mentioned large amounts of snow together with very high wind speeds could enhance this effect.

These model simulations and simulations of the carbon balance development of other disturbed ecosystems (e.g., Lindroth et al., 2009; Thornton et al., 2002; Thürig et al., 2005) suggest that generally ecosystems after disturbance are at first a carbon source and afterwards switch to a strong carbon sink that is gradually diminishing, while the recovery time from source to sink is longer with higher amount of litter or CWD, respectively. This would confirm the hypothesis of Odum (1969), which has been shown in section 1.5. However, simulating the development of carbon balances in disturbed areas is still subject to major uncertainties. For example, the microclimate and thus conditions for mineralization and re-growth on disturbed areas is different from intact forest ecosystems as well as from grassland. Under natural conditions, the competition between grass or other herbaceous species and upcoming trees can be intense and is changing dynamically in dependence on the specific environmental conditions (Grote R., personal communication).

Therefore, the carbon release of non-cleared wind-throws does most probably not follow a simple pattern which is only a function of biomass, but changing structural and micro-climate conditions have to be taken into account.

3.2.2.3 Long-term simulation

Despite the major uncertainties regarding to long-term simulations of the carbon balance in disturbed forest ecosystems we took a glance into the farer future.

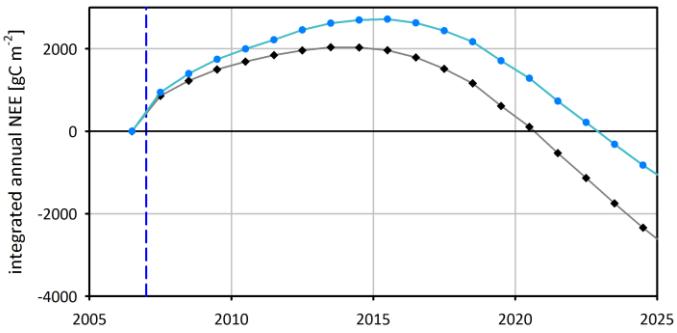

Figure 49: integrated annual NEE (simulated) from 2006 to 2025 in consideration of the underestimation of the model (light-blue dots). Blue dashed line shows the disturbance event. X-axis shows the year.

As such a "first-shot" a simulation from 2006 to 2025 was conducted to get an idea about the long-term carbon balance development at this site. According to the model simulations and assuming an average underestimation (average difference between observation based estimates and simulation) of about 82 g C $m^{-2}yr^{-1}$ of the model (light-blue dots in Figure 49), total-

ly over 2700 g C m^{-2} were emitted from the site from 2007 to 2015 when annual NEE is negative again. Another seven years later almost all carbon that was emitted after disturbance has been fixed again by the ecosystem given that no further disturbance event occurs during that time. Another severe storm event or bark-beetle outbreak could switch the ecosystem to a net carbon source for another long period of time. Thus, the "biome-time-scale" – the time period after disturbance till all disturbance-related emitted carbon has been gained again by the ecosystem – would be about 20 years for this ecosystem and this type and severity of disturbance.

3.2.3 Comparison with other disturbed forest ecosystems

In this section the carbon balance of the Lackenberg site is discussed in relation to other topic related publications.

Table 10 shows annual NEE of several forest ecosystems ("intact" and "recently disturbed") and should just give an idea about their magnitudes of CO_2 exchange.

Table 10: NEE of several ecosystems within Europe.

Study	Ecosystem (forest type)	NEE [g C $m^{-2}yr^{-1}$]
	intact ecosystems	
Gruenwald and Bernhofer (2007)	Norway spruce, Germany	-395 to -698
Rebmann et al. (2010)	Norway spruce, Germany	-63 to -246
Valentini et al. (1996)	Beech, Italy	-470
Knohl et al. (2003)	Beech, Germany	-490 to -494
Etzold et al. (2011)	mixed deciduous forest (montane level), Switzerland	-366 to -662
	Norway spruce forest (subalpine level), Switzerland	-47 to -274
Lagergren et al. (2008)	Scots pine, Finland	≈ -199
	Beech, Denmark	≈ -196
	Norway spruce; Scots Pine; mixed deciduous, Sweden	≈ +52
Clement et al. (2012)	Sitka Spruce plantation, Scotland	≈ -600
	recently disturbed ecosystems	
Kowalski et al. (2004)	Coppice-oak, Italy; Sitka spruce, Britain; Scots pine, Finland, Maritime pine , France (all after clear-cutting)	+100 to +420
Lindroth et al. (2009)	Norway spruce, Sweden (one year after storm, cleared wind-throw)	+897 to +1259
Knohl et al. (2002)	Norway Spruce, Russia (regeneration after wind-throw)	+180*
This work	Norway Spruce, Germany (regeneration after wind-throw)	+167 to +347

Generally, an intact spruce forest in the temperate region of central Europe is expected to be a strong annual carbon sink (Gruenwald and Bernhofer, 2007). This has been shown to be valid in several cases for relatively undisturbed conditions (e.g., Van Dijk and Dolman, 2004), and could also be captured very well with the model used in this study (Grote et al., 2011a)

However, to our knowledge there is no comparable long-term investigation of NEE in a wind-throw disturbed ecosystem, where all biomass remained on site. Knohl et al (2002) estimated carbon dioxide exchange for one season only, in the center of a large wind-throw area in Fyedorovskoye (near Nelidovo, about 300 km NW of Moscow) Russia, in 1998, two years after a storm event. Over the

* 3-months measurement period

three-month measurement period from July to October, NEE was +180 g C m^{-2}. A rough extrapolation to annual NEE yielded about +400 g C m^{-2}. The higher net carbon loss compared to our results from the Lackenberg site is likely due to the difference in soil moisture (much higher at Fyedorovskoye), leading to enhanced ecosystem respiration. Additionally, Fyedorovskoye was affected by other heavy windstorms before 1996 (1969, 1987). Therefore, a higher amount of deadwood was likely contributing to R_{eco} at the Russian site.

Lindroth et al. (2009) estimated NEE in a Norway spruce ecosystem in Sweden after a severe wind-disturbance by the storm Gudrun (2005). One year after the storm event the ecosystem was a large source of carbon, with annual net carbon loss of over 1000 g C m^{-2}. The authors attribute this high carbon emission (compared to NEE estimates after clear-cutting, e.g., in Kowalski et al., 2004) to the intensive disturbance of the soil layer by heavy machinery used to clear the wind-throw area.

Amiro et al. (2003) reported that a Canadian boreal forest was a net carbon sink (at least in summer) a few years after fire-disturbance. In further work, Amiro et al. (2006) showed that 4 and 8 years after disturbance (fire and harvest, respectively) boreal forests were net sources of carbon with annual NEE ranging from 50 to 130 g C m^{-2}, while a burned site was a net carbon sink (annual NEE: -68 g C m^{-2}) 13 years after disturbance. Using a chronosequence approach (similar ecosystems at different successional stages) with an age-range of 180 site years, Amiro et al. (2010) summarized that after stand-replacing disturbance all ecosystems return to net carbon sinks, at the latest, 20 years after the disturbance event. They reported that maximum annual NEE after disturbance ranged from +1270 (in Florida) to +200 g C m^{-2} (in boreal forests). Comparing these reported values to each other, or to the presented results, is quite difficult, because of the range of disturbance types, severity of disturbance, types of ecosystem, post-disturbance-management, climate, and vegetation zone the ecosystems are located in.

However, one general emerging result is that, especially in the first few years, the severity of soil perturbation associated with the post-disturbance management plays a major role in the longer term carbon balance development. Severe disruption of the upper soil layer, as caused by heavy machinery, can lead to an enormous CO_2 efflux immediately after disturbance (Janssens et al., 2001; Lindroth et al., 2009).

In contrast, in disturbed ecosystems that are left in their natural state, carbon is mobilized much more slowly, resulting in lower ecosystem CO_2 efflux. On the other hand, it must be expected that the structural robustness of deadwood most likely leads to long-term but more moderate CO_2 emissions in such ecosystems (Brown et al., 2012; Knohl et al., 2002). No heavy machinery was used at the Lackenberg site (except on the periphery, outside the windfall area). Thus, our results of a con-

sistent, albeit smaller, carbon loss in the years after disturbance are consistent with the results of both Knohl et al. (2002) and Lindroth et al. (2009).

At the Lackenberg site, trends identified after five years of carbon exchange measurements indicate that the wind-throw disturbed Norway spruce ecosystem is well on its way of regeneration toward becoming a net annual carbon sink. The LandscapeDNDC simulations reveal that the sizable carbon uptake even in the first summer seasons after the disturbance is predominantly due to grasses and other ground cover vegetation, rather than new trees. This aspect is generally neglected in larger scale models (Edburg et al., 2011; e.g., Eliasson et al., 2013; Williams et al., 2012), although the dependence of recovery speed on tree species composition (Gough et al., 2013) and the importance of plant driven processes for soil carbon dynamics (Litton et al., 2003) is well known. Large uncertainties exist in the model representation of litter pools. In fact, the decomposition process of coarse woody debris is quite different from that of fine litter in and directly above the ground, and (among other things) depends on wood properties and microclimate (Herrmann and Bauhus, 2013). As with all such models, heterotrophic respiration (and especially pertaining to coarse woody debris overlong time periods) is fraught with a lack of direct measurements for evaluation and comparison. The present work exemplifies the need to build up the database and process knowledge on these aspects.

4 Summary and Conclusion

The Lackenberg site within the Bavarian Forest National Park, Bavaria, Germany, has been shown to offer ideal conditions for estimating the carbon balance development in an upland disturbed forest ecosystem and to get a better idea of the processes controlling CO_2 exchange in such disturbed ecosystems.

As a centerpiece of this study the net ecosystem exchange, as well as the component fluxes GEP and R_{eco} were estimated over a five year measurement period at the Lackenberg site. Measured fluxes of NEE showed that, in daytime in summer, GEP already exceeds respiration. The main environmental drivers for carbon exchange on this site were found to be soil temperature, mainly controlling ecosystem respiration, and photosynthetic photon flux density, mainly controlling carbon assimilation (GEP). Using these biophysical parameters, an appropriate gap-filling model to replace missing NEE values could be found. Due to the necessity for continuous time-series of these driving parameters, we developed a simple model for incoming short-wave radiation, requiring only screen-level relative humidity data (and site specific astronomical information) as presented in the Appendix.

Annual sums of NEE after gap-filling showed that the Lackenberg site is still a marked source of carbon with annual NEE of 347 ±104, 255 ±77, 221 ±66, 240 ±52, and 167 ±50 g C m^{-2} from 2009 to 2013. However, summertime GEP of the non-cleared wind-throw area was already high and exhibited a consistently positive trend. In contrast, ecosystem respiration showed no clear overall trend, but high inter-annual variability. Despite the gradually increasing annual GEP, NEE is still dominated by R_{eco} which again mainly depends on the annual course of weather conditions. The length of the vegetation period, which is not easy to estimate precisely in a grass and spruce dominated ecosystem, seems to have an additional strong effect on the annual NEE.

A comparison with other gap-filling procedures indicates that the “local gap-filling” results are in good agreement with the NEE estimates when using other gap-filling procedures. However, it has also been shown that annual NEE estimates can be very sensitive to the application of a u*-filter, depending on the gap-fill procedure used. Such systematic differences in NEE can amount to ± 100 g C m^{-2}.

Snow covered periods are not negligible in terms of carbon exchange at the Lackenberg site. CO_2-flux measurements during snow-covered periods averaged about 0.9 µmol m^{-2} s^{-1}, with little variation. The isolating snow-pack (up to 2 m deep) kept soil temperatures relatively high and allowed persistent soil microbial activity.

Simulations of the carbon exchange, using a biogeochemical model LandscapeDNDC (Haas et al., 2013), have shown that this model can reasonably represent the measured carbon dioxide fluxes

through the early recovery period, apart from a slight but systematic underestimation of ecosystem respiration at very high fluxes and during winter. The model served as a valuable tool to examine the partitioning of carbon sinks and sources in various compartments in the disturbed ecosystem and to explain the variability between years. In our case the slow year-to-year increase of the spruce contribution to assimilation could be nicely demonstrated, but the partitioning of heterotrophic respiration processes into below ground, litter, and coarse woody debris components remains a formidable challenge. Long-term simulations of the carbon balance development at the study site with this model indicate that the ecosystem will most likely switch from carbon source to carbon sink within about the next ten years. Always assumed, that no further disturbance event will hit the young re-growing forest before that time.

In summary the answers to the research questions of section 1.6 are:

- Three to six years after the storm net CO_2 exchange ranged from 221 ±11 to 347 ±17 g C $m^{-2}yr^{-1}$ and tends to decrease during the measurement period.
- In the same time period annual GEP estimates ranged from 393 to 529 g C m^{-2}. R_{eco} ranged from 656 to 786 g C $m^{-2}yr^{-1}$.
- While GEP shows a gradually increase during the measurement period R_{eco} was highly variable and has a strong influence on the annual net exchange despite the already strong GEP values. Environmental drivers and the length of the growing season are assumed to be mainly responsible for this high variability in annual R_{eco} and thus in annual NEE, as well.
- A review of the current literature about carbon exchange in disturbed ecosystems leads to the recognition, that there are marked differences in annual NEE between unmanaged and managed disturbed forest ecosystems. One of the main differences is likely the status of the upper soil layer after disturbance. Marked destruction e.g., by deadwood-clearing through heavy machinery most likely leads to an enormous carbon efflux, in contrast to unmanaged disturbed ecosystems (Lindroth et al., 2009). However, remaining deadwood in disturbed ecosystems which have been left in their natural state will most likely lead to moderate but continuous long-term carbon efflux (Knohl et al., 2002).
- The carbon release of non-cleared wind-throws does most probably not follow a simple pattern which is only a function of biomass. Thus, changing structural and micro-climate conditions have to be taken into account.
- Simulations of the carbon balance development with the modeling framework Landscape DNDC have shown that the ecosystem will most likely switch from net carbon source to net carbon sink within the next ten years.

The principal innovative contributions of the present dissertation are summarized as follows:

- It was the first study to observe and examine carbon exchange of an intact wind-throw-disturbed forest ecosystem for multiple years post disturbance
- The combination of observations and modelling of main ecosystem components through the disturbance event and the re-growth period. Modelling also sheds light on the transient roles of different carbon pools and plant functional types in the period after disturbance.
- This study also contains a valuable contribution to gap-fill modelling for upland, cool climate spruce forest ecosystems.
- A new and universally applicable parameterization model for global radiation was developed in this study, dependent on screen level relative humidity only

Appendix - Global Radiation Model

Following section has been submitted for publication in an international scientific journal. Title: *"A simple new model for incoming solar radiation dependent only on screen-level relative humidity"*

Introduction

Insolation at the Earth's surface (global incoming shortwave radiation, R_g) is the primary energy source for the majority of biogeochemical or physical land-surface processes, as well as for the operation of photovoltaic (PV) power production systems. Therefore, it is one of the most important drivers for land surface models that calculate energy-, water-, and carbon balances, and site-specific information about R_g is essential to estimate the viability PV systems. With knowledge of albedo and temperature, R_g is the starting point for estimates of net radiation, evapotranspiration and the energy balance. Assumptions about the spectral composition of R_g lead to estimates of photosynthetically active radiation (PAR) and practical ecosystem-scale models of photosynthesis, biogeochemical cycling, carbon uptake, and plant growth (e.g., Arora, 2002; Baldocchi and Meyers, 1998; Bonan, 2008a; Sellers et al., 1997; Wang and Jarvis, 1990; Williams et al., 1996). At the site level, such models are ideally driven with directly measured values of PAR, R_g or net radiation at high temporal resolution. However, such radiation measurements are not standard at most climate stations, and even at FLUXNET stations (e.g., Baldocchi et al., 2001) data series often suffer from missing values. If direct surface radiation measurements are unavailable, it is thus necessary to model or parameterize them based on whatever data available.

Commonly, models of R_g are based on the ratio of R_g (at the surface) over the value of down-welling solar radiation at the top of the atmosphere (extraterrestrial solar radiation, R_E), defining the overall atmospheric transmissivity, $\widetilde{T}_R$ (e.g., Fortin et al., 2008). This transmissivity depends on path length through the atmosphere, atmospheric absorption characteristics, and cloudiness. Full models of global incoming shortwave radiation treat radiative transmission explicitly, from the top of the atmosphere to the surface, including scattering and absorption processes by ozone, water vapor, clouds and aerosol throughout the atmosphere (e.g., Jia et al., 2013). Such models require detailed information about the state of the atmosphere, are computationally expensive, and require too much input information to be practical for most site-specific applications. Reanalysis datasets and satellite derived energy balance products often include estimates of surface solar radiation, but they are usually limited to coarse spatial resolutions and typically refer to averages between 3-hourly to daily (e.g., Babst et al., 2008; Jia et al., 2013; Zib et al., 2012). Vuichard and Papale (2015) present a method for deriving half-hourly estimates of R_g based on ERA-Interim reanalysis data, using a spatial and temporal downscaling approach. Their analysis was performed for a set of over 150 sites (part of the so-called FLUXNET-Synthesis Dataset, see Vuichard and Papale, 2015) and indicated a fairly good

performance of the approach. However, the method is quite involved and setting it up for individual sites and time periods is likely very time consuming. For spatially and temporally explicit estimates of R_g at individual locations and time periods, empirical models or parameterizations based on readily available meteorological data have traditionally been the methods of choice.

Empirical models of R_g must address the fact that cloudiness has commonly both the strongest and the most variable effect on atmospheric transmissivity for shortwave radiation. Unfortunately, neither cloudiness, nor sunshine duration are standard variables reported by climate stations, and thus such models need to revert to using a suitable proxy for cloudiness. As cloudiness also affects the thermal regime at the surface, one obvious such proxy is the daily range of air temperatures (Baigorria et al., 2004; Bristow and Campbell, 1984; Goodin et al., 1999; Lee, 2010). Among the most frequently used R_g models of this kind are those by Hargreaves and Samani (1982), and by Mahmood and Hubbard (2002), which require only the daily range (minimum and maximum) of air temperature as input variable. Since only one daily value is used as input in these models, they are also limited to produce daily mean estimates of R_g only. Daily means can then be distributed over a daily course using prescribed (e.g., sinusoidal) functions (e.g., Berninger, 1994). However, if surface radiation data are needed to parameterize processes at sub-daily resolution (e.g., to gap-fill eddy-covariance based CO_2 exchange time-series; e.g., Reichstein et al., 2005), such estimates introduce considerable uncertainty, as they are unable to respond to short-term atmospheric variability.

At a mountain-top carbon exchange flux station on the Lackenberg (1308 m elevation) in the Bavarian Forest National Park (southern Germany, see Lindauer et al., 2014) we found that cloud cover, and thus R_g and PAR, typically varied strongly over the course of the day. As the relationship between carbon assimilation by photosynthesis and shortwave radiation is strongly non-linear (e.g., Reichstein et al., 2005), daily mean values of a cloudiness-proxy were not sufficient to drive our carbon assimilation model at times when we were lacking all but standard climate station data. We also found that the atmospheric moisture regime that supports or suppresses the formation of clouds in elevated layers of the troposphere appears to be fairly well coupled to surface humidity – at least at the Lackenberg site. This very heuristic and speculative notion led us to use standard measurements of relative humidity as a proxy for cloud cover, haziness, and thus variability of atmospheric transmissivity. Surprisingly, we have found no evidence that a relation between relative humidity and atmospheric transmissivity has ever been explored before. In this work, we present a simple empirical model of R_g at sub-daily (e.g., half-hourly) resolution that requires only relative humidity as meteorological input. Relative humidity is a standard observation variable at most climate stations. We test the model at a wide range of observation sites, and evaluate it against independent data sets. We also investigate its accuracy at hourly and daily resolutions.

Methods

Generally, short-wave incoming radiation at the surface (global radiation – R_g) can be expressed as:

$$R_g = R_E \, \tilde{T}_R \ , \tag{A1}$$

where R_E is the extraterrestrial radiation on top of the atmosphere and $\tilde{T}_R$ is the atmospheric transmissivity. This transmissivity can be expressed as a net sky transmissivity, T_R, modified by the influence of the optical path-length through the atmosphere, L_P:

$$R_g = R_E \, L_P \, T_R \tag{A2}$$

The extraterrestrial radiation, R_E, can be calculated as (e.g., Stull, 2000):

$$R_E = S \sin \Psi \ , \tag{A3}$$

where S is the solar constant (1368 Wm^{-2}) and Ψ is the local elevation angle of the sun. The influence of the path-length through the atmosphere was considered, for instance, in Holtslag and van Ulden (1983), where the equivalent of our L_P is described by:

$$L_P = a_1 \sin \Psi + a_2 \ , \tag{A4}$$

where a_1 and a_2 are empirical coefficients. Stull (2000) proposed the values $a_1 = 0.2$, and $a_2 = 0.6$ for a clear-sky and average “clean” atmosphere. Thus, we find R_0 as the reference surface radiation under clear skies and optimal transmissivity:

$$R_0 = R_E \, L_P = R_E \, (0.2 \sin \Psi + 0.6) \tag{A5}$$

Lindauer et al. (2014) showed an ad-hoc empirical relation between the ratio of R_g and R_0 (effective local transmissivity, T_R) and relative air humidity to model R_g (Figure 22). Based on this method we developed the following equation:

$$R_g = \underbrace{R_E \, L_P}_{R_0} \underbrace{(1\text{-}rHf)^b}_{T_R} \ , \tag{A6}$$

where rHf denotes the local relative humidity at the surface (fraction, 0…1) and b is an empirical parameter.

Table A 1: Parameters of sites selected for model development and evaluation. The first part contains 15 sites from the U.S. Surface Climate Observing Reference Networks (data from 2012) which were used for model development and parameterization. The second part (below the bold line) shows parameters for six sites used for additional model evaluation. Station names in the first column are followed by the common codes for states (for the USA stations) and countries. T_{avg}, T_{max},T_{min} are the average, maximum and minimum air temperatures for the data period used; Prec is the annual precipitation; rH_{avg} and $rH_{avg(daytime)}$ are the overall average and daytime average relative humidities; CI is the continentality index (see text). Data source references are: a) Diamond et al. 2013; b) Cleverley 2011; c) Grote et al., 2009c; d) Eder et al. 2014; e) Hanan et al., 2004; f) Lindauer et al. 2014; g) Falge et al. 2005.

Station	Data Source	Lat. [°]	Lon. [°]	Elev. [m]	T_{avg} [°C]	T_{max} [°C]	T_{min} [°C]	Prec. [mm]	rH_{avg} [%]	$rH_{avg(daytime)}$ [%]	CI [°C]
Austin, TX, USA	a	30.62	98.08	149	20.3	11.6	27.5	583	61	55	15.9
Baker, NV, USA	a	39.01	114.21	1620	10.4	28.1	-13.2	300	41	35	22
Barrow, AK, USA	a	71.32	156.61	3	-10.8	12.8	-39.6	114	83	86	34.9
Bodega, CA, USA	a	38.32	123.07	36	11	9.4	12.2	870	86	83	2.8
Boulder, CO, USA	a	40.04	105.54	1655	3.1	19.8	-17.4	739	52	46	18.3
Champaign, IL, USA	a	40.05	88.37	225	12.3	29.9	-11.2	727	71	62	26.6
Everglades City, FL, USA	a	25.90	81.32	5	23.1	29.5	8.3	1290	78	67	10.2
Fairbanks, AK, USA	a	64.97	147.51	136	-2	20.6	-34.4	299	63	57	41.2
Mauna Loa, HI, USA	a	19.54	155.58	3397	7.1	12.3	0	164	31	34	3.8
Mercury, NV, USA	a	36.62	116.02	1155	18.3	35.4	0.3	90	28	23	22
Northgate, ND, USA	a	48.97	102.17	570	4.8	-7.9	21.3	415	72	64	29.2
Oakley, KS, USA	a	38.87	100.96	934	13.1	34.7	-13.8	362	53	44	27.8
Sitka, AK, USA	a	57.06	135.33	8	5.4	17.9	-15.2	2300	89	85	12.9
Tucson, AZ, USA	a	32.24	111.17	728	21.6	34	5.2	232	30	25	16.3
Yuma, AZ, USA	a	32.84	114.19	43	23.8	39	7.8	62.5	28	24	19.8
Alice Springs, AUS	b	-22.28	-133.25	600	22.2	40.5	-0.2	277	34	28	-18
Bontioli, Burkina Faso	c	10.84	-3.15	330	28.9	35.4	22.8	940	51	48	-2.8
Fendt (TERENO), D	d	47.80	-11.07	580	8.6	32.5	-21.9	1200	77	70	16.2
Krüger National Park, ZAF	e	-25.02	31.5	250	21.8	38.6	2.8	600	60	58	8.3
Lackenberg, D	f	49.10	-13.3	1308	4.8	24	-18.9	1400	76	75	16.8
Manaus, BRA	g	-2.58	60.12	92	25.1	34.1	17.5	2431	88	82	0.7

For model development and parameterization we looked for freely available weather information with high quality and resolution that cover a wide range of environmental conditions. Therefore, we used data derived from U.S. Surface Climate Observing Reference Networks. For additional evaluation, we used data from independent sites with consistent data that are not involved in the process of model development and parameterization. These sites are Alice Springs (data from 2011 - 2013) in Australia (part of the Australian Terrestrial Ecosystem Research Network, TERN, www.tern.org.au),Fendt (data from 2011 - 2013) in southern Germany (part of the German TERrestrial Environmental Observatories, TERENO, www.TERENO.net), Lackenberg (data from 2011-2013) also in southern Germany, Manaus in Brazil (data from 1996), Kruger National Park in South Africa (data from 2001-2002), and Bontioli (data from 2004-2005) in Burkina Faso.

High resolution meteorological data that include humidity and radiation are available at all of these sites. Table A 1 shows general information about the selected sites.

These sites cover a wide range of latitudes, longitudes, elevations, average air humidity, and continentality. A continentality index (CI) was calculated as the difference between the average monthly air temperature in January and July (e.g., Botta-Dukát et al., 2005; Holmlund and Schneider, 1997).

Figure A 1 illustrates the relation between $R_0\ R_g^{-1}$ and rHf (a), and shows the resulting scatterplot of modelled vs. observed R_g values (b) at Boulder, CO in 2011.

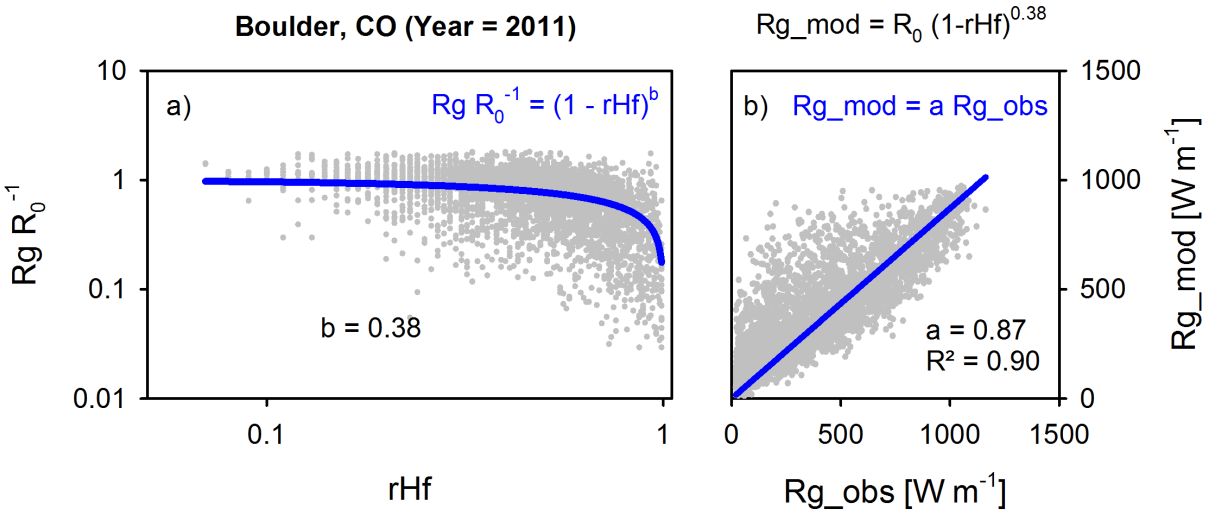

Figure A 1: $R_g\ R_0^{-1}$ against rHf at Boulder in 2011. The blue line shows the power-law regression with an estimated parameter of b = 0.38. **b)** modelled values of R_g against observed Values of R_g. The blue line is the linear regression with slope a = 0.87.

This analysis was done for every site listed in the first part of Table A 1 (above the bold horizontal line). Parameters b, and a, the coefficient of determination (R^2), as well as the root mean square error (RMSE), and the normalized RMSE are listed in Table A 2. These parameters and model evaluation measures were estimated with three years of data (2011 - 2013) at each site, to account for the year to year variability.

In addition to R^2 we use the RMSE (root mean square error) and normalized RMSE for testing the predictive power of the model in equation (6).

$$RMSE=\sqrt{\frac{1}{n}\sum_{i=1}^{n}(p_i-o_i)^2} \tag{A7}$$

Where p_i is a predicted or modelled value, respectively at time i and o_i is a observed value at time i. By dividing RMSE by the average of observed values, $\bar{o}$, one gets the normalized RMSE:

$$NRMSE=\frac{RMSE}{\bar{o}} \tag{A8}$$

Results

Table A 2 shows the averages of b, a, R^2, RMSE, and NRMSE of the three years for every site. The first part shows again the sites in the U.S, which were used for model development and parameterization. The shape-parameter, b, ranges between 0.17 and 0.53 with an average of 0.34, and the slope parameter, a, ranges from 0.74 to 0.99, with an average of 0.92. The average R^2 value of all sites is 0.92, indicating a very good overall performance of the model. The NRMSE ranges between 24 and 74% with an average of 40%.

Table A 2: Parameters of the regression functions in Figure A 1 and measures of predictive power (see text for definitions).

	power-law		**linear regression**									
Site	b	σ_b	a	σ_a	R^2	σ_{R^2}	RMSE [Wm^{-2}]	σRMSE [Wm^{-2}]	NMRSE	σNRMSE	rHf_{DT}	σ_{rHfDT}
Austin	0.41	0.04	0.92	0.01	0.94	0.01	124.4	5.9	33%	3%	0.52	0.03
Baker	0.31	0.05	0.94	0.01	0.92	0.01	147.4	7.9	37%	2%	0.36	0.03
Barrow	0.20	0.02	0.81	0.01	0.88	0.01	97.2	2.5	53%	3%	0.87	0.01
Bodega	0.17	0.01	0.90	0.02	0.90	0.02	136.4	6.6	42%	3%	0.83	0.02
Boulder	0.40	0.02	0.88	0.02	0.90	0.01	158.5	1.7	44%	2%	0.50	0.04
Champaign	0.35	0.03	0.90	0.02	0.91	0.02	135.5	9.6	43%	4%	0.66	0.04
Everglades	0.30	0.01	0.93	0.01	0.93	0.01	137.0	3.7	35%	2%	0.68	0.01
Fairbanks	0.45	0.01	0.90	0.01	0.91	0.02	99.0	5.1	46%	5%	0.56	0.02
Mauna Loa	0.17	0.05	0.95	0.01	0.94	0.01	153.6	9.1	31%	3%	0.39	0.04
Mercury	0.53	0.19	0.99	0.04	0.96	0.01	114.5	7.8	28%	1%	0.23	0.02
Northgate	0.25	0.04	0.92	0.01	0.90	0.02	132.3	11.1	44%	4%	0.67	0.03
Oakley	0.33	0.02	0.94	0.01	0.94	0.01	120.7	6.1	32%	2%	0.47	0.03
Sitka	0.49	0.06	0.74	0.01	0.84	0.02	119.1	5.3	74%	4%	0.85	0.02
Tucson	0.39	0.08	0.98	0.00	0.96	0.01	118.7	6.6	27%	2%	0.25	0.01
Yuma	0.40	0.15	0.99	0.02	0.97	0.01	105.5	1.7	24%	2%	0.24	0.01
Average	**0.34**		**0.91**		**0.92**		**126.7**		**40%**			

We did not detect any trend in the variation of shape-parameter b. In contrast, the slope-parameter

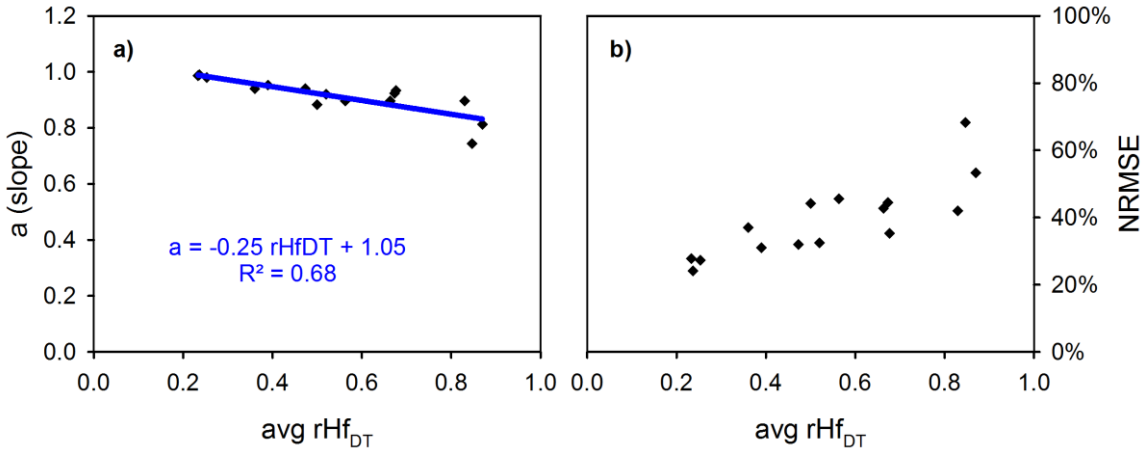

Figure A 2: a) slope of linear regressions against annual average daytime humidity (rHf_{DT}); **b)** NRMSE against rHf_{DT}

a as well as the random uncertainty (NRMSE) show a linear relation to the annual average daytime relative humidity rHf_{DT} (Figure A 2a, b).

In summary, R_g can be modeled based on equation (A6), using the average value of b = 0.34, and dividing it by the site-specific climatology influence:

$$R_g = \frac{R_0 \, (1\text{-}rHf)^{0.34}}{1.05\text{-}0.25 \, rHf_{DT}} \qquad (A9)$$

Applying this site-climate correction reduces the systematic bias of the model and raises the average slope in Table A 2 from 0.92 to 0.98, but this gain in accuracy comes at a slight cost in random uncertainty: average NRMSE increases from 40 to 43%.

To examine the applicability we used this generalized model (equation A9) to the sites listed in the lower part of Table A 1 to test the model performance at independent sites which have not been used in the model development.

Table A 3: Parameters of the linear regression functions after using equation A9 at independent sites.

	linear regression				
Site	slope	R^2	RMSE [Wm^{-2}]	NMRSE	rHf_{DT}
Alice Springs (2011)	**0.98**	**0.94**	**152.2**	**32%**	0.36
Alice Springs (2012)	**0.96**	**0.95**	**134.4**	**26%**	0.28
Alice Springs 2013)	**0.97**	**0.95**	**140.6**	**28%**	0.25
Bontioli (2004)	**1.13**	**0.95**	**156.8**	**38%**	0.48
Bontioli (2005)	**1.13**	**0.96**	**144.0**	**33%**	0.29
Fendt (2011)	**0.98**	**0.89**	**145.1**	**55%**	0.71
Fendt (2012)	**1.05**	**0.88**	**151.9**	**58%**	0.70
Fendt (2013)	**1.07**	**0.87**	**158.6**	**65%**	0.71
Krüger National Park (2001)	**1.06**	**0.91**	**169.2**	**55%**	0.63
Krüger National Park (2002)	**1.03**	**0.92**	**163.5**	**50%**	0.58
Lackenberg (2011)	**0.97**	**0.88**	**131.4**	**52%**	0.73
Lackenberg (2012)	**0.98**	**0.89**	**126.9**	**49%**	0.75
Lackenberg (2013)	**0.97**	**0.88**	**130.2**	**59%**	0.77
Manaus (1996)	**1.05**	**0.92**	**144.8**	**41%**	0.82

Table A 3 shows parameters of the linear regression functions after using equation A9 at the independent sites. There, the slope parameter, a, ranges from 0.96 to 1.13, with an average of 1.02. The average R^2 value of all sites is 0.91 and the NRMSE ranges between 26 and 74% with an average of 65%. These values are fairly in the range of those in Table A 2, and indicate that equation A9 can generally be used for modelling R_g at any site.

Apart from model performance at an hourly temporal resolution, the question could arise if the relationship between global radiation and air humidity also holds for more aggregated data. Therefore, we tested the relationship with daily input values of air humidity and compared the results with those obtained with a conventional method. For this exercise, we used the same model as described before for all sites in the investigation but restrict ourselves to the year 2012. R_0 and rH are simply replaced by daily values instead of hourly values. It should be noted that relative humidity is calculated from daytime values only to be consistent with the period where the radiation data are originating from. We compared the daily sum of measured R_g values with the daily sum of modelled hourly R_g values (Figure A 3a), with the results of this daily model (Figure A 3b), and with R_g values derived after the method of Hargreaves and Samani (1982) (Figure A 3c).

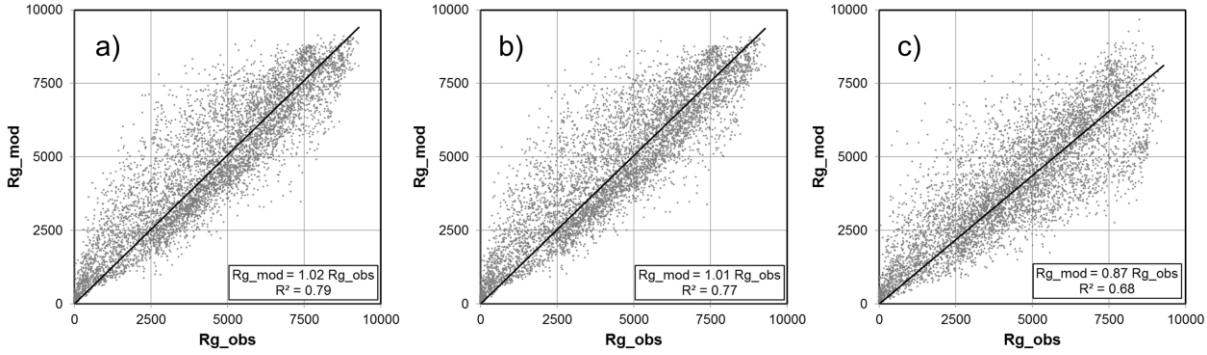

Figure A 3: R_g – daily values derived from hourly air humidity (a), daily air humidity (b), and minimum and maximum air temperature after Hargreaves and Samani (1982) (c) compared with daily aggregated observations. Units in W m^{-2}.

These results show that using sub-daily values performs better than using daily values, and that using daily values is still superior to using the method of Hargreaves and Samani (1982).

Discussion and Conclusions

To our knowledge, this work is the first study to present a relation between relative humidity and atmospheric transmissivity as a basis for modeling down welling solar radiation (global radiation) at the land surface.

The model has been tested for a variety of sites that represent a range of global terrestrial microclimates. Thus, we are confident to propose it for general applicability. However, a rigorous cause-and-effect chain between screen-level relative humidity, turbidity, cloud cover and transmissivity over the entire atmosphere above a given site is not straightforward to establish, and we don't attempt to try. At our Lackenberg site, the necessity of filling large gaps in radiation data was literally the mother of invention, to guide our intuition towards exploring relative humidity as a proxy. We were surprised that our simple method worked as well as it did, and even more so, when we found that it performs

well for a wide range of elevations and latitudes globally. As a variable, relative humidity combines the moisture and temperature characteristics of air, and thus expresses the state of the air relative to condensation conditions. Our finding that relative humidity near the surface evidently correlates well with haze and cloud conditions aloft indicates that, overall, the general shape of atmospheric profiles of moisture and temperature is fairly robust. For given local climatic conditions, relative shifts in the profiles due to airmass changes appear to be anchored well to their surface values. Nevertheless, it should be noted that the relation between transmissivity and relative humidity near the surface is likely uncoupled under certain conditions. Such conditions include the presence of surface advection (e.g., near coast lines or in katabatic flows), non-convective lifting (e.g., orographic or frontal lifting), or strong dust/aerosol loading in arid/semi-arid environments. Some of our test sites may be affected by such factors at times. The relation linking atmospheric transmissivity to relative humidity in our model for global radiation is non-linear: the sensitivity of radiation to changes in relative humidity is particularly large under moist conditions and decreases with decreasing humidity. Therefore, the uncertainty of our radiation model is less at dry (continental) sites than in humid regions (see Tables A 1-A 3).

It has been demonstrated that the model is applicable to sub-daily as well as daily temporal resolution of relative humidity. Even with daily resolution, and thus with the same detail of input required for conventional approaches, the new model outperforms the most commonly used approaches today (e.g., model of Hargreaves and Samani, 1982 - Figure A 3b and c; or model of Mahmood and Hubbard, 2002 - data not shown). However, we have also shown that the accuracy increases when sub daily resolution values are used, which underlines the importance of the non-linearity in the relation between transmissivity and humidity. Although the model performance statistics reported by Vuichard and Papale (2015) are different from the ones used here, and are not given for individual sites, it appears that the present model performs nearly as well as their ERA-interim based method. However, as mentioned, retrieval and downscaling of site-specific reanalysis time-series is quite demanding. In addition, Vuichard and Papale's method includes an intermediate step of de-biasing that requires pre-existing representative site-level data of global radiation. The comparative simplicity and general applicability of the present model, without recourse to pre-existing data except relative humidity, comes at a relatively small cost of uncertainty.

List of Abbreviations and Symbols

BFNP	Bavarian Forest National Park
Bo	Bowen ratio
CH_4	Methane
CO_2	Carbon dioxide
CWD	Coarse woody debris
DOC	Dissolved organic carbon
E_0	Activation energy
EC	Eddy covariance
F_a	Water vapor flux
F_c	Eddy flux of a scalar c
G	Soil heat flux
GEP	Gross ecosystem production
GEP_{1000}	Carbon uptake at PPFD = 1000 µmol m^{-2} s^{-1}
GEP_{sat}	Maximum carbon uptake at infinitive PPFD
GHG	Greenhouse gas
H_2O	Water
HTs	Sensible heat flux
L_P	Influence of path-length through the atmosphere
LUE	Light-use-efficiency
LvE	Latent heat flux
MAE	Mean absolute error
n	Number
NBE	Net biome exchange
NEE	Net ecosystem exchange
NRMSE	Normalized root mean square error
PAR	Photosynthetic active radiation
PPFD	Photosynthetically active photon flux density
R^2	Coefficient of determination
R_a	Autotrophic respiration
R_E	extraterrestrial incoming short-wave radiation
R_{eco}	Ecosystem respiration
R_g	Global radiation
R_h	Heterotrophic respiration
rH	Relative humidity
rHf	Relative humidity – fraction (0…1)
RMSE	Root mean square error
R_{net}	Net radiation
R_{ref}	Respiration at a reference temperature of 10 °C
S	Solar constant
SOC	Soil organic carbon
T_0	Constant temperature of 223.8 K declared by Lloyd and Taylor (1994)
T_{air}	Air temperature
$\widetilde{T_R}$	Atmospheric transmissivity
T_R	Net sky transmissivity
T_{ref}	Reference temperature of 10°C
T_{soil}	Soil temperature
u	Horizontal wind component
u_*	Friction velocity
v	Lateral wind component
VWC	Volumetric water content
w	Vertical wind component
WUE	Water-use-efficiency
x	Direction of the mean wind
y	Direction of the lateral wind
Z	Direction of the vertical wind
α	Apparent quantum yield efficiency
ε	Random Error
ρ_d	Density of dry air
X_s	Mixing ratio of component s
Ψ	Local elevation angle of the sun

List of Figures

List of Tables

References

Acevedo, O.C., Moraes, O.L.L., Degrazia, G.A., Fitzjarrald, D.R., Manzi, A.O., and Campos, J.G., 2009. Is friction velocity the most appropriate scale for correcting nocturnal carbon dioxide fluxes? Agricultural and Forest Meteorology 149(1), 1-10. DOI: www.dx.doi.org/10.1016/j.agrformet.2008.06.014

Aerts, R., 1996. Nutrient resorption from senescing leaves of perennials: Are there general patterns? Journal of Ecology 84(4), 597-608. DOI: www.dx.doi.org/10.2307/2261481

Amiro, B.D., 2001. Paired-tower measurements of carbon and energy fluxes following disturbance in the boreal forest. Global Change Biology 7(3), 253-268. DOI: www.dx.doi.org/10.1046/j.1365-2486.2001.00398.x

Amiro, B.D., Barr, A.G., Barr, J.G., Black, T.A., Bracho, R., Brown, M., Chen, J., Clark, K.L., Davis, K.J., Desai, A.R., Dore, S., Engel, V., Fuentes, J.D., Goldstein, A.H., Goulden, M.L., Kolb, T.E., Lavigne, M.B., Law, B.E., Margolis, H.A., Martin, T., McCaughey, J.H., Misson, L., Montes-Helu, M., Noormets, A., Randerson, J.T., Starr, G., and Xiao, J., 2010. Ecosystem carbon dioxide fluxes after disturbance in forests of North America. Journal of Geophysical Research: Biogeosciences 115, pp. G00K02. DOI: www.dx.doi.org/10.1029/2010JG001390

Amiro, B.D., Barr, A.G., Black, T.A., Iwashita, H., Kljun, N., McCaughey, J.H., Morgenstern, K., Murayama, S., Nesic, Z., Orchansky, A.L., and Saigusa, N., 2006. Carbon, energy and water fluxes at mature and disturbed forest sites, Saskatchewan, Canada. Agricultural and Forest Meteorology 136(3-4), 237-251. DOI: www.dx.doi.org/10.1016/j.agrformet.2004.11.012

Amiro, B.D., MacPherson, J.I., Desjardins, R.L., Chen, J.M., and Liu, J., 2003. Post-fire carbon dioxide fluxes in the western Canadian boreal forest: evidence from towers, aircraft and remote sensing. Agricultural and Forest Meteorology 115(1-2), 91-107. DOI: www.dx.doi.org/10.1016/S0168-1923(02)00170-3

Andersson, P., Berggren, D., and Nilsson, I., 2002. Indices for nitrogen status and nitrate leaching from Norway spruce (Picea abies (L.) Karst.) stands in Sweden. Forest Ecology and Management 157(1-3), 39-53. DOI: www.dx.doi.org/10.1016/S0378-1127(00)00651-4

Angelstam, P. and Kuulivainen, T., 2004. Boreal forest disturbance regimes, successional dynamics and landscape structures - a European perspective. Ecological Bulletins 51, 117-136

Anthoni, P.M., Law, B.E., and Unsworth, M.H., 1999. Carbon and water vapor exchange of an open-canopied ponderosa pine ecosystem. Agricultural and Forest Meteorology 95(3), 151-168. DOI: www.dx.doi.org/10.1016/S0168-1923(99)00029-5

Arora, V., 2002. Modeling vegetation as a dynamic component in soil-vegetation-atmosphere transfer schemes and hydrological models. Reviews of Geophysics 40(2). DOI: www.dx.doi.org/10.1029/2001RG000103

Aubinet, M., 2008. Eddy covariance CO_2 flux measurements in nocturnal conditions: An analysis of the problem. Ecological Applications 18(6), 1368-1378. DOI: www.dx.doi.org/10.1890/06-1336.1

Aubinet, M., Feigenwinter, C., Heinesch, B., Bernhofer, C., Canepa, E., Lindroth, A., Montagnani, L., Rebmann, C., Sedlak, P., and van Gorsel, E., 2010. Direct advection measurements do not help to solve the night-time CO_2 closure problem: Evidence from three different forests. Agricultural

and Forest Meteorology 150(5), 655-664. DOI: www.dx.doi.org/10.1016/j.agrformet.2010.01.016

Aubinet, M., Vesala,T. and Papale,D., 2012. Eddy Covariance : A Practical Guide to Measurement and Data Analysis, Springer Netherlands, Dordrecht,

Aurela, M., Laurila, T., and Tuovinen, J.P., 2002. Annual CO_2 balance of a subarctic fen in northern Europe: Importance of the wintertime efflux. Journal of Geophysical Research-Atmospheres 107(D21), ACH 17-1-ACH 17-2. DOI: www.dx.doi.org/10.1029/2002JD002055

Babst, F., Mueller, R., and Hollmarm, R., 2008. Verification of NCEP reanalysis shortwave radiation with mesoscale remote sensing data. Ieee Geoscience and Remote Sensing Letters 5(1), 34-37. DOI: www.dx.doi.org/10.1109/LGRS.2007.907537

Baigorria, G.A., Villegas, E.B., Trebejo, I., Carlos, J.F., and Quiroz, R., 2004. Atmospheric transmissivity: Distribution and empirical estimation around the central andes. International Journal of Climatology 24(9), 1121-1136. DOI: www.dx.doi.org/10.1002/joc.1060

Baldocchi, D.D., 2003. Assessing the eddy covariance technique for evaluating carbon dioxide exchange rates of ecosystems: past, present and future. Global Change Biology 9(4), 479-492. DOI: www.dx.doi.org/10.1046/j.1365-2486.2003.00629.x

Baldocchi, D.D., 2008. Breathing of the terrestrial biosphere: lessons learned from a global network of carbon dioxide flux measurement systems. Australian Journal of Botany 56(1), 1-26. DOI: www.dx.doi.org/10.1071/BT07151

Baldocchi, D.D., Falge, E., Gu, L.H., Olson, R., Hollinger, D., Running, S., Anthoni, P., Bernhofer, C., Davis, K., Evans, R., Fuentes, J., Goldstein, A., Katul, G., Law, B., Lee, X.H., Malhi, Y., Meyers, T., Munger, W., Oechel, W., U, K., Pilegaard, K., Schmid, H.P., Valentini, R., Verma, S., Vesala, T., Wilson, K., and Wofsy, S., 2001. FLUXNET: A new tool to study the temporal and spatial variability of ecosystem-scale carbon dioxide, water vapor, and energy flux densities. Bulletin of the American Meteorological Society 82(11), 2415-2434. DOI: www.dx.doi.org/10.1175/1520-0477(2001)082<2415:FANTTS>2.3.CO;2

Baldocchi, D.D. and Meyers, T., 1998. On using eco-physiological, micrometeorological and biogeochemical theory to evaluate carbon dioxide, water vapor and trace gas fluxes over vegetation: a perspective. Agricultural and Forest Meteorology 90(1-2), 1-25. DOI: www.dx.doi.org/10.1016/S0168-1923(97)00072-5

Baldocchi, D.D. and Xu, L. 2005. Carbon exchange of deciduous broadleaved forests in temperate and Mediterranean regions. In: Griffith, H., Jarvis, P.J. (Eds.), The Carbon Balance of Forest Biomes, Garland Science/BIOS Scientific Publishers, 187-213.

Ball, J.T., Woodrow, I.E. and Berry, J.A. 1987. A model predicting stomatal conductance and its contribution to the control of photosynthesis under different environmental conditions. In: Biggins, J. (Ed.), Progress in photosynthesis research, Martinus-Nijhoff Publishers, Dordrecht, The Netherlands, 221-224.

Barford, C.C., Wofsy, S.C., Goulden, M.L., Munger, J.W., Pyle, E.H., Urbanski, S.P., Hutyra, L., Saleska, S.R., Fitzjarrald, D., and Moore, K., 2001. Factors controlling long- and short-term sequestration of atmospheric CO_2 in a mid-latitude forest. Science 294(5547), 1688-1691. DOI: www.dx.doi.org/10.1126/science.1062962

Berger, T.W., Untersteiner, H., Toplitzer, M., and Neubauer, C., 2009. Nutrient fluxes in pure and mixed stands of spruce (Picea abies) and beech (Fagus sylvatica). Plant and Soil 322(1-2), 317-342. DOI: www.dx.doi.org/10.1007/s11104-009-9918-z

Bergh, J., McMurtrie, R.E., and Linder, S., 1998. Climatic factors controlling the productivity of Norway spruce: A model-based analysis. Forest Ecology and Management 110(1-3), 127-139. DOI: www.dx.doi.org/10.1016/S0378-1127(98)00280-1

Bergholm, J., Majdi, H., and Persson, T., 2007. Nitrogen Budget of a Spruce Forest Ecosystem After Six-year Addition of Ammonium Sulphate in Southwest Sweden. Water Air Soil Pollut: Focus 7(1-3), 225-234. DOI: www.dx.doi.org/10.1007/s11267-006-9104-8

Berninger, F., 1994. Simulated irradiance and temperature estimates as a possible source of bias in the simulation of photosynthesis. Agricultural and Forest Meteorology 71(1), 19-32. DOI: www.dx.doi.org/10.1016/0168-1923(94)90098-1

Bolin, B., Sukumar, R., Ciais, P., Cramer, W., Jarvis, P., Kheshgi, H., Nobre, C., Semenov, S. and Steffen, W. 2000. Global Perspective. In: Watson, R.T., Noble, I.R., Ravindranath, N.H., Verardo, D.J., Dokken, D.J. (Eds.), IPCC, Land Use, Land-Use Change, and Forestry. A Special Report of the IPCC, Cambridge University Press, Cambridge, UK, 23-51.

Bonan, G.B., 2008a. Ecological Climatology: Concepts and Applications. 2nd Edition, Cambridge University Press, Cambridge, pp. 550.

Bonan, G.B., 2008b. Forests and climate change: Forcings, feedbacks, and the climate benefits of forests. Science 320(5882), 1444-1449. DOI: www.dx.doi.org/10.1126/science.1155121

Bond-Lamberty, B., Wang, C.K., and Gower, S.T., 2004. Net primary production and net ecosystem production of a boreal black spruce wildfire chronosequence. Global Change Biology 10(4), 473-487. DOI: www.dx.doi.org/10.1111/j.1529-8817.2003.0742.x

Borken, W., Kossmann, G., and Matzner, E., 2007. Biomass, morphology and nutrient contents of fine roots in four Norway spruce stands. Plant and Soil 292(1-2), 79-93. DOI: www.dx.doi.org/10.1007/s11104-007-9204-x

Botta-Dukát, Z., Chytrý, M., Hájková, P., and Havlová, M., 2005. Vegetation of lowland wet meadows along a climatic continentality gradient in Central Europe. Preslia 77, 89-111

Bowling, D. and Massman, W., 2011. Persistent wind-induced enhancement of diffusive CO_2 transport in a mountain forest snowpack. Journal of Geophysical Research-Biogeosciences 116. DOI: www.dx.doi.org/10.1029/2011JG001722

Bristow, K.L. and Campbell, G.S., 1984. On the Relationship Between Incoming Solar-Radiation and Daily Maximum and Minimum Temperature. Agricultural and Forest Meteorology 31(2), 159-166. DOI: www.dx.doi.org/10.1016/0168-1923(84)90017-0

Brooks, P.D., McKnight, D., and Elder, K., 2005. Carbon limitation of soil respiration under winter snowpacks: potential feedbacks between growing season and winter carbon fluxes. Global Change Biology 11(2), 231-238. DOI: www.dx.doi.org/10.1111/j.1365-2486.2004.00877.x

Brown, M.G., Black, T., Nesic, Z., Fredeen, A.L., Foord, V.N., Spittlehouse, D.L., Bowler, R., Burton, P.J., Trofymow, J., Grant, N.J., and Lessard, D., 2012. The carbon balance of two lodgepole pine stands recovering from mountain pine beetle attack in British Columbia. Agricultural and Forest Meteorology 153, 82-93. DOI: www.dx.doi.org/10.1016/j.agrformet.2011.07.010

Brunner, I., Bakker, M., Bjork, R., Hirano, Y., Lukac, M., Aranda, X., Borja, I., Eldhuset, T., Helmisaari, H., Jourdan, C., Konopka, B., Lopez, B., Miguel Perez, C., Persson, H., and Ostonen, I., 2013. Fine-root turnover rates of European forests revisited: an analysis of data from sequential coring and ingrowth cores. Plant and Soil 362(1-2), 357-372. DOI: www.dx.doi.org/10.1007/s11104-012-1313-5

Buchmann, N. and Schulze, E.D., 1999. Net CO_2 and H_2O fluxes of terrestrial ecosystems. Global Biogeochemical Cycles 13(3), 751-760. DOI: www.dx.doi.org/10.1029/1999GB900016

Burba, G. and Anderson,D.J., 2010. A Brief Practical Guide to Eddy Covariance Flux Measurements: Principles and Workflow Examples for Scientific and Industrial Applications, LI-COR Biosciences, Lincoln, USA, 1-211.

Canadell, J.G., Kirschbaum, M.U.F., Kurz, W.A., Sanz, M.J., Schlamadinger, B., and Yamagata, Y., 2007a. Factoring out natural and indirect human effects on terrestrial carbon sources and sinks. Environmental Science & Policy 10(4), 370-384. DOI: www.dx.doi.org/10.1016/j.envsci.2007.01.009

Canadell, J.G., Mooney, H.A., Baldocchi, D.D., Berry, J.A., Ehleringer, J.R., Field, C.B., Gower, S.T., Hollinger, D.Y., Hunt, J.E., Jackson, R.B., Running, S.W., Shaver, G.R., Steffen, W., Trumbore, S.E., Valentini, R., and Bond, B.Y., 2000. Carbon metabolism of the terrestrial biosphere: A multitechnique approach for improved understanding. Ecosystems 3(2), 115-130. DOI: www.dx.doi.org/10.1007/s100210000014

Canadell, J.G., Ciais, P., Dhakal, S., Dolman, H., Friedlingstein, P., Gurney, K.R., Held, A., Jackson, R.B., Le Quere, C., Malone, E.L., Ojima, D.S., Patwardhan, A., Peters, G.P., and Raupach, M.R., 2010. Interactions of the carbon cycle, human activity, and the climate system: a research portfolio. Current Opinion in Environmental Sustainability 2(4), 301-311. DOI: www.dx.doi.org/10.1016/j.cosust.2010.08.003

Canadell, J.G., Le Quere, C., Raupach, M.R., Field, C.B., Buitenhuis, E.T., Ciais, P., Conway, T.J., Gillett, N.P., Houghton, R., and Marland, G., 2007b. Contributions to accelerating atmospheric CO_2 growth from economic activity, carbon intensity, and efficiency of natural sinks. Proceedings of the National Academy of Sciences of the United States of America 104(47), 18866-18870. DOI: www.dx.doi.org/10.1073/pnas.0702737104

Chapin, F.S., Matson,P.A. and Mooney,H.A., 2002. Principles of terrestrial ecosystem ecology, Springer, New York, pp. 436.

Chapin, F.S., Woodwell, G., Randerson, J., Rastetter, E., Lovett, G., Baldocchi, D., Clark, D., Harmon, M., Schimel, D., Valentini, R., Wirth, C., Aber, J., Cole, J., Goulden, M., Harden, J., Heimann, M., Howarth, R., Matson, P., McGuire, A., Melillo, J., Mooney, H., Neff, J., Houghton, R., Pace, M., Ryan, M., Running, S., Sala, O., Schlesinger, W.H., and Schulze, E.-D., 2006. Reconciling carbon-cycle concepts, terminology, and methods. Ecosystems 9(7), 1041-1050. DOI: www.dx.doi.org/10.1007/s10021-005-0105-7

Chen, J.Q., Brosofske, K.D., Noormets, A., Crow, T.R., Bresee, M.K., Le Moine, J.M., Euskirchen, E.S., Mather, S.V., and Zheng, D., 2004. A working framework for quantifying carbon sequestration in disturbed land mosaics. Environmental Management 33, pp. S210-S221. DOI: www.dx.doi.org/10.1007/s00267-003-9131-4

Ciais, P., Schelhaas, M.J., Zaehle, S., Piao, S.L., Cescatti, A., Liski, J., Luyssaert, S., Le-Maire, G., Schulze, E.D., Bouriaud, O., Freibauer, A., Valentini, R., and Nabuurs, G.J., 2008. Carbon accumulation in European forests. Nature Geoscience 1(7), 425-429. DOI: www.dx.doi.org/10.1038/ngeo233

Cienciala, E., Eckersten, H., Lindroth, A., and Hallgren, J.E., 1994. Simulated and Measured Water-Uptake by Picea-Abies Under Nonlimiting Soil-Water Conditions. Agricultural and Forest Meteorology 71(1-2), 147-164. DOI: www.dx.doi.org/10.1016/0168-1923(94)90105-8

Clement, R.J., Jarvis, P.G., and Moncrieff, J.B., 2012. Carbon dioxide exchange of a Sitka spruce plantation in Scotland over five years. Agricultural and Forest Meteorology 153(0), 106-123. DOI: www.dx.doi.org/10.1016/j.agrformet.2011.07.012

Cleverly, J., 2011. Alice Springs Mulga OzFlux site. OzFlux: Australian and New Zealand Flux Research and Monitoring Network, hdl 102(100), pp. 8697. DOI: www.dx.doi.org/10.3334/ORNLDAAC/761

Dale, V.H., Joyce, L.A., McNulty, S., Neilson, R.P., Ayres, M.P., Flannigan, M.D., Hanson, P.J., Irland, L.C., Lugo, A.E., Peterson, C.J., Simberloff, D., Swanson, F.J., Stocks, B.J., and Wotton, B.M., 2001. Climate change and forest disturbances. Bioscience 51(9), 723-734. DOI: www.dx.doi.org/10.1641/0006-3568(2001)051[0723:CCAFD]2.0.CO;2

Dale, V.H., Joyce, L.A., McNulty, S., and Neilson, R.P., 2000. The interplay between climate change, forests, and disturbances. Science of The Total Environment 262(3), 201-204

Desai, A.R., Bolstad, P.V., Cook, B.D., Davis, K.J., and Carey, E.V., 2005. Comparing net ecosystem exchange of carbon dioxide between an old-growth and mature forest in the upper Midwest, USA. Agricultural and Forest Meteorology 128(1-2), 33-55. DOI: www.dx.doi.org/10.1016/j.agrformet.2004.09.005

Diamond, H.J., Karl, T.R., Palecki, M.A., Baker, C.B., Bell, J.E., Leeper, R.D., Easterling, D.R., Lawrimore, J.H., Meyers, T.P., Helfert, M.R., Goodge, G., and Thorne, P.W., 2013. U.S. Climate Reference Network after One Decade of Operations: Status and Assessment. Bulletin of the American Meteorological Society 94(4), 485-498. DOI: www.dx.doi.org/doi: 10.1175/BAMS-D-12-00170.1

Donat, M.G., Pardowitz, T., Leckebusch, G.C., Ulbrich, U., and Burghoff, O., 2011. High-resolution refinement of a storm loss model and estimation of return periods of loss-intensive storms over Germany. Nat.Hazards Earth Syst.Sci. 11(10), 2821-2833. DOI: www.dx.doi.org/10.5194/nhess-11-2821-2011

Dore, S., Kolb, T.E., Montes-Helu, M., Sullivan, B.W., Winslow, W.D., Hart, S.C., Kaye, J.P., Koch, G.W., and Hungate, B.A., 2008. Long-term impact of a stand-replacing fire on ecosystem CO2 exchange of a ponderosa pine forest. Global Change Biology 14(8), 1801-1820. DOI: www.dx.doi.org/10.1111/j.1365-2486.2008.01613.x

Dragoni, D., Schmid, H.P., Grimmond, C.S.B., and Loescher, H.W., 2007. Uncertainty of annual net ecosystem productivity estimated using eddy covariance flux measurements. Journal of Geophysical Research: Biogeosciences 112(D17), pp. D17102. DOI: www.dx.doi.org/10.1029/2006JD008149

Dragoni, D., Schmid, H.P., Wayson, C.A., Potter, H., Grimmond, C., and Randolph, J.C., 2011. Evidence of increased net ecosystem productivity associated with a longer vegetated season in a deciduous forest in south-central Indiana, USA. Global Change Biology 17(2), 886-897. DOI: www.dx.doi.org/10.1111/j.1365-2486.2010.02281.x

Durand, J.L., Schaufele, R., and Gastal, F., 1999. Grass leaf elongation rate as a function of developmental stage and temperature: Morphological analysis and modelling. Annals of Botany 83(5), 577-588. DOI: www.dx.doi.org/10.1006/anbo.1999.0864

Edburg, S.L., Hicke, J.A., Lawrence, D.M., and Thornton, P.E., 2011. Simulating coupled carbon and nitrogen dynamics following mountain pine beetle outbreaks in the western United States. Journal of Geophysical Research: Biogeosciences 116(G4), pp. G04033. DOI: www.dx.doi.org/10.1029/2011JG001786

Eder, F., De Roo, F., Kohnert, K., Desjardins, R., Schmid, H.P., and Mauder, M., 2014. Evaluation of Two Energy Balance Closure Parametrizations. Boundary-Layer Meteorol 151(2), 195-219. DOI: www.dx.doi.org/10.1007/s10546-013-9904-0

Ehman, J.L., Schmid, H.P., Grimmond, C.S.B., Randolph, J.C., Hanson, P.J., Wayson, C.A., and Cropley, F.D., 2002. An initial intercomparison of micrometeorological and ecological inventory estimates of carbon exchange in a mid-latitude deciduous forest. Global Change Biology 8(6), 575-589. DOI: www.dx.doi.org/10.1046/j.1365-2486.2002.00492.x

Elbers, J.A., Jacobs, C.M., Kruijt, B., Jans, W.W., and Moors, E.J., 2011. Assessing the uncertainty of estimated annual totals of net ecosystem productivity: A practical approach applied to a mid latitude temperate pine forest. Agricultural and Forest Meteorology 151(12), 1823-1830. DOI: www.dx.doi.org/10.1016/j.agrformet.2011.07.020

Eliasson, P., Svensson, M., Olsson, M., and Ågren, G.I., 2013. Forest carbon balances at the landscape scale investigated with the Q model and the CoupModel - Responses to intensified harvests. Forest Ecology and Management 290(0), 67-78. DOI: www.dx.doi.org/10.1016/j.foreco.2012.09.007

Elling, W., Bauer, E., Klemm, G., and Koch, H., 1987. Klima und Böden - Waldstandorte.1, pp. 255

Etzold, S., Ruehr, N.K., Zweifel, R., Dobbertin, M., Zingg, A., Pluess, P., Haesler, R., Eugster, W., and Buchmann, N., 2011. The Carbon Balance of Two Contrasting Mountain Forest Ecosystems in Switzerland: Similar Annual Trends, but Seasonal Differences. Ecosystems 14(8), 1289-1309. DOI: www.dx.doi.org/10.1007/s10021-011-9481-3

Falge, E., Aubinet, M., Bakwin, P., Baldocchi, D., Berbigier, P., Bernhofer, C., Black, A., Ceulemans, R., Davis, K., and Dolman, A., 2005. FLUXNET Marconi Conference gap-filled flux and meteorology data, 1992ΓÇô2000. Data set.Available on-line [http//www.daac.ornl.gov] from Oak Ridge National Laboratory Distributed Active Archive Center, Oak Ridge, Tennessee, USA doi 10. DOI: www.dx.doi.org/110.3334/ORNLDAAC/811

Falge, E., Baldocchi, D., Olson, R., Anthoni, P., Aubinet, M., Bernhofer, C., Burba, G., Ceulemans, R., Clement, R., Dolman, H., Granier, A., Gross, P., Grunwald, T., Hollinger, D., Jensen, N.O., Katul, G., Keronen, P., Kowalski, A., Lai, C.T., Law, B.E., Meyers, T., Moncrieff, H., Moors, E., Munger, J.W., Pilegaard, K., Rannik, U., Rebmann, C., Suyker, A., Tenhunen, J., Tu, K., Verma, S., Vesala, T., Wilson, K., and Wofsy, S., 2001. Gap filling strategies for defensible annual sums of net ecosystem exchange. Agricultural and Forest Meteorology 107(1), 43-69. DOI: www.dx.doi.org/10.1016/S0168-1923(00)00225-2

Falge, E., Ryel, R.J., Alsheimer, M., and Tenhunen, J.D., 1997. Effects of stand structure and physiology on forest gas exchange: a simulation study for Norway spruce. Trees-Structure and Function 11(7), 436-448. DOI: www.dx.doi.org/10.1007/s004680050105

Falkowski, P., Scholes, R.J., Boyle, E., Canadell, J., Canfield, D., Elser, J., Gruber, N., Hibbard, K., Hogberg, P., Linder, S., Mackenzie, F.T., Moore, B., Pedersen, T., Rosenthal, Y., Seitzinger, S., Smetacek, V., and Steffen, W., 2000. The global carbon cycle: A test of our knowledge of earth as a system. Science 290(5490), 291-296. DOI: www.dx.doi.org/10.1126/science.290.5490.291

FAO, 2010. Global Forest Resources Assessment 2010. Main report.163

Farquhar, G.D., Von Caemmerer, S., and Berry, J.A., 1980. A biochemical model of photosynthetic CO_2 assimilation in leaves of C_3 species. Planta 149, 78-90

Fink, A.H., Brucher, T., Ermert, V., Kruger, A., and Pinto, J.G., 2009. The European storm Kyrill in January 2007: synoptic evolution, meteorological impacts and some considerations with respect to climate change. Natural Hazards and Earth System Sciences 9(2), 405-423. DOI: www.dx.doi.org/10.5194/nhess-9-405-2009

Finkelstein, P.L. and Sims, P.F., 2001. Sampling error in eddy correlation flux measurements. Journal of Geophysical Research-Atmospheres 106(D4), 3503-3509. DOI: www.dx.doi.org/10.1029/2000JD900731

Foken, T., Aubinet, M., Finnigan, J.J., Leclerc, M.Y., Mauder, M., and U, K., 2011. Results of A Panel Discussion About the Energy Balance Closure Correction for Trace Gases. Bulletin of the American Meteorological Society 92(4), pp. ES13-ES18. DOI: www.dx.doi.org/10.1175/2011BAMS3130.1

Foken, T., Gockede, M., Mauder, M., Mahrt, L., Amiro, B., and Munger, W., 2004. Post-field data quality control. Handbook of Micrometeorology: A Guide for Surface Flux Measurement and Analysis 29, 181-208. DOI: www.dx.doi.org/10.1007/1-4020-2265-4_9

Foken, T. and Wichura, B., 1996. Tools for quality assessment of surface-based flux measurements. Agricultural and Forest Meteorology 78(1-2), 83-105. DOI: www.dx.doi.org/10.1016/0168-1923(95)02248-1

Foken, T., 2008. Micrometeorology, Springer, Berlin, pp. 306.

Foken, T., Leuning, R., Oncley, S., Mauder, M. and Aubinet, M. 2012. Corrections and Data Quality Control. In: Aubinet, M., Vesala, T., Papale, D. (Eds.), Eddy Covariance, Springer Netherlands, 85-131.

Fortin, J.G., Anctil, F., Parent, L.E., and Bolinder, M.A., 2008. Comparison of empirical daily surface incoming solar radiation models. Agricultural and Forest Meteorology 148(8-9), 1332-1340. DOI: www.dx.doi.org/10.1016/j.agrformet.2008.03.012

Friend, A.D., Arneth, A., Kiang, N.Y., Lomas, M., Ogee, J., Roedenbeckk, C., Running, S.W., Santaren, J.D., Sitch, S., Viovy, N., Woodward, F., I, and Zaehle, S., 2007. FLUXNET and modelling the global carbon cycle. Global Change Biology 13(3), 610-633. DOI: www.dx.doi.org/10.1111/j.1365-2486.2006.01223.x

Gardiner, B., Blennow, K., Carnus, J.M., Fleischner, P., Ingemarson, F., Landmann, G., Lindner, M., Marzano, M., Nicoll, B., Orazio, C., Peyron, J.L., Reviron, M.P., Schelhaas, M.J., Schuck, A., Spielmann, M., and Usbeck, T., 2010. Destructive storms in European forests: past and forthcoming impacts., pp. 138

Goetz, S.J., Bond-Lamberty, B., Law, B.E., Hicke, J.A., Huang, C., Houghton, R.A., McNulty, S., O'Halloran, T., Harmon, M., Meddens, A.J.H., Pfeifer, E.M., Mildrexler, D., and Kasischke, E.S., 2012. Observations and assessment of forest carbon dynamics following disturbance in North America. Journal of Geophysical Research: Biogeosciences 117(G2), pp. G02022. DOI: www.dx.doi.org/10.1029/2011JG001733

Goodale, C.L., Apps, M.J., Birdsey, R.A., Field, C.B., Heath, L.S., Houghton, R.A., Jenkins, J.C., Kohlmaier, G.H., Kurz, W., Liu, S.R., Nabuurs, G.J., Nilsson, S., and Shvidenko, A.Z., 2002. Forest carbon sinks in the Northern Hemisphere. Ecological Applications 12(3), 891-899. DOI: www.dx.doi.org/10.2307/3060997

Goodin, D.G., Hutchinson, J.M.S., Vanderlip, R.L., and Knapp, M.C., 1999. Estimating solar irradiance for crop modeling using daily air temperature data. Agronomy Journal 91(5), 845-851. DOI: www.dx.doi.org/10.2134/agronj1999.915845x

Gough, C.M., Hardiman, B.S., Nave, L.E., Bohrer, G., Maurer, K.D., Vogel, C.S., Nadelhoffer, K.J., and Curtis, P.S., 2013. Sustained carbon uptake and storage following moderate disturbance in a Great Lakes forest. Ecological Applications 23(5), 1202-1215. DOI: www.dx.doi.org/10.1890/12-1554.1

Gough, C.M., Vogel, C.S., Harrold, K.H., George, K., and Curtis, P.S., 2007. The legacy of harvest and fire on ecosystem carbon storage in a north temperate forest. Global Change Biology 13(9), 1935-1949. DOI: www.dx.doi.org/10.1111/j.1365-2486.2007.01406.x

Gough, C.M., Vogel, C.S., Schmid, H.P., and Curtis, P.S., 2008. Controls on annual forest carbon storage: Lessons from the past and predictions for the future. Bioscience 58(7), 609-622. DOI: www.dx.doi.org/10.1641/B580708

Gower, S.T., Haynes, B.E., Fassnacht, K.S., Running, S.W., and Hunt, E.R., 1993. Influence of Fertilization on the Allometric Relations for 2 Pines in Contrasting Environments. Canadian Journal of Forest Research-Revue Canadienne de Recherche Forestiere 23(8), 1704-1711. DOI: www.dx.doi.org/10.1139/x93-212

Grassi, G., Colom, M.R., and Minotta, G., 2001. Effects of nutrient supply on photosynthetic acclimation and photoinhibition of one-year-old foliage of Picea abies. Physiologia Plantarum 111(2), 245-254. DOI: www.dx.doi.org/10.1034/j.1399-3054.2001.1110217.x

Groffman, P.M., Driscoll, C.T., Fahey, T.J., Hardy, J.P., Fitzhugh, R.D., and Tierney, G.L., 2001. Colder soils in a warmer world: A snow manipulation study in a northern hardwood forest ecosystem. Biogeochemistry 56(2), 135-150. DOI: www.dx.doi.org/10.1023/A:1013039830323

Grote, R., 1998. Integrating dynamic morphological properties into forest growth modeling. II. Allocation and mortality. Forest Ecology and Management 111(2/3), 193-210. DOI: www.dx.doi.org/10.1016/S0378-1127(98)00328-4

Grote, R., Lavoir, A.V., Rambal, S., Staudt, M., Zimmer, I., and Schnitzler, J.-P., 2009a. Modelling the drought impact on monoterpene fluxes from an evergreen Mediterranean forest canopy. Oecologia 160(2), 213-223. DOI: www.dx.doi.org/10.1007/s00442-009-1298-9

Grote, R., Kiese, R., Grünwald, T., Ourcival, J.-M., and Granier, A., 2011a. Modelling forest carbon balances considering tree mortality and removal. Agricultural and Forest Meteorology 151, 179-190. DOI: www.dx.doi.org/10.1016/j.agrformet.2010.10.002

Grote, R., Korhonen, J., and Mammarella, I., 2011b. Challenges for evaluating process-based models of gas exchange at forest sites with fetches of various species. Forest Systems 20(3), 389-406. DOI: www.dx.doi.org/10.5424/fs/20112003-11084

Grote, R., Lehmann, E., Brümmer, C., Brüggemann, N., Szarzynski, J., and Kunstmann, H., 2009b. Modelling and observation of biosphere-atmosphere interactions in natural savannah in

Burkina Faso, West Africa. Physics and Chemistry of the Earth 34(4-5), 251-260. DOI: www.dx.doi.org/10.1016/j.pce.2008.05.003

Grote, R., 2007. Sensitivity of volatile monoterpene emission to changes in canopy structure: a model-based exercise with a process-based emission model. New Phytologist 173(3), 550-561. DOI: www.dx.doi.org/10.1111/j.1469-8137.2006.01946.x

Grote, R., Lehmann, E., Bruemmer, C., Brueggemann, N., Szarzynski, J., and Kunstmann, H., 2009c. Modelling and observation of biosphere-atmosphere interactions in natural savannah in Burkina Faso, West Africa. Physics and Chemistry of the Earth 34(4-5), 251-260. DOI: www.dx.doi.org/10.1016/j.pce.2008.05.003

Gruenwald, T. and Bernhofer, C., 2007. A decade of carbon, water and energy flux measurements of an old spruce forest at the Anchor Station Tharandt. Tellus Series B-Chemical and Physical Meteorology 59(3), 387-396. DOI: www.dx.doi.org/10.1111/j.1600-0889.2007.00259.x

Gu, L., Falge, E.M., Boden, T., Baldocchi, D.D., Black, T.A., Saleska, S.R., Suni, T., Verma, S.B., Vesala, T., and Wofsy, S.C., 2005. Objective threshold determination for nighttime eddy flux filtering. Agricultural and Forest Meteorology 128(3), 179-197. DOI: www.dx.doi.org/10.1016/j.agrformet.2004.11.006

Haas, E., Klatt, S., Froehlich, A., Kraft, P., Werner, C., Kiese, R., Grote, R., Breuer, L., and Butterbach-Bahl, K., 2013. LandscapeDNDC: a process model for simulation of biosphere-atmosphere-hydrosphere exchange processes at site and regional scale. Landscape Ecology 28(4), 615-636. DOI: www.dx.doi.org/10.1007/s10980-012-9772-x

Hagen, S.C., Braswell, B.H., Linder, E., Frolking, S., Richardson, A.D., and Hollinger, D.Y., 2006. Statistical uncertainty of eddy flux-based estimates of gross ecosystem carbon exchange at Howland Forest, Maine. Journal of Geophysical Research-Atmospheres 111(D8). DOI: www.dx.doi.org/10.1029/2005JD006154

Hanan, N., Scholes, R., and Cougenour, M., 2004. SAFARI 2000 Meteorological Tower Measurements, Kruger National Park, 2000-2002.

Hargreaves, G.H. and Samani, Z.A., 1982. Estimating potential evapotranspiration. Journal of the Irrigation and Drainage Division 108(3), 225-230

Harmon, M.E., Bond-Lamberty, B., Tang, J., and Vargas, R., 2011. Heterotrophic respiration in disturbed forests: A review with examples from North America. Journal of Geophysical Research: Biogeosciences 116, pp. G00K04. DOI: www.dx.doi.org/10.1029/2010JG001495

Heimann, M. and Reichstein, M., 2008. Terrestrial ecosystem carbon dynamics and climate feedbacks. Nature 451(7176), 289-292. DOI: www.dx.doi.org/10.1038/nature06591

Herrmann, S. and Bauhus, J., 2013. Effects of moisture, temperature and decomposition stage on respirational carbon loss from coarse woody debris (CWD) of important European tree species. Scandinavian Journal of Forest Research 28(4), 346-357. DOI: www.dx.doi.org/10.1080/02827581.2012.747622

Hojstrup, J., 1981. A Simple-Model for the Adjustment of Velocity Spectra in Unstable Conditions Downstream of An Abrupt Change in Roughness and Heat-Flux. Boundary-Layer Meteorology 21(3), 341-356. DOI: www.dx.doi.org/10.1007/BF00119278

Hojstrup, J., 1993. A Statistical-Data Screening-Procedure. Measurement Science & Technology 4(2), 153-157. DOI: www.dx.doi.org/10.1088/0957-0233/4/2/003

Hollinger, D.Y. and Richardson, A.D., 2005. Uncertainty in eddy covariance measurements and its application to physiological models. Tree Physiology 25(7), 873-885. DOI: www.dx.doi.org/10.1093/treephys/25.7.873

Holmlund, P. and Schneider, T., 1997. The effect of continentality on glacier response and mass balance. Annals of Glaciology 24, 272-276. DOI: www.dx.doi.org/10.1029/2011JF002064

Holst, J., Grote, R., Offermann, C., Ferrio, J.P., Gessler, A., Mayer, H., and Rennenberg, H., 2010. Water fluxes within beech stands in complex terrain. International Journal of Biometeorology 54, 23-36. DOI: www.dx.doi.org/10.1007/s00484-009-0248-x

Holtslag, A.A.M. and Vanulden, A.P., 1983. A Simple Scheme for Daytime Estimates of the Surface Fluxes from Routine Weather Data. Journal of Climate and Applied Meteorology 22(4), 517-529. DOI: www.dx.doi.org/10.1175/1520-0450(1983)022<0517:ASSFDE>2.0.CO;2

Hommeltenberg, J., Schmid, H.P., Drösler, M., and Werle, P., 2014. Can a bog drained for forestry be a stronger carbon sink than a natural bog forest? Biogeosciences 11(13), 3477-3493. DOI: www.dx.doi.org/10.5194/bg-11-3477-2014

Houghton, R.A., 2003. Why are estimates of the terrestrial carbon balance so different? Global Change Biology 9(4), 500-509. DOI: www.dx.doi.org/10.1046/j.1365-2486.2003.00620.x

Howard, E.A., Gower, S.T., Foley, J.A., and Kucharik, C.J., 2004. Effects of logging on carbon dynamics of a jack pine forest in Saskatchewan, Canada. Global Change Biology 10(8), 1267-1284. DOI: www.dx.doi.org/10.1111/j.1365-2486.2004.00804.x

Hussain, M., Gruenwald, T., Tenhunen, J., Li, Y., Mirzae, H., Bernhofer, C., Otieno, D., Dinh, N., Schmidt, M., Wartinger, M., and Owen, K., 2011. Summer drought influence on CO_2 and water fluxes of extensively managed grassland in Germany. Agriculture Ecosystems & Environment 141(1-2), 67-76. DOI: www.dx.doi.org/10.1016/j.agee.2011.02.013

IGBP Terrestrial Carbon Working Group, 1998. The Terrestrial Carbon Cycle: Implications for the Kyoto Protocol. Science 280(5368), 1393-1394. DOI: www.dx.doi.org/10.1126/science.280.5368.1393

Ilvesniemi, H., Kahkonen, M.A., Pumpanen, J., Rannik, U., Wittmann, C., Peramaki, M., Keronen, P., Hari, P., Vesala, T., and Salkinoja-Salonen, M., 2005. Wintertime CO_2 evolution from a boreal forest ecosystem. Boreal Environment Research 10(5), 401-408

IPCC, 2013. Climate Change 2013: The Physical Science Basis. Contribution of Working Group I to the Fifth Assessment Report of the Intergovernmental Panel on Climate Change., pp. 1535

Jackson, R.B., Mooney, H.A., and Schulze, E.D., 1997. A global budget for fine root biomass, surface area, and nutrient contents. Proceedings of the National Academy of Sciences of the United States of America 94(14), 7362-7366. DOI: www.dx.doi.org/10.1073/pnas.94.14.7362

Janisch, J.E. and Harmon, M.E., 2002. Successional changes in live and dead wood carbon stores: implications for net ecosystem productivity. Tree Physiology 22(2-3), 77-89. DOI: www.dx.doi.org/10.1093/treephys/22.2-3.77

Janssens, I.A., Freibauer, A., Schlamadinger, B., Ceulemans, R., Ciais, P., Dolman, A.J., Heimann, M., Nabuurs, G.J., Smith, P., Valentini, R., and Schulze, E.D., 2005. The carbon budget of terrestrial ecosystems at country-scale - a European case study. Biogeosciences 2(1), 15-26. DOI: www.dx.doi.org/10.5194/bg-2-15-2005

Janssens, I.A., Lankreijer, H., Matteucci, G., Kowalski, A.S., Buchmann, N., Epron, D., Pilegaard, K., Kutsch, W., Longdoz, B., Grunwald, T., Montagnani, L., Dore, S., Rebmann, C., Moors, E.J., Grelle, A., Rannik, U., Morgenstern, K., Oltchev, S., Clement, R., Gudmundsson, J., Minerbi, S., Berbigier, P., Ibrom, A., Moncrieff, J., Aubinet, M., Bernhofer, C., Jensen, N.O., Vesala, T., Granier, A., Schulze, E.D., Lindroth, A., Dolman, A.J., Jarvis, P.G., Ceulemans, R., and Valentini, R., 2001. Productivity overshadows temperature in determining soil and ecosystem respiration across European forests. Global Change Biology 7(3), 269-278. DOI: www.dx.doi.org/10.1046/j.1365-2486.2001.00412.x

Jia, B.H., Xie, Z.H., Dai, A.G., Shi, C.X., and Chen, F., 2013. Evaluation of satellite and reanalysis products of downward surface solar radiation over East Asia: Spatial and seasonal variations. Journal of Geophysical Research-Atmospheres 118(9), 3431-3446. DOI: www.dx.doi.org/10.1002/jgrd.50353

Kaimal, J.C., Izumi, Y., Wyngaard, J.C., and Cote, R., 1972. Spectral Characteristics of Surface-Layer Turbulence. Quarterly Journal of the Royal Meteorological Society 98(417), 563-589. DOI: www.dx.doi.org/10.1002/qj.49709841707

Kaimal, J.C. and Finnigan,J.J., 1994. Atmospheric boundary layer flows : their structure and measurement, Oxford University Press, New York, pp. 289.

Kirschbaum, M.U.F., Eamus, D., Gifford, R.M., Roxburgh, S.H. and Sands, P.J. 2001. Definitions Of Some Ecological Terms Commonly Used In Carbon Accounting. In: Kirschbaum, M.U.F., Mueller, R. (Eds.), Net Ecosystem Exchange CRC Workshop Proceedings, Cooperative Research Centre for Greenhouse Accounting, Canberra, Australia, 2-5.

Kljun, N., Calanca, P., Rotachhi, M.W., and Schmid, H.P., 2004. A simple parameterisation for flux footprint predictions. Boundary-Layer Meteorology 112(3), 503-523. DOI: www.dx.doi.org/10.1023/B:BOUN.0000030653.71031.96

Knohl, A., Kolle, O., Minayeva, T.Y., Milyukova, I.M., Vygodskaya, N.N., Foken, T., and Schulze, E.D., 2002. Carbon dioxide exchange of a Russian boreal forest after disturbance by wind throw. Global Change Biology 8(3), 231-246. DOI: www.dx.doi.org/10.1046/j.1365-2486.2002.00475.x

Knohl, A., Schulze, E.D., Kolle, O., and Buchmann, N., 2003. Large carbon uptake by an unmanaged 250-year-old deciduous forest in Central Germany. Agricultural and Forest Meteorology 118(3-4), 151-167. DOI: www.dx.doi.org/10.1016/S0168-1923(03)00115-1

Kochendorfer, J., Castillo, E.G., Haas, E., Oechel, W.C., and Paw, K.T., 2011. Net ecosystem exchange, evapotranspiration and canopy conductance in a riparian forest. Agricultural and Forest Meteorology 151(5), 544-553. DOI: www.dx.doi.org/10.1016/j.agrformet.2010.12.012

Kolari, P., Kulmala, L., Pumpanen, J., Launiainen, S., Ilvesniem, H., Hari, P., and Nikinmaa, E., 2009. CO(2) exchange and component CO(2) fluxes of a boreal Scots pine forest. Boreal Environment Research 14(4), 761-783

Kolle, O. and Rebmann, C., 2007. Eddy Soft Documentation of a Software Package to Acquire and Process Eddy Covariance Data.10

Kormann, R. and Meixner, F.X., 2001. An analytical footprint model for non-neutral stratification. Boundary-Layer Meteorology 99(2), 207-224. DOI: www.dx.doi.org/10.1023/A:1018991015119

Körner, C., 2003. Slow in, rapid out - Carbon flux studies and Kyoto targets. Science 300(5623), 1242-1243. DOI: www.dx.doi.org/10.1126/science.1084460

Kowalski, A.S., Loustau, D., Berbigier, P., Manca, G., Tedeschi, V., Borghetti, M., Valentini, R., Kolari, P., Berninger, F., Rannik, U., Hari, P., Rayment, M., Mencuccini, M., Moncrieff, J., and Grace, J., 2004. Paired comparisons of carbon exchange between undisturbed and regenerating stands in four managed forests in Europe. Global Change Biology 10(10), 1707-1723. DOI: www.dx.doi.org/10.1111/j.1365-2486.2004.00846.x

Kozlowski, T.T., 2002. Physiological ecology of natural regeneration of harvested and disturbed forest stands: implications for forest management. Forest Ecology and Management 158(1-3), 195-221. DOI: www.dx.doi.org/10.1016/S0378-1127(00)00712-X

Lagergren, F., Lindroth, A., Dellwik, E., Ibrom, A., Lankreijer, H., Launiainen, S., Mölder, M., Kolari, P., Pilegaard, K., and Vesala, T., 2008. Biophysical controls on CO_2 fluxes of three Northern forests based on long-term eddy covariance data. Tellus B 60(2), 143-152. DOI: www.dx.doi.org/10.1111/j.1600-0889.2006.00324.x

Lasslop, G., Reichstein, M., Kattge, J., and Papale, D., 2008. Influences of observation errors in eddy flux data on inverse model parameter estimation. Biogeosciences 5(5), 1311-1324. DOI: www.dx.doi.org/10.5194/bg-5-1311-2008

Lasslop, G., Reichstein, M., Papale, D., Richardson, A.D., Arneth, A., Barr, A., Stoy, P., and Wohlfahrt, G., 2010. Separation of net ecosystem exchange into assimilation and respiration using a light response curve approach: critical issues and global evaluation. Global Change Biology 16(1), 187-208. DOI: www.dx.doi.org/10.1111/j.1365-2486.2009.02041.x

Law, B.E., Falge, E., Gu, L., Baldocchi, D.D., Bakwin, P., Berbigier, P., Davis, K., Dolman, A.J., Falk, M., Fuentes, J.D., Goldstein, A., Granier, A., Grelle, A., Hollinger, D., Janssens, I.A., Jarvis, P., Jensen, N.O., Katul, G., Mahli, Y., Matteucci, G., Meyers, T., Monson, R., Munger, W., Oechel, W., Olson, R., Pilegaard, K., Paw, K.T., Thorgeirsson, H., Valentini, R., Verma, S., Vesala, T., Wilson, K., and Wofsy, S., 2002. Environmental controls over carbon dioxide and water vapor exchange of terrestrial vegetation. Agricultural and Forest Meteorology 113(1-4), 97-120. DOI: www.dx.doi.org/10.1016/S0168-1923(02)00104-1

Law, B.E., Sun, O.J., Campbell, J., Van Tuyl, S., and Thornton, P.E., 2003. Changes in carbon storage and fluxes in a chronosequence of ponderosa pine. Global Change Biology 9(4), 510-524. DOI: www.dx.doi.org/10.1046/j.1365-2486.2003.00624.x

Le Quéré, C., 2010. Trends in the land and ocean carbon uptake. Current Opinion in Environmental Sustainability 2(4), 219-224. DOI: www.dx.doi.org/10.1016/j.cosust.2010.06.003

Le Quéré, C., Andres, R.J., Boden, T., Conway, T., Houghton, R.A., House, J.I., Marland, G., Peters, G.P., van der Werf, G., Ahlström, A., Andrew, R.M., Bopp, L., Canadell, J.G., Ciais, P., Doney, S.C., Enright, C., Friedlingstein, P., Huntingford, C., Jain, A.K., Jourdain, C., Kato, E., Keeling, R.F., Klein Goldewijk, K., Levis, S., Levy, P., Lomas, M., Poulter, B., Raupach, M.R., Schwinger, J., Sitch, S., Stocker, B.D., Viovy, N., Zaehle, S., and Zeng, N., 2012. The global carbon budget 1959-2011. Earth Syst.Sci.Data Discuss. 5(2), 1107-1157. DOI: www.dx.doi.org/10.5194/essdd-5-1107-2012

Le Quéré, C., Peters, G.P., Andres, R.J., Andrew, R.M., Boden, T., Ciais, P., Friedlingstein, P., Houghton, R.A., Marland, G., Moriarty, R., Sitch, S., Tans, P., Arneth, A., Arvanitis, A., Bakker, D.C.E., Bopp, L., Canadell, J.G., Chini, L.P., Doney, S.C., Harper, A., Harris, I., House, J.I., Jain, A.K., Jones, S.D., Kato, E., Keeling, R.F., Klein Goldewijk, K., Körtzinger, A., Koven, C., Lefévre, N., Omar, A., Ono, T., Park, G.H., Pfeil, B., Poulter, B., Raupach, M.R., Regnier, P., Rödenbeck, C., Saito, S., Schwinger, J., Segschneider, J., Stocker, B.D., Tilbrook, B., van Heuven, S., Viovy, N., Wanninkhof, R., Wiltshire, A., Zaehle, S., and Yue, C., 2013. Global carbon budget 2013. Earth Syst.Sci.Data Discuss. 6(2), 689-760

Le Quéré, C., Raupach, M.R., Canadell, J.G., Marland, G., Bopp, L., Ciais, P., Conway, T.J., Doney, S.C., Feely, R.A., Foster, P., Friedlingstein, P., Gurney, K., Houghton, R.A., House, J.I., Huntingford, C., Levy, P.E., Lomas, M.R., Majkut, J., Metzl, N., Ometto, J.P., Peters, G.P., Prentice, I.C., Randerson, J.T., Running, S.W., Sarmiento, J.L., Schuster, U., Sitch, S., Takahashi, T., Viovy, N., van der Werf, G.R., and Woodward, F.I., 2009. Trends in the sources and sinks of carbon dioxide. Nature Geoscience 2(12), 831-836. DOI: www.dx.doi.org/10.1038/ngeo689

Lee, K.H., 2010. Constructing a non-linear relationship between the incoming solar radiation and bright sunshine duration. International Journal of Climatology 30(12), 1884-1892. DOI: www.dx.doi.org/10.1002/joc.2032

Lee, X., Finnigan, J. and Paw, U. 2004. Coordinate Systems and Flux Bias Error. In: Lee, X., Massman, W., Law, B. (Eds.), Handbook of Micrometeorology, Springer Netherlands, 33-66.

Lee, X. and Massman, W.J., 2011. A Perspective on Thirty Years of the Webb, Pearman and Leuning Density Corrections. Boundary-Layer Meteorology 139(1), 37-59. DOI: www.dx.doi.org/10.1007/s10546-010-9575-z

Lehning, A., Zimmer, W., Zimmer, I., and Schnitzler, J.-P., 2001. Modeling of annual variations of oak (*Quercus robur* L.) isoprene synthase activity to predict isoprene emission rates. Journal of Geophysical Research 106(D3), 3157-3166. DOI: www.dx.doi.org/10.1029/2000JD900631

Li, C.S., Aber, J., Stange, F., Butterbach-Bahl, K., and Papen, H., 2000. A process-oriented model of N2O and NO emissions from forest soils: 1. Model development. Journal of Geophysical Research-Atmospheres 105(D4), 4369-4384. DOI: www.dx.doi.org/10.1029/1999JD900949

Li, C., Frolking, S., and Frolking, T.A., 1992. A model of nitrous oxide evolution from soil driven by rainfall events: 1. Model structure and Sensitivity. Journal of Geophysical Research 97(9), 9759-9776. DOI: www.dx.doi.org/10.1029/92JD00509

Li, S.G., Asanuma, J., Eugster, W., Kotani, A., Liu, J.J., Urano, T., Oikawa, T., Davaa, G., Oyunbaatar, D., and Sugita, M., 2005a. Net ecosystem carbon dioxide exchange over grazed steppe in central Mongolia. Global Change Biology 11(11), 1941-1955. DOI: www.dx.doi.org/10.1111/j.1365-2486.2005.01047.x

Li, Z.Q., Yu, G.R., Wen, X.F., Zhang, L.M., Ren, C.Y., and Fu, Y.L., 2005b. Energy balance closure at ChinaFLUX sites. Science in China Series D-Earth Sciences 48, 51-62. DOI: www.dx.doi.org/10.1360/05zd0005

Lindauer, M., Schmid, H.P., Grote, R., Mauder, M., Steinbrecher, R., and Wolpert, B., 2014. Net ecosystem exchange over a non-cleared wind-throw-disturbed upland spruce forest - Measurements and simulations. Agricultural and Forest Meteorology 197(0), 219-234. DOI: www.dx.doi.org/10.1016/j.agrformet.2014.07.005

Lindroth, A., Lagergren, F., Grelle, A., Klemedtsson, L., Langvall, O., Weslien, P., and Tuulik, J., 2009. Storms can cause Europe-wide reduction in forest carbon sink. Global Change Biology 15(2), 346-355. DOI: www.dx.doi.org/10.1111/j.1365-2486.2008.01719.x

Liptzin, D., Williams, M.W., Helmig, D., Seok, B., Filippa, G., Chowanski, K., and Hueber, J., 2009. Process-level controls on CO_2 fluxes from a seasonally snow-covered subalpine meadow soil, Niwot Ridge, Colorado. Biogeochemistry 95(1), 151-166. DOI: www.dx.doi.org/10.1007/s10533-009-9303-2

Litton, C.M., Ryan, M.G., Knight, D.H., and Stahl, P.D., 2003. Soil-surface carbon dioxide efflux and microbial biomass in relation to tree density 13 years after a stand replacing fire in a lodgepole pine ecosystem. Global Change Biology 9(5), 680-696. DOI: www.dx.doi.org/10.1046/j.1365-2486.2003.00626.x

Liu, S., Bond-Lamberty, B., Hicke, J., Vargas, R., Zhao, S., Chen, J.M., Edburgh, S.L., Hu, Y., Liu, J., McGuire, A.D.D., Xiao, J., Keane, R., Yuan, W., Tang, J., Luo, Y., Potter, C.S., and Oeding, J., 2011. Simulating the Impacts of Disturbances on Forest Carbon Cycling in North America: Processes, Data, Models, and Challenges. Journal of Geophysical Research: Biogeosciences . DOI: www.dx.doi.org/10.1029/2010JG001585

Lloyd, J. and Taylor, J.A., 1994. On the Temperature-Dependence of Soil Respiration. Functional Ecology 8(3), 315-323

Loescher, H.W., Law, B.E., Mahrt, L., Hollinger, D.Y., Campbell, J., and Wofsy, S.C., 2006. Uncertainties in, and interpretation of, carbon flux estimates using the eddy covariance technique. Journal of Geophysical Research-Atmospheres 111(D21). DOI: www.dx.doi.org/10.1029/2005JD006932

Longuetaud, F., Mothe, F., Leban, J.M., and Makela, A., 2006. Picea abies sapwood width: Variations within and between trees. Scandinavian Journal of Forest Research 21(1), 41-53. DOI: www.dx.doi.org/10.1080/02827580500518632

Lovett, G., Cole, J., and Pace, M., 2006. Is net ecosystem production equal to ecosystem carbon accumulation? Ecosystems 9(1), 152-155. DOI: www.dx.doi.org/10.1007/s10021-005-0036-3

Luyssaert, S., Schulze, E., Boerner, A., Knohl, A., Hessenmoeller, D., Law, B.E., Ciais, P., and Grace, J., 2008. Old-growth forests as global carbon sinks. Nature 455(7210), 213-215. DOI: www.dx.doi.org/10.1038/nature07276

Magnani, F., Mencuccini, M., Borghetti, M., Berbigier, P., Berninger, F., Delzon, S., Grelle, A., Hari, P., Jarvis, P.G., Kolari, P., Kowalski, A.S., Lankreijer, H., Law, B.E., Lindroth, A., Loustau, D., Manca, G., Moncrieff, J.B., Rayment, M., Tedeschi, V., Valentini, R., and Grace, J., 2007. The human footprint in the carbon cycle of temperate and boreal forests. Nature 447(7146), 848-850. DOI: www.dx.doi.org/10.1038/nature05847

Mahmood, R. and Hubbard, K.G., 2002. Effect of time of temperature observation and estimation of daily solar radiation for the northern Great Plains, USA. Agronomy Journal 94(4), 723-733. DOI: www.dx.doi.org/10.2134/agronj2002.0723

Mahrt, L., 2010. Computing turbulent fluxes near the surface: Needed improvements. Agricultural and Forest Meteorology 150(4), 501-509. DOI: www.dx.doi.org/10.1016/j.agrformet.2010.01.015

Mäkelä, A., Hari, P., Berninger, F., Hanninen, H., and Nikinmaa, E., 2004. Acclimation of photosynthetic capacity in Scots pine to the annual cycle of temperature. Tree Physiology 24(4), 369-376. DOI: www.dx.doi.org/10.1093/treephys/24.4.369

Massman, W.J., 2006. Advective transport of CO_2 in permeable media induced by atmospheric pressure fluctuations: 1. An analytical model. Journal of Geophysical Research: Biogeosciences 111(G3), pp. G03004. DOI: www.dx.doi.org/10.1029/2006JG000163

Massman, W. and Clement, R. 2004. Uncertainty in Eddy Covariance Flux Estimates Resulting from Spectral Attenuation. In: Lee, X., Massman, W., Law, B. (Eds.), Handbook of Micrometeorology, Springer Netherlands, 67-99.

Mast, M.A., Wickland, K.P., Striegl, R.T., and Clow, D.W., 1998. Winter fluxes of CO_2 and CH_4 from subalpine soils in Rocky Mountain National Park, Colorado. Global Biogeochemical Cycles 12(4), 607-620. DOI: www.dx.doi.org/10.1029/98GB02313

Mauder, M., Cuntz, M., Druee, C., Graf, A., Rebmann, C., Schmid, H.P., Schmidt, M., and Steinbrecher, R., 2013. A strategy for quality and uncertainty assessment of long-term eddy-covariance measurements. Agricultural and Forest Meteorology 169, 122-135. DOI: www.dx.doi.org/10.1016/j.agrformet.2012.09.006

Mauder, M., Desjardins, R.L., Pattey, E., and Worth, D., 2010. An Attempt to Close the Daytime Surface Energy Balance Using Spatially-Averaged Flux Measurements. Boundary-Layer Meteorology 136(2), 175-191. DOI: www.dx.doi.org/10.1007/s10546-010-9497-9

Mauder, M., Oncley, S., Vogt, R., Weidinger, T., Ribeiro, L., Bernhofer, C., Foken, T., Kohsiek, W., De Bruin, H., and Liu, H., 2007. The energy balance experiment EBEX-2000. Part II: Intercomparison of eddy-covariance sensors and post-field data processing methods. Boundary-Layer Meteorology 123(1), 29-54. DOI: www.dx.doi.org/10.1007/s10546-006-9139-4

McFarlane, K.J. and Yanai, R.D., 2006. Measuring nitrogen and phosphorus uptake by intact roots of mature Acer saccharum Marsh., Pinus resinosa Ait., and Picea abies (L.) Karst. Plant and Soil 279(1-2), 163-172. DOI: www.dx.doi.org/10.1007/s11104-005-0838-2

Medlyn, B.E., Barton, C.V.M., Broadmeadow, M.S.J., Ceulemans, R., De Angelis, P., Forstreuter, M., Freeman, M., Jackson, S.B., Kellomaeki, S., Laitat, E., Rey, A., Roberntz, P., Sigurdsson, B.D., Strassemeyer, J., Wang, K., Curtis, P.S., and Jarvis, P.G., 2001. Stomatal conductance of forest species after long-term exposure to elevated CO_2 concentration: A synthesis. New Phytologist 149(2), 247-264. DOI: www.dx.doi.org/10.1046/j.1469-8137.2001.00028.x

Medlyn, B.E. and Jarvis, P.G., 1999. Design and use of a database of model parameters from elevated CO_2 experiments. Ecological Modelling 124(1), 69-83

Meir, P., Kruijt, B., Broadmeadow, M., Barbosa, E., Kull, O., Carswell, F., Nobre, A., and Jarvis, P.G., 2002. Acclimation of photosynthetic capacity to irradiance in tree canopies in relation to leaf nitrogen concentration and leaf mass per unit area. Plant Cell and Environment 25(3), 343-357. DOI: www.dx.doi.org/10.1046/j.0016-8025.2001.00811.x

Menzel,A.: 1997, 'Phänologie von Waldbäumen unter sich ändernden Klimabedingungen – Auswertung der Beobachtungen in den Internationalen Phänologischen Gärten und Möglichkeiten der Modellierung von Phänodaten', Forest Faculty**,** München.

Menzel, A. and Fabian, P., 1999. Growing season extended in Europe. Nature 397(6721), pp. 659. DOI: www.dx.doi.org/10.1038/17709

Michaelis, L. and Menten, M.L., 1913. Die kinetik der invertinwirkung. Biochem.Z 49(333-369), pp. - 352

Moffat, A.M., Papale, D., Reichstein, M., Hollinger, D.Y., RICHARDSON, A.D., Barr, A.G., Beckstein, C., Braswell, B.H., Churkina, G., Desai, A.R., Falge, E., Gove, J.H., Heimann, M., Hui, D., Jarvis, A.J., Kattge, J., Noormets, A., and Stauch, V.J., 2007. Comprehensive comparison of gap-filling techniques for eddy covariance net carbon fluxes. Agricultural and Forest Meteorology 147(3-4), 209-232. DOI: www.dx.doi.org/10.1016/j.agrformet.2007.08.011

Moncrieff, J.B., Malhi, Y., and Leuning, R., 1996. The propagation of errors in long-term measurements of land-atmosphere fluxes of carbon and water. Global Change Biology 2(3), 231-240. DOI: www.dx.doi.org/10.1111/j.1365-2486.1996.tb00075.x

Monson, R.K., Burns, S.P., Williams, M.W., Delany, A.C., Weintraub, M., and Lipson, D.A., 2006a. The contribution of beneath-snow soil respiration to total ecosystem respiration in a high-elevation, subalpine forest. Global Biogeochemical Cycles 20(3). DOI: www.dx.doi.org/10.1029/2005GB002684

Monson, R.K., Lipson, D.L., Burns, S.P., Turnipseed, A.A., Delany, A.C., Williams, M.W., and Schmidt, S.K., 2006b. Winter forest soil respiration controlled by climate and microbial community composition. Nature 439(7077), 711-714. DOI: www.dx.doi.org/10.1038/nature04555

Moore, B.A. and Allard, G.B., 2011. Abiotic disturbances and their influence on forest health: A review. Forest Health and Biosecurity Working Paper FBS E 35

Moore, C.J., 1986. Frequency response corrections for eddy correlation systems. Boundary-Layer Meteorology 37(1), 17-35. DOI: www.dx.doi.org/10.1007/BF00122754

Morgenstern, K., Black, T.A., Humphreys, E.R., Griffis, T.J., Drewitt, G.B., Cai, T.B., Nesic, Z., Spittlehouse, D.L., and Livingstone, N.J., 2004. Sensitivity and uncertainty of the carbon balance of a Pacific Northwest Douglas-fir forest during an El Nino La Nina cycle. Agricultural and Forest Meteorology 123(3-4), 201-219. DOI: www.dx.doi.org/10.1016/j.agrformet.2003.12.003

Munich Re, 2007. Zwischen Hoch und Tief - Wetterrisiken in Mitteleuropa., 1-60

Nabuurs, G.J., PΣivinen, R., Sikkema, R., and Mohren, G.M.J., 1997. The role of European forests in the global carbon cycle--A review. Biomass and Bioenergy 13(6), 345-358. DOI: www.dx.doi.org/10.1016/S0961-9534(97)00036-6

Nave, L.E., Gough, C.M., Maurer, K.D., Bohrer, G., Hardiman, B.S., Le Moine, J., Munoz, A.B., Nadelhoffer, K.J., Sparks, J.P., Strahm, B.D., Vogel, C.S., and Curtis, P.S., 2011. Disturbance and the resilience of coupled carbon and nitrogen cycling in a north temperate forest. Journal of Geophysical Research: Biogeosciences 116(G4), pp. G04016. DOI: www.dx.doi.org/10.1029/2011JG001758

Odum, E.P., 1969. The strategy of ecosystem development. Science 164(3877), 262-270

Osone, Y. and Tateno, M., 2005. Nitrogen absorption by roots as a cause of interspecific variations in leaf nitrogen concentration and photosynthetic capacity. Functional Ecology 19(3), 460-470. DOI: www.dx.doi.org/10.1111/j.1365-2435.2005.00970.x

Overpeck, J.T., Rind, D., and Goldberg, R., 1990. Climate-Induced Changes in Forest Disturbance and Vegetation. Nature 343(6253), 51-53. DOI: www.dx.doi.org/10.1038/343051a0

Pan, Y., Birdsey, R.A., Fang, J., Houghton, R., Kauppi, P.E., Kurz, W.A., Phillips, O.L., Shvidenko, A., Lewis, S.L., Canadell, J.G., Ciais, P., Jackson, R.B., Pacala, S.W., McGuire, A., Piao, S., Rautiainen, A., Sitch, S., and Hayes, D., 2011. A Large and Persistent Carbon Sink in the World's Forests. Science 333(6045), 988-993. DOI: www.dx.doi.org/10.1126/science.1201609

Papale, D., Reichstein, M., Aubinet, M., Canfora, E., Bernhofer, C., Kutsch, W., Longdoz, B., Rambal, S., Valentini, R., Vesala, T., and Yakir, D., 2006. Towards a standardized processing of Net Ecosystem Exchange measured with eddy covariance technique: algorithms and uncertainty estimation. Biogeosciences 3(4), 571-583. DOI: www.dx.doi.org/10.5194/bg-3-571-2006

Paw U, K.T., Baldocchi, D.D., Meyers, T.P., and Wilson, K.B., 2000. Correction Of Eddy-Covariance Measurements Incorporating Both Advective Effects And Density Fluxes. Boundary-Layer Meteorology 97(3), 487-511. DOI: www.dx.doi.org/10.1023/A:1002786702909

Payeur-Poirier, J.L., Coursolle, C., Margolis, H.A., and Giasson, M.A., 2012. CO_2 fluxes of a boreal black spruce chronosequence in eastern North America. Agricultural and Forest Meteorology 153(0), 94-105. DOI: www.dx.doi.org/10.1016/j.agrformet.2011.07.009

Peters, E., Wythers, K., Bradford, J., and Reich, P., 2012. Influence of Disturbance on Temperate Forest Productivity. Ecosystems , 1-16. DOI: www.dx.doi.org/10.1007/s10021-012-9599-y

Peters, W., Krol, M., van der Werf, G., Houweling, S., Jones, C., Hughes, J., Schaefer, K., Masarie, K., Jacobson, A., Miller, J., Cho, C., Ramonet, M., Schmidt, M., Ciattaglia, L., Apadula, F., Helta, D., Meinhardt, F., di Sarra, A., Piacentino, S., Sferlazzo, D., Aalto, T., Hatakka, J., Strom, J., Haszpra, L., Meijer, H., van der Laan, S., Neubert, R., Jordan, A., Rodo, X., Morgui, J., Vermeulen, A., Popa, E., Rozanski, K., Zimnoch, M., Manning, A., Leuenberger, M., Uglietti, C., Dolman, A.J., Ciais, P., Heimann, M., and Tans, P.P., 2010. Seven years of recent European net terrestrial carbon dioxide exchange constrained by atmospheric observations. Global Change Biology 16(4), 1317-1337. DOI: www.dx.doi.org/10.1111/j.1365-2486.2009.02078.x

Pickett, S.T.A. and White,P.S., 1985. The ecology of natural disturbance and patch dynamics, Academic Press, San Diego, pp. 472.

Pickett, S.T.A., Wu, J. and Cadenasso, M.L. 1999. Patch dynamics and the ecology of disturbed ground: A framework for synthesis. In: Walker, L.R. (Ed.), Ecosystems of Disturbed Ground, Elsevier, Amsterdam, 707-722.

Potter, C., Tan, P.N., Steinbach, M., Klooster, S., Kumar, V., Myneni, R., and Genovese, V., 2003. Major disturbance events in terrestrial ecosystems detected using global satellite data sets. Global Change Biology 9(7), 1005-1021. DOI: www.dx.doi.org/10.1046/j.1365-2486.2003.00648.x

Pregitzer, K.S. and Euskirchen, E.S., 2004. Carbon cycling and storage in world forests: biome patterns related to forest age. Global Change Biology 10(12), 2052-2077. DOI: www.dx.doi.org/10.1111/j.1365-2486.2004.00866.x

Prentice, I.C., Farquhar, G.D., Fashham, M.J.R., Goulden, M.L., Heimann, M., Jaramillo, V.J., Kheshgi, H.S., Le Quéré, C., Scholes, R.J., Wallace, D.W.R., Archer, D., Ashmore, M.R., Aumont, O., Baker, D., Battle, M., Bender, M., Bopp, L.P., Bousquet, P., Caldeira, K., Ciais, P., Cramer, W., Dentener, F., Enting, I.G., Field, C.B., Holland, E.A., Houghton, R.A., House, J.I., Ishida, A., Jain, A.K., Janssens, I., Joos, F., Kaminski, T., Kicklighter, D.W., Kohfeld, K.E., Knorr, W., Law, R., Lenton, T., Lindsay, K., Maier-Reimer, E., Manning, A., Matear, R.J., McGuire, A.D., Melillo, J.M., Meyer, R., Mund, M., Orr, J.C., Piper, S., Plattner, K., Rayner, P.J., Sitch, S., Slater, R., Taguchi, S., Tans, P.P., Tian, H.Q., Weirig, M.F., Whorf, T. and Yool, A. 2002. The carbon cycle and

atmospheric carbon dioxide. In: Houghton, J.T. (Ed.), Climate Change 2001: The scientific basis: contribution of Working Group I to the Third Assessment Report of the Intergouvernmental Panel on Climate Change, Cambridge University Press, Cambridge, 183-237.

Randerson, J.T., Chapin, F.S., Harden, J.W., Neff, J.C., and Harmon, M.E., 2002. Net ecosystem production: A comprehensive measure of net carbon accumulation by ecosystems. Ecological Applications 12(4), 937-947. DOI: www.dx.doi.org/10.2307/3061028

Rannik, U., Kolari, P., Vesala, T., and Hari, P., 2006. Uncertainties in measurement and modelling of net ecosystem exchange of a forest. Agricultural and Forest Meteorology 138(1-4), 244-257. DOI: www.dx.doi.org/10.1016/j.agrformet.2006.05.007

Raupach, M.R., 2011. CARBON CYCLE Pinning down the land carbon sink. Nature Climate Change 1(3), 148-149. DOI: www.dx.doi.org/10.1038/nclimate1123

Rebmann, C., Zeri, M., Lasslop, G., Mund, M., Kolle, O., Schulze, E.D., and Feigenwinter, C., 2010. Treatment and assessment of the CO_2-exchange at a complex forest site in Thuringia, Germany. Agricultural and Forest Meteorology 150(5), 684-691. DOI: www.dx.doi.org/10.1016/j.agrformet.2009.11.001

Reichstein, M., Falge, E., Baldocchi, D., Papale, D., Aubinet, M., Berbigier, P., Bernhofer, C., Buchmann, N., Gilmanov, T., Granier, A., Grunwald, T., Havrankova, K., Ilvesniemi, H., Janous, D., Knohl, A., Laurila, T., Lohila, A., Loustau, D., Matteucci, G., Meyers, T., Miglietta, F., Ourcival, J.M., Pumpanen, J., Rambal, S., Rotenberg, E., Sanz, M., Tenhunen, J., Seufert, G., Vaccari, F., Vesala, T., Yakir, D., and Valentini, R., 2005. On the separation of net ecosystem exchange into assimilation and ecosystem respiration: review and improved algorithm. Global Change Biology 11(9), 1424-1439. DOI: www.dx.doi.org/10.1111/j.1365-2486.2005.001002.x

Richardson, A.D. and Hollinger, D.Y., 2005. Statistical modeling of ecosystem respiration using eddy covariance data: Maximum likelihood parameter estimation, and Monte Carlo simulation of model and parameter uncertainty, applied to three simple models. Agricultural and Forest Meteorology 131(3-4), 191-208. DOI: www.dx.doi.org/10.1016/j.agrformet.2005.05.008

Richardson, A.D., Hollinger, D.Y., Burba, G.G., Davis, K.J., Flanagan, L.B., Katul, G.G., William Munger, J., Ricciuto, D.M., Stoy, P.C., Suyker, A.E., Verma, S.B., and Wofsy, S.C., 2006. A multi-site analysis of random error in tower-based measurements of carbon and energy fluxes. Agricultural and Forest Meteorology 136(1-2), 1-18. DOI: www.dx.doi.org/10.1016/j.agrformet.2006.01.007

Richardson, A.D., Mahecha, M.D., Falge, E., Kattge, J., Moffat, A.M., Papale, D., Reichstein, M., Stauch, V.J., Braswell, B.H., Churkina, G., Kruijt, B., and Hollinger, D.Y., 2008. Statistical properties of random CO2 flux measurement uncertainty inferred from model residuals. Agricultural and Forest Meteorology 148(1), 38-50. DOI: www.dx.doi.org/10.1016/j.agrformet.2007.09.001

Richardson, A., Aubinet, M., Barr, A., Hollinger, D., Ibrom, A., Lasslop, G. and Reichstein, M. 2012. Uncertainty Quantification. In: Aubinet, M., Vesala, T., Papale, D. (Eds.), Eddy Covariance, Springer Netherlands, 173-209.

Rötzer, T., Grote, R., and Pretzsch, H., 2004. The timing of bud burst and its effect on tree growth. International Journal of Biometeorology 48(3), 109-118. DOI: www.dx.doi.org/10.1007/s00484-003-0191-1

Running, S.W., 2008. Climate change - Ecosystem disturbance, carbon, and climate. Science 321(5889), 652-653. DOI: www.dx.doi.org/10.1126/science.1159607

Ruppert, J., Mauder, M., Thomas, C., and L³ers, J., 2006. Innovative gap-filling strategy for annual sums of CO2 net ecosystem exchange. Agricultural and Forest Meteorology 138(1-4), 5-18. DOI: www.dx.doi.org/10.1016/j.agrformet.2006.03.003

Rykiel, E.J., 1985. Towards A Definition of Ecological Disturbance. Australian Journal of Ecology 10(3), 361-365. DOI: www.dx.doi.org/10.1111/j.1442-9993.1985.tb00897.x

Sarmiento, J., Gloor, M., Gruber, N., Beaulieu, C., Jacobson, A., Fletcher, S., Pacala, S., and Rodgers, K., 2010. Trends and regional distributions of land and ocean carbon sinks. Biogeosciences 7(8), 2351-2367. DOI: www.dx.doi.org/10.5194/bg-7-2351-2010

Schelhaas, M.J., Hengeveld, G., Moriondo, M., Reinds, G.J., Kundzewicz, Z.W., Ter Maat, H., and Bindi, M., 2010. Assessing risk and adaptation options to fires and windstorms in European forestry. Mitigation and Adaptation Strategies for Global Change 15(7), 681-701. DOI: www.dx.doi.org/10.1007/s11027-010-9243-0

Schelhaas, M.J., Nabuurs, G.J., and Schuck, A., 2003. Natural disturbances in the European forests in the 19th and 20th centuries. Global Change Biology 9(11), 1620-1633. DOI: www.dx.doi.org/10.1046/j.1529-8817.2003.00684.x

Schimel, D.S., House, J.I., Hibbard, K.A., Bousquet, P., Ciais, P., Peylin, P., Braswell, B.H., Apps, M.J., Baker, D., Bondeau, A., Canadell, J., Churkina, G., Cramer, W., Denning, A.S., Field, C.B., Friedlingstein, P., Goodale, C., Heimann, M., Houghton, R.A., Melillo, J.M., Moore, B., Murdiyarso, D., Noble, I., Pacala, S.W., Prentice, I.C., Raupach, M.R., Rayner, P.J., Scholes, R.J., Steffen, W.L., and Wirth, C., 2001. Recent patterns and mechanisms of carbon exchange by terrestrial ecosystems. Nature 414(6860), 169-172. DOI: www.dx.doi.org/10.1038/35102500

Schindlbacher, A., Zechmeister-Boltenstern, S., Glatzel, G., and Jandl, R., 2007. Winter soil respiration from an Austrian mountain forest. Agricultural and Forest Meteorology 146(3), 205-215. DOI: www.dx.doi.org/10.1016/j.agrformet.2007.06.001

Schmid, H.P., 1997. Experimental design for flux measurements: matching scales of observations and fluxes. Agricultural and Forest Meteorology 87(2-3), 179-200. DOI: www.dx.doi.org/10.1016/S0168-1923(97)00011-7

Schmid, H.P., Grimmond, C.S.B., Cropley, F., Offerle, B., and Su, H.B., 2000. Measurements of CO2 and energy fluxes over a mixed hardwood forest in the mid-western United States. Agricultural and Forest Meteorology 103(4), 357-374. DOI: www.dx.doi.org/10.1016/S0168-1923(00)00140-4

Schmid, H.P., Su, H.B., Vogel, C.S., and Curtis, P.S., 2003. Ecosystem-atmosphere exchange of carbon dioxide over a mixed hardwood forest in northern lower Michigan. Journal of Geophysical Research vol.108, no.D14, ACH6-19. DOI: www.dx.doi.org/10.1029/2002JD003011

Schopf, R., Steinbrecher, R., and Schmid, H.P., 2008. Borkenkaeferbefall auf Windwurfflächen: Prozessanalyse für Handlungsoptionen. Forschungsantrag zum Projekt: VGU-06070204028, Bayerisches Staatsministerium für Umwelt und Gesundheit.

Schulze, E.D. and Heimann, M. 1998. Carbon and water exchange of terrestrial ecosystems. In: Galloway, J., Melillo, J.M. (Eds.), Asian change in the context of global change, Cambridge University Press, Cambridge, 145-161.

Schulze, E.D., Lloyd, J., Kelliher, F.M., Wirth, C., Rebmann, C., Luhker, B., Mund, M., Knohl, A., Milyukova, I.M., Schulze, W., Ziegler, W., Varlagin, A.B., Sogachev, A.F., Valentini, R., Dore, S., Grigoriev, S., Kolle, O., Panfyorov, M.I., Tchebakova, N., and Vygodskaya, N.N., 1999. Productivity of forests in the Eurosiberian boreal region and their potential to act as a carbon sink - a synthesis. Global Change Biology 5(6), 703-722. DOI: www.dx.doi.org/10.1046/j.1365-2486.1999.00266.x

Schulze, E.D., Wirth, C., and Heimann, M., 2000. Climate change - managing forests after Kyoto. Science 289(5487), 2058-2059. DOI: www.dx.doi.org/10.1126/science.289.5487.2058

Seidl, R., Schelhaas, M.J., and Lexer, M.J., 2011. Unraveling the drivers of intensifying forest disturbance regimes in Europe. Global Change Biology 17(9), 2842-2852. DOI: www.dx.doi.org/10.1111/j.1365-2486.2011.02452.x

Sellers, P.J., Dickinson, R.E., Randall, D.A., Betts, A.K., Hall, F.G., Berry, J.A., Collatz, G.J., Denning, A.S., Mooney, H.A., Nobre, C.A., Sato, N., Field, C.B., and Henderson-Sellers, A., 1997. Modeling the exchanges of energy, water, and carbon between continents and the atmosphere. Science 275(5299), 502-509. DOI: www.dx.doi.org/10.1126/science.275.5299.502

Sellin, A. and Kupper, P., 2004. Within-crown variation in leaf conductance of Norway spruce: effects of irradiance, vapour pressure deficit, leaf water status and plant hydraulic constraints. Annals of Forest Science 61(5), 419-429. DOI: www.dx.doi.org/10.1051/forest:2004035

Späth, C., 2010. Der Nationalpark Bayerischer Wald und seine Wälder, GRIN Verlag, München, pp. 120.

Spielvogel, S., Prietzel, J., and Koegel-Knabner, I., 2006. Soil organic matter changes in a spruce ecosystem 25 years after disturbance. Soil Science Society of America Journal 70(6), 2130-2145. DOI: www.dx.doi.org/10.2136/sssaj2005.0027

Stauch, V.J., Jarvis, A.J., and Schulz, K., 2008. Estimation of net carbon exchange using eddy covariance CO_2 flux observations and a stochastic model. J.Geophys.Res 113, pp. D03101. DOI: www.dx.doi.org/10.1029/2007JD008603

Stoy, P.C., Katul, G.G., Siqueira, M.B.S., Juang, J.Y., Novick, K.A., Uebelherr, J.M., and Oren, R., 2006. An evaluation of models for partitioning eddy covariance-measured net ecosystem exchange into photosynthesis and respiration. Agricultural and Forest Meteorology 141(1), 2-18. DOI: www.dx.doi.org/10.1016/j.agrformet.2006.09.001

Stull, R.B., 2000. Meteorology for scientists and engineers, Brooks/Cole Thomson Learning, Pacific Grove, Calif., pp. 502.

Thornley, J.H.M. and Cannell, M.G.R., 2000. Managing forests for wood yield and carbon storage: a theoretical study. Tree Physiology 20(7), 477-484. DOI: www.dx.doi.org/10.1093/treephys/20.7.477

Thornton, P.E., Law, B.E., Gholz, H.L., Clark, K.L., Falge, E., Ellsworth, D.S., Golstein, A.H., Monson, R.K., Hollinger, D., Falk, M., Chen, J., and Sparks, J.P., 2002. Modeling and measuring the effects of disturbance history and climate on carbon and water budgets in evergreen needleleaf forests. Agricultural and Forest Meteorology 113(1-4), 185-222. DOI: www.dx.doi.org/10.1016/S0168-1923(02)00108-9

Thürig, E., Palosuo, T., Bucher, J., and Kaufmann, E., 2005. The impact of windthrow on carbon sequestration in Switzerland: a model-based assessment. Forest Ecology and Management 210(1-3), 337-350. DOI: www.dx.doi.org/10.1016/j.foreco.2005.02.030

Tjoelker, M.G., Craine, J.M., Wedin, D., Reich, P.B., and Tilman, D., 2005. Linking leaf and root trait syndromes among 39 grassland and savannah species. New Phytologist 167(2), 493-508. DOI: www.dx.doi.org/10.1111/j.1469-8137.2005.01428.x

Ukonmaanaho, L., Merila, P., Nojd, P., and Nieminen, T.M., 2008. Litterfall production and nutrient return to the forest floor in Scots pine and Norway spruce stands in Finland. Boreal Environment Research 13, 67-91

Ulanova, N.G., 2000. The effects of windthrow on forests at different spatial scales: a review. Forest Ecology and Management 135(1-3), 155-167. DOI: www.dx.doi.org/10.1016/S0378-1127(00)00307-8

Urban, O., Ac, A., Kalina, J., Priwitzer, T., Sprtova, M., Spunda, V., and Marek, M., V, 2007. Temperature dependences of carbon assimilation processes in four dominant species from mountain grassland ecosystem. Photosynthetica 45(3), 392-399. DOI: www.dx.doi.org/10.1007/s11099-007-0066-5

Valentini, R., DeAngelis, P., Matteucci, G., Monaco, R., Dore, S., and Mugnozza, G.E.S., 1996. Seasonal net carbon dioxide exchange of a beech forest with the atmosphere. Global Change Biology 2(3), 199-207. DOI: www.dx.doi.org/10.1111/j.1365-2486.1996.tb00072.x

Valentini, R., Matteucci, G., Dolman, A.J., Schulze, E.D. and Jarvis, P.G. 2003. The carbon sink strength of forests in Europe: a synthesis of results. In: Valentini, R. (Ed.), Fluxes of Carbon, Water and Energy of European Forests, 225-232.

Van Dijk, A.I.J.M. and Dolman, A.J., 2004. Estimates of CO_2 uptake and release among European forests based on eddy covariance data. Global Change Biology 10(9), 1445-1459. DOI: www.dx.doi.org/10.1111/j.1365-2486.2004.00831.x

van Gorsel, E., Delpierre, N., Leuning, R., Black, A., Munger, J.W., Wofsy, S., Aubinet, M., Feigenwinter, C., Beringer, J., Bonal, D., Chen, B.Z., Chen, J.Q., Clement, R., Davis, K.J., Desai, A.R., Dragoni, D., Etzold, S., Grunwald, T., Gu, L.H., Heinesch, B., Hutyra, L.R., Jans, W.W.P., Kutsch, W., Law, B.E., Leclerc, M.Y., Mammarella, I., Montagnani, L., Noormets, A., Rebmann, C., and Wharton, S., 2009. Estimating nocturnal ecosystem respiration from the vertical turbulent flux and change in storage of CO2. Agricultural and Forest Meteorology 149(11), 1919-1930. DOI: www.dx.doi.org/10.1016/j.agrformet.2009.06.020

Vickers, D. and Mahrt, L., 1997. Quality control and flux sampling problems for tower and aircraft data. Journal of Atmospheric and Oceanic Technology 14(3), 512-526. DOI: www.dx.doi.org/10.1175/1520-0426(1997)014<0512:QCAFSP>2.0.CO;2

Vickers, D., Irvine, J., Martin, J.G., and Law, B.E., 2012. Nocturnal subcanopy flow regimes and missing carbon dioxide. Agricultural and Forest Meteorology 152, 101-108. DOI: www.dx.doi.org/10.1016/j.agrformet.2011.09.004

Vuichard, N. and Papale, D., 2015. Filling the gaps in meteorological continuous data measured at FLUXNET sites with ERA-Interim reanalysis. Earth Syst.Sci.Data 7(2), 157-171. DOI: www.dx.doi.org/10.5194/essd-7-157-2015

Wang, D., Lin, J., Sun, R., Xia, L., and Lian, G., 2003. Optimum nitrogen rate for a high productive rice-wheat system and its impact on the groundwater in the taihu lake area. Acta Pedologica Sinica 40(3), 426-432. DOI: www.dx.doi.org/cnki:ISSN:0564-3929.0.2003-03-015

Wang, T., Ciais, P., Piao, S.L., Ottlé, C., Brender, P., Maignan, F., Arain, A., Cescatti, A., Gianelle, D., Gough, C., Gu, L., Lafleur, P., Laurila, T., Marcolla, B., Margolis, H., Montagnani, L., Moors, E., Saigusa, N., Vesala, T., Wohlfahrt, G., Koven, C., Black, A., Dellwik, E., Don, A., Hollinger, D., Knohl, A., Monson, R., Munger, J., Suyker, A., Varlagin, A., and Verma, S., 2011. Controls on winter ecosystem respiration in temperate and boreal ecosystems. Biogeosciences 8(7), 2009-2025. DOI: www.dx.doi.org/10.5194/bg-8-2009-2011

Wang, Y.P. and Jarvis, P.G., 1990. Influence of Crown Structural-Properties on Par Absorption, Photosynthesis, and Transpiration in Sitka Spruce - Application of A Model (Maestro). Tree Physiology 7(1-4), 297-316. DOI: www.dx.doi.org/10.1093/treephys/7.1-2-3-4.297

Webb, E.K., Pearman, G.I., and Leuning, R., 1980. Correction of flux measurements for density effects due to heat and water vapour transfer. Quarterly Journal of the Royal Meteorological Society 106(447), 85-100. DOI: www.dx.doi.org/10.1002/qj.49710644707

Wharton, S., Schroeder, M., Paw, U., Falk, M., and Bible, K., 2009. Turbulence considerations for comparing ecosystem exchange over old-growth and clear-cut stands for limited fetch and complex canopy flow conditions. Agricultural and Forest Meteorology 149(9), 1477-1490. DOI: www.dx.doi.org/10.1016/j.agrformet.2009.04.002

Wilczak, J., Oncley, S., and Stage, S., 2001. Sonic Anemometer Tilt Correction Algorithms. Boundary-Layer Meteorology 99(1), 127-150. DOI: www.dx.doi.org/10.1023/A:1018966204465

Williams, C.A., Collatz, G., Masek, J., and Goward, S.N., 2012. Carbon consequences of forest disturbance and recovery across the conterminous United States. Global Biogeochemical Cycles 26. DOI: www.dx.doi.org/10.1029/2010GB003947

Williams, M., Rastetter, E.B., Fernandes, D.N., Goulden, M.L., Wofsy, S.C., Shaver, G.R., Melillo, J.M., Munger, J.W., Fan, S.M., and Nadelhoffer, K.J., 1996. Modelling the soil-plant-atmosphere continuum in a Quercus-Acer stand at Harvard forest: The regulation of stomatal conductance by light, nitrogen and soil/plant hydraulic properties. Plant Cell and Environment 19(8), 911-927. DOI: www.dx.doi.org/10.1111/j.1365-3040.1996.tb00456.x

Williams, M.W., Helmig, D., and Blanken, P., 2009. White on green: under-snow microbial processes and trace gas fluxes through snow, Niwot Ridge, Colorado Front Range. Biogeochemistry 95(1), 1-12. DOI: www.dx.doi.org/10.1007/s10533-009-9330-z

Wilpert, K., 1990. Die Jahrringstruktur von Fichten in Abhängigkeit vom Bodenwasserhaushalt auf Pseudogley und Parabraunerde: ein Methodenkonzept zur Erfassung standortsspezifischer Wasserstreßdisposition. Freiburger bodenkundl.Abhandlungen 24, pp. 184

Wilson, K., Goldstein, A., Falge, E., Aubinet, M., Baldocchi, D., Berbigier, P., Bernhofer, C., Ceulemans, R., Dolman, H., and Field, C., 2002. Energy balance closure at FLUXNET sites. Agricultural and Forest Meteorology 113(1-4), 223-243. DOI: www.dx.doi.org/10.1016/S0168-1923(02)00109-0

Withington, J.M., Reich, P.B., Oleksyn, J., and Eissenstat, D.M., 2006. Comparisons of structure and life span in roots and leaves among temperate trees. Ecological Monographs 76(3), 381-397. DOI: www.dx.doi.org/10.1890/0012-9615(2006)076[0381:COSALS]2.0.CO;2

Wohlfahrt, G., Bahn, M., Tappeiner, U., and Cernusca, A., 2000. A model of whole plant gas exchange for herbaceous species from mountain grassland sites differing in land use. Ecological Modelling 125(2-3), 173-201. DOI: www.dx.doi.org/10.1016/S0304-3800(99)00180-5

Wohlfahrt, G., Bahn, M., Tappeiner, U., and Cernusca, A., 2001. A multi-component, multi-species model of vegetation-atmosphere CO_2 and energy exchange for mountain grasslands. Agricultural and Forest Meteorology 106(4), 261-287. DOI: www.dx.doi.org/10.1016/S0168-1923(00)00224-0

Wolpert,B.: 2012, 'Emission and abundance of biogenic volatile organic compounds in wind-throw areas of upland spruce forests in Bavaria', *PhD Thesis* Technische Universität München**,** München, Germany, pp. 161.

Zeeman, M.J., Hiller, R., Gilgen, A.K., Michna, P., Pluess, P., Buchmann, N., and Eugster, W., 2010. Management and climate impacts on net CO_2 fluxes and carbon budgets of three grasslands along an elevational gradient in Switzerland. Agricultural and Forest Meteorology 150(4), 519-530. DOI: www.dx.doi.org/10.1016/j.agrformet.2010.01.011

Zha, T., Kellomaki, S., Wang, K.Y., and Rouvinen, I., 2004. Carbon sequestration and ecosystem respiration for 4 years in a Scots pine forest. Global Change Biology 10(9), 1492-1503. DOI: www.dx.doi.org/10.1111/j.1365-2486.2004.00835.x

Zianis, D. and Mencuccini, M., 2005. Aboveground net primary productivity of a beech (*Fagus moesiaca*) forest: a case study of Naousa forest, northern Greece. Tree Physiology 25(6), 713-722. DOI: www.dx.doi.org/10.1093/treephys/25.6.713

Zib, B.J., Dong, X.Q., Xi, B.K., and Kennedy, A., 2012. Evaluation and Intercomparison of Cloud Fraction and Radiative Fluxes in Recent Reanalyses over the Arctic Using BSRN Surface Observations. Journal of Climate 25(7), 2291-2305. DOI: www.dx.doi.org/10.1175/JCLI-D-11-00147.1

Zimov, S.A., Davidov, S.P., Voropaev, Y.V., Prosiannikov, S.F., Semiletov, I.P., Chapin, M.C., and Chapin, F.S., 1996. Siberian CO_2 efflux in winter as a CO_2 source and cause of seasonality in atmospheric CO_2. Climatic Change 33(1), 111-120. DOI: www.dx.doi.org/10.1007/BF00140516

Acknowledgements

My research was conducted at the Karlsruhe Institute of Technology (KIT), Institute of Meteorology and Climate Research, Department of Atmospheric Environmental Research (IMK-IFU), Garmisch-Partenkirchen, Germany, in the research group “Transport Processes in the Atmospheric Boundary Layer (TABLe)” within the division of “Ecosystem-Atmosphere Interactions” in collaboration with the chair for Atmospheric Environmental Research, Technical University Munich. It was supported, in part, by the Bavarian Ministry of the Environment and Public Health (UGV06080204000), the German Helmholtz Association with its research program Atmosphere and Climate (ATMO), and the KIT Graduate School for Climate and Environment – GRACE.

The work was supervised by Professor Dr. Hans Peter Schmid (IMK-IFU). I wish to thank him for providing me the opportunity to work in this project, for critical discussions on scientific questions, stimulating new ideas and helpful guidance in research problems. I am very thankful for the numerous chances to visit conferences and workshops, which were very beneficial for my personal development as a young scientist.

I am grateful to Professor Dr. Harald Kunstmann who unhesitatingly agreed to be my second referee.

Furthermore, I am grateful to my colleagues Dr. Janina Hommeltenberg, Katja Heidbach, Elisabeth Eckart Carsten Jahn and, particularly, Dr. Benjamin Wolpert for perfect collaboration in theoretical research and practical field work, and for refreshing coffee breaks.

Moreover I wish to thank Dr. Rainer Steinbrecher, and Dr. Matthias Mauder for sharing their profound scientific knowledge and for helping me in technical issues and practical field work. Also many thanks to Dr. Rüdiger Grote for his support with the LandscapeDNDC model simulations and Dr. Matthias Zeeman for his help with the Monte Carlo simulation.

This work was embedded in the project “Borkenkäferbefall auf Windwurfflächen: Prozessanalyse für Handlungsoptionen“ funded by the Bavarian State Ministry of the Environment and Public Health. I express my thanks to the coordinator of the project, Professor Dr. Reinhard Schopf, and the administration of the National Park Bavarian Forest, especially Dr. Heinrich Rall, Dr. Claus Bässler, and Burkhard Beudert.

Garmisch-Partenkirchen, Dezember 2015